Intensity Correlations in the Multiple Scattering of Light by Cold Atomic Gases

Research Thesis

In Partial Fulfillment of The Requirements for the Degree of Doctor of Philosophy

Ohad Assaf

Submitted to the Senate of the Technion - Israel Institute of Technology

Av 5768 Haifa August 2007

.

To my wife and son, Anat and Eitan

To my parents, Shosh and Israel

To my brothers, Itay and Yoav

.

The research thesis was done under the supervision of Prof. Eric Akkermans in the department of physics.

I wish to thank Prof. Akkermans, from the bottom of my heart, for his great devotion in guiding me, his crucial contribution to this research, and the generous financial support he has provided me with.

The generous financial help of the Technion is gratefully acknowledged.

.

Contents

List of Figures

.

List of Tables

.

List of symbols

l - elastic mean free path.
L - linear dimension of the slab.
b - optical depth.
$\mathcal{T}$ - transmission coefficient.
I - light intensity/ the unit matrix.
$Corr$ - correlation function.
C - normalized correlation function.
$\mathcal{D}$ - Diffuson.
Γ - natural width of the atomic excited state.
j_g - total angular momentum quantum number of the atomic ground state.
j_e - total angular momentum quantum number of the atomic excited state.
J - shorthand for $2j_g + 1$.
$a_{j_g j_e}$ - shorthand for $\frac{1}{3}\frac{2j_e+1}{2j_g+1}$.
$\mathcal{V}^{(i)}$ - intensity vertex.
$\mathcal{V}^{(c)}$ - correlation vertex.
$\mathcal{W}$ - intensity propagator between two successive scattering events.
T_i - spectral decomposition tensors.
H - magnetic field/ Hamiltonian of the system light + atom.
s - dimensionless magnetic field.

.

Abstract

A light beam multiply scattered by a cloud of randomly distributed scatterers leads to a very complex interference, or speckle, pattern. The characteristics of a speckle pattern are usually studied using the average transmitted intensity and the intensity correlation function of the scattered light. In particular, the intensity fluctuations for the case of classical scatterers are given by the Rayleigh law, which states that the root mean square of the transmitted intensity equals its configuration average. In this thesis we study the average and the correlation functions of the transmitted intensity of light multiply scattered by a cold atomic gas. We show that the internal structure of atoms, *e.g.* Zeeman degeneracy, enhances significantly the intensity correlation. This enhancement results from contributions of the internal degrees of freedom of the scatterers, that do not contribute to the average intensity. These additional contributions are, however, sensitive to an applied magnetic field which reduces sharply the correlation enhancement. The corresponding behavior of the correlation has a resonant-like shape, and its width is narrower than the one obtained in other related phenomena like the Hanle effect. This may have an experimental significance, since the width of the resonance-like peak is directly related to experiments resolution. The enhanced correlation is also sensitive to the motion of scatterers. This motion leads to a rapid decay of the correlation as a function of time.

.

CHAPTER 1

Introduction

In this work we study the intensity correlation of light multiply scattered by a cloud of randomly distributed atoms. As such, this work involves two different fields of physics [1, 2] (Appendix D). The first one is atomic physics, namely the interaction of light and atoms. This is a well established field which has been extensively studied since the early years of the twentieth century. The second field is coherent transport of waves in random media, which is a central part of mesoscopic physics. This field is much younger than atomic physics, and most of the progress has been achieved mainly during the last two decades of the twentieth century, although a few important contributions have been published beforehand, *e.g.* in the context of light waves [3, 4]. Coherent multiple scattering of waves in disordered media appears in many areas in physics, such as astrophysics, but the main focus during the last decades is on solid state physics or, more precisely, the transport of electrons in conductors. The impurities in a conductor are randomly distributed, and scatter electrons. This determines the conduction properties of the substance. Owing to the progress in technology, which allows cooling metallic samples down to sub-kelvin temperatures, the coherence length of conduction electrons became comparable to the size of the conductor [5]. This new situation led to new theoretical developments to take into account the wave properties of the electrons inside the conductor. This new field is known as mesoscopic physics. It concerns systems which, despite being macroscopic, involve interference effects due to the long range coherence of the waves.

The study of coherent multiple scattering of light in disordered media presents experimental advantages relative to the problem of electronic conduction. For example, light that is shined upon a scattering medium and then is detected along some direction allows angular, or directional, analysis of multiple scattering, which is much more difficult in the case of electrons. Moreover, lasers provide a common source of extremely coherent waves, which are also easily tunable, so that the scattering cross section may be controlled by simply changing the light wavelength. The use of light

thus allowed the experimental observation of mesoscopic phenomena, such as coherent backscattering, which was discovered theoretically and experimentally during the mid eighties of the last century [6, 7, 8, 9]. The coherent backscattering is often referred to as a *weak localization* effect, to indicate that it is observed when the scattering events can be considered independent of each other. The condition for weak localization is usually expressed as $kl \gg 1$, where k is the wave number of the scattered wave and l is the *elastic mean free path* of the wave inside the medium. In this regime, the multiply scattered wave is treated within the framework of diffusion theory, where interference effects amounts to some corrections to the diffusion result, called *weak localization corrections*. In the strong localization regime, $kl \sim 1$, a very different behavior is obtained, such as a metal-insulator transition (Anderson transition) in three dimensions. In this work, we restrict ourselves to the weak localization regime.

Within the diffusion approximation, the disorder-averaged multiply scattered intensity depends essentially on 4 parameters: the size of the disordered sample, the light wavelength, the total scattering cross section of the wave off a single scatterer, and the density of scatterers in the medium. It does not depend, for example, on the dynamics of the scatterers, at least as long as this dynamics does not affect the coherence of the wave. More information, both about the sample and the scattered wave, may be gained using *correlation functions*. Here we focus on two kinds of correlation functions: angular and temporal. The first kind is the correlation between the intensity, incoming and scattered along different directions (different *channels*). The second kind usually amounts to correlation between the scattered intensity of a single channel at two different times. In both cases, the full correlation function is given by a perturbation series, where each order corresponds to the number of possible *crossings*. The term "crossing" denotes the situation in which two diffusion processes cross each other in a coherent way. The small parameter in this perturbation series is the probability of the crossing event to occur, which for a cubic sample of linear dimension L is given roughly by λ^2/lL (λ is the wavelength of the wave), and is typically much smaller than unity. The zeroth order, $C^{(1)}$, corresponds to the absence of crossing [5, 10]. This is the dominant contribution to the channel correlation function, namely, where the wave is incident and detected along some specific directions. Since this is the case considered in the present work, we restrict our study to the zeroth order contribution. The $C^{(1)}$ function is often called *short range* correlation, since it decays exponentially with the relative angle of the two channels or with

the time separation between measurements (temporal correlation). There is a general behavior that characterizes the correlation $C^{(1)}$ for classical scatterers. This is the Rayleigh law, which states that for small relative angles, or time separations, we have $\overline{II'} = 2\bar{I}\bar{I'}$. Here I and I' denotes two intensities, corresponding to two channels or two times, and $\overline{\cdots}$ is a disorder configuration average. In particular, for $I = I'$, the Rayleigh law becomes $\overline{I^2} = 2\bar{I}^2$. It characterizes also the light coming from the sun (chaotic light). The next two orders, $C^{(2)}$ and $C^{(3)}$, correspond to cases where two diffusion processes cross each other once and twice, respectively. These contributions are referred to as *long ranged* [11, 12], because they decay much slower than $C^{(1)}$ as a function of the relative angle or time: $C^{(2)}$ decays as a power low while $C^{(3)}$ is constant. As a result, $C^{(2)}$ and $C^{(3)}$ contribute significantly only when many channels are integrated to find, for example, the total transmission coefficient. In particular, the infinite-range $C^{(3)}$ contribution is at the basis of the so-called universal conductance fluctuations observed in electronic transport [13]. Information about the dynamics of scatterers may be obtained using the temporal correlation function, since the decay of this function is due to the motion of the scatterers. This motion leads to a difference between the positions of the scatterer at times 0 and t, say. If this difference is sufficiently large and random, the scattering amplitudes at times 0 and t are no longer coherent, and the correlation between them is suppressed. This field is called *diffusing wave spectroscopy* [14].

The development of new techniques for cooling atoms using light, in the 1990'th, raised the question of coherent multiple scattering of light in a gas of cold atoms. This is mainly due to the fact that information about the atomic sample is obtained by studying the multiply scattered light. For cold enough atoms, the Doppler effect can be neglected and the coherence length of the light may be on the order of the sample size. Resonant multiple scattering corresponds to photons that are resonant with a given atomic transition. In this case, a large scattering cross section is obtained, which is also very easily tunable. Thus, the experimentalist is able to control the mean free path of the light inside the medium, and to vary it over orders of magnitude just by changing slightly the laser frequency. A major difference of the resonant multiple scattering of light by atoms, relative to classical scatterers, is the interaction between light polarization and the internal degrees of freedom of the scatterers, and in particular the Zeeman degeneracy [2, 15, 16]. The effect of atomic internal degrees of freedom was shown to reduce significantly the coherent backscattering of light [17, 18, 19]. This is because constructive

interference between counter propagating scattering paths, in the presence of an atomic Zeeman degeneracy, occurs only for a certain reciprocity condition for the Zeeman m quantum numbers. Therefore, the backscattering peak is reduced relatively to scatterers that do not possess internal structure, for which constructive interference always occur between counter propagating paths. For light resonant with an atomic transition which involves a non-degenerate ground state, the height of the coherent backscattering peak is found to be about its classical value [20]. This result confirms the prediction, according to which Zeeman degeneracy has an effect on the multiple scattering process. Until now, however, no study has been devoted to the effect of a Zeeman degeneracy on the correlation functions.

In this work we calculate the transmitted intensity correlation of a light beam, multiply scattered in a gas of cold atoms, within the diffusion approximation. We consider two level atoms, with ground and excited states which are generally Zeeman degenerate. Our main results are as follows:

(1) We find that when the atomic ground state is Zeeman degenerate, the transmitted intensity correlation is well enhanced above the classical Rayleigh law. In the case of angular correlation, the enhancement decays for relative angles of the order λ/L, as in the classical case. In the case of temporal correlation, the enhanced correlation holds at very short times, as discussed below. For a non-degenerate atomic ground state we recover the classical results, and in particular the Rayleigh law. The origin of the enhanced correlation is the mixing of spatial disorder, related to the classical position of scatterers, and internal disorder, corresponding to the randomness in the internal states of scatterers. The classical Rayleigh law amounts to the enhancement of the multiply scattered intensity correlation relative, say, to the incoming laser beam. The enhanced correlation above Rayleigh may thus be intuitively explained as a result of the enhanced disorder due to the additional degrees of freedom (Zeeman quantum numbers).

(2) The enhanced correlation is not unique to quantum systems or to multiple scattering processes. It is shown that a similar result is obtained even in the limit of a single scattering, as long as the scatterers have some internal degeneracy. Moreover, the internal degrees of freedom may be of any kind, classical or quantum in nature.

(3) The effect of an external magnetic field on the enhanced correlation

is studied. The magnetic field removes the atomic degeneracy and thus affects the correlation function. In a sense, the magnetic field may be said to reduce the internal disorder, by taking many atomic transitions far from resonance, thus reducing their occurrence. We show that there is a sharp reduction of the enhanced correlation as a function of the magnitude of the external field. The Full Width at Half Maximum (FWHM) of this reduction scales as $l/L \equiv 1/b$, a parameter which is controllable and in principle may be infinitely small. This might be very useful in spectroscopy, since the FWHM is directly related to the resolution of the experiment. In the multiple scattering regime, where $l/L \ll 1$, the FWHM of the resonance-like field dependent correlation curve, is orders of magnitude smaller than the FWHM of the Hanle or Franken effects used in standard level-crossing spectroscopy.

(4) Dephasing mechanisms, such as Doppler shifts, are expected to reduce and limit the enhancement of the intensity correlation. Of these mechanisms we focus on the dynamics of scatterers, which classically leads to an exponential reduction of the correlation as a function of time. We give a criterion for the time period over which the enhanced correlation holds. The decrease of the correlation with time is roughly similar to the classical case, namely exponential, with a decay rate equal to b^2/τ_b. Here τ_b is the typical time for the scatterers to move a distance comparable to λ. This means that as we get more and more into the multiple scattering regime, namely, when we increase b, the time window to observe the enhanced correlation gets shorter and shorter.

This thesis contains two main parts. The first, which includes Chapters 2,3, and 4, provides an introductory survey of the essential theory which is at the basis of our work. Chapter 2 describes the theory of multiple scattering within the diffusion approximation. In Chapter 3 we discuss the correlation function $C^{(1)}$ in the specific case we consider here, namely, the *slab* geometry. Chapter 4 is devoted to the preliminaries of the interaction between light and atoms. The second part of this thesis (Chapters 5 and 6) contains our original contribution. In Chapter 5 we develop and calculate the correlation function of the light for the case of atomic scatterers. In Chapter 6, we study the effect of an applied magnetic field. Also in Chapter 6, we discuss the time dependence of the correlation function due to the dynamics of the scatterers.

.

CHAPTER 2

Multiple scattering of light

In this chapter and in the next one we survey the theory of multiple scattering of light in random media. The present chapter concerns the propagation of intensity, and the next one is devoted to intensity correlation functions. As the rest of this thesis, we assume *weak disorder*. There are two essential consequences of this assumption: first, it allows for a perturbative treatment of the problem and second, it permits the consideration of the individual scattering events as being independent of each other. Thus, we ignore cooperative effects of the scatterers. Moreover, it is assumed that the coherence length of the scattered wave is always larger than the sample size, meaning that we neglect dephasing mechanisms such as Doppler effect. We also assume that there is no absorption in the medium. The medium has, however, a significant effect on the coherence between two *different* wave amplitudes. Also, in Chapters 2 and 3 we do not take into account the possibility that the scatterers have an internal structure, and they are treated as point-like classical objects. Internal degrees of freedom of the scatterers are considered from Chapter 4 on.

This chapter starts with a study of the Green function of the wave equation, including its temporal and spatial dependence. Next we discuss in a general way the intensity propagation. Then, we introduce the *Diffuson* function, which plays a central role in this work. Finally, we consider the diffusive limit and the corresponding diffusion equation for the intensity propagation.

The description given in the present and the next chapters is based mainly on [2].

2.1 Green function of the wave equation

The behavior of electromagnetic fields in a material medium with no charge and current densities is governed by the Maxwell's equations (SI units)

$$\begin{aligned} \nabla \cdot \mathbf{D} &= 0 \\ \nabla \cdot \mathbf{B} &= 0 \\ \nabla \times \mathbf{E} + \frac{\partial \mathbf{B}}{\partial t} &= 0 \\ \nabla \times \mathbf{H} - \frac{\partial \mathbf{D}}{\partial t} &= 0 \end{aligned} \tag{1}$$

where $\mathbf{E}$ is the electric field, $\mathbf{D} = \varepsilon(\mathbf{r})\mathbf{E}$, $\mathbf{H}$ is the magnetic field, and $\mathbf{B} = \mu_0\mathbf{H}$. We assume that the dielectric coefficient of the medium depends weakly on the position, namely $\varepsilon(\mathbf{r}) = \bar{\varepsilon} + \delta\varepsilon(\mathbf{r})$, and differs only slightly from ε_0. We now limit ourselves for simplicity to a scalar wave, and further assume harmonic temporal dependence for the electric field, namely $E = \psi(\mathbf{r})\exp(i\omega t)$. Then, taking the curl of both sides of the third Maxwell's equation, using the identity $\nabla \times (\nabla \times \mathbf{V}) = \nabla(\nabla \cdot \mathbf{V}) - \Delta\mathbf{V}$, and with the help of the first and fourth of the equations (1), leads to the wave equation

$$\left(\Delta + \frac{\omega^2}{c^2}\frac{\delta\varepsilon(\mathbf{r})}{\varepsilon_0} + \frac{\omega^2}{c^2}\frac{\bar{\varepsilon}}{\varepsilon_0}\right)\psi(\mathbf{r}) = 0 \tag{2}$$

where $c^2 = 1/\mu_0\varepsilon_0$ is the speed of light in vacuum. Denoting $\mu(\mathbf{r}) = \delta\varepsilon(\mathbf{r})/\bar{\varepsilon}$, we obtain the Helmholz equation

$$[\Delta + k^2(\mu(\mathbf{r}) + 1)]\psi(\mathbf{r}) = 0 \tag{3}$$

Here k is the light wave number in vacuum, but since we have assumed that ε is very close to ε_0, it can be considered also as the wave number inside the medium.

As is standard in optics, each multiple scattering event is considered as a secondary source. Therefore, one uses the Green function of (3), $G(\mathbf{r}', \mathbf{r})$, which is interpreted as the amplitude of the wave at point $\mathbf{r}$, of a point source that is placed at point $\mathbf{r}'$. This function is defined as

$$[\Delta + k^2(\mu(\mathbf{r}) + 1)]G(\mathbf{r}', \mathbf{r}) = \delta(\mathbf{r}' - \mathbf{r}) \tag{4}$$

To see why the Green function is interpreted as above, we assume for the moment that a charge density $\rho(\mathbf{r})$ is present inside the medium. Equation (3) should then be modified by putting $\rho(\mathbf{r})$ in its *r.h.s* instead of 0. The solution of this source-included wave equation can be expressed as

$$\psi(\mathbf{r}) = \int G(\mathbf{r}', \mathbf{r})\rho(\mathbf{r}')d\mathbf{r}' \tag{5}$$

which is the sum of contributions to the wave amplitude due to all "point sources" in the medium.

We first calculate the free Green function of (3), which satisfies

$$[\Delta + k^2]G_0(\mathbf{r}', \mathbf{r}) = \delta(\mathbf{r}' - \mathbf{r}) \tag{6}$$

since $\mu(\mathbf{r}) = 0$ in this case. For an infinite and isotropic medium, $G_0(\mathbf{r}', \mathbf{r}) = G_0(\mathbf{r}' - \mathbf{r})$. Fourier transforming (6) yields

$$(k^2 - Q^2)G_0(\mathbf{Q}) = 1 \tag{7}$$

where $\mathbf{Q}$ is the Fourier variable of $\mathbf{r}' - \mathbf{r}$ and $Q = |\mathbf{Q}|$. The free Green function is thus written formally, in Fourier space, as

$$G_0(\mathbf{Q}) = \frac{1}{k^2 - Q^2 \pm i0} \tag{8}$$

where $i0$ denotes an infinitesimally small complex value, which is needed in order to prevent divergence of this expression. Transforming back to the real space one finds

$$G_0(\mathbf{R}) = -\frac{1}{4\pi}\frac{e^{\pm ikR}}{R} \tag{9}$$

with $\mathbf{R} = \mathbf{r}' - \mathbf{r}$ and $R = |\mathbf{R}|$. The sign of $i0$ in (8), and thus of the exponent in (9), determines whether it is an *advanced* or a *retarded* Green function, which are complex conjugate of each other. These terms correspond to whether the Green function describes the evolution of the wave towards the positive (retarded) or negative (advanced) direction of time. To see this, we insert in (9) $k = \omega/c$ and write the Fourier transform

$$G_0(\mathbf{R}, t) = -\frac{1}{4\pi R}\int_{-\infty}^{\infty} d\omega e^{i\omega(t \pm R/c)} \tag{10}$$

The sign of the exponent in the integrand therefore determines whether the evolution is toward positive or negative times.

In a material medium, the Green function (8) (or (9)) is modified due to the scattering potential. This potential is, up to a proportionality factor, the fluctuation of the dielectric coefficient of the medium $\mu(\mathbf{r})$. For our purpose, all we need are a few general features of this potential, which are its average and correlation values. We consider a white noise potential, characterized by

$$\begin{aligned} \overline{\mu(\mathbf{r})} &= 0 \\ \overline{\mu(\mathbf{r})\mu(\mathbf{r}')} &= B\delta(\mathbf{r}' - \mathbf{r}) \end{aligned} \tag{11}$$

where all higher order cumulants are zero. Here $\overline{\cdots}$ denotes the *disorder average*, meaning an average over different realizations (configurations) of the

medium. In the present case, these realizations correspond solely to the position of the particles building up the medium (atoms, molecules), assumed to be random. The second condition in (11) means that the potential correlation is short-range, namely that the scattering events are independent, where B characterizes the strength of the potential. The independent scatterings assumption is also related to the weak disorder approximation which is discussed later on. The disordered potential satisfying (11) is a special case of the so called Gaussian disordered potential for which, generally, the correlation in (11) is not a δ-function.

In order to build the Green function of the wave, it is necessary to take into account all the scattering events that might take place. This is formally written as

$$G = G_0 + G_0VG_0 + G_0VG_0VG_0 + \cdots = G_0 + G_0VG \tag{12}$$

where V formally represents a scattering event, and in real space is proportional to $\mu(\mathbf{r})$, so that we may write

$$\begin{aligned} G(\mathbf{r},\mathbf{r}') = G_0(\mathbf{r},\mathbf{r}') + \int d\mathbf{r}_1 G_0(\mathbf{r},\mathbf{r}_1)\mu(\mathbf{r}_1)G_0(\mathbf{r}_1,\mathbf{r}') \\ + \int d\mathbf{r}_1 d\mathbf{r}_2 G_0(\mathbf{r},\mathbf{r}_1)\mu(\mathbf{r}_1)G_0(\mathbf{r}_1,\mathbf{r}_2)\mu(\mathbf{r}_2)G_0(\mathbf{r}_2,\mathbf{r}') + \cdots \end{aligned} \tag{13}$$

When dealing with random disordered media one usually considers the disorder-averaged Green function $\overline{G}$. Using the model (11) leads for the disorder average of (13) to terms containing products of an even number of μ's. For example, the disorder average taken over the third term on the *r.h.s* of (13) gives

$$\overline{G_0(\mathbf{r},\mathbf{r}_1)\mu(\mathbf{r}_1)G_0(\mathbf{r}_1,\mathbf{r}_2)\mu(\mathbf{r}_2)G_0(\mathbf{r}_2,\mathbf{r}')} = BG_0(\mathbf{r},\mathbf{r}_1)G_0(\mathbf{r}_1,\mathbf{r}_2)G_0(\mathbf{r}_2,\mathbf{r}')\delta(\mathbf{r}_1-\mathbf{r}_2) \ . \tag{14}$$

We are left, therefore, with a series written formally as

$$\overline{G} = G_0 + B^2G_0G_0G_0 + B^4G_0G_0G_0G_0G_0 + \cdots \tag{15}$$

where $\overline{G}$ is the disorder averaged Green function. This expansion may be written in a more compact way using the *self energy* Σ, given by the relation

$$\overline{G} = G_0 + G_0\Sigma G_0 + G_0\Sigma G_0\Sigma G_0 + \cdots = G_0 + G_0\Sigma\overline{G} \tag{16}$$

This expression is called the Dyson equation. Σ accounts for all *irreducible* scattering diagrams, namely those that cannot be split into several successive independent scattering events. These processes may include one scatterer, two scatterers, *etc.*, so that Σ is expanded into a perturbation series where the first order corresponds to one scatteter that is involved in the process, the second order to two scatterers, *etc.* It can be shown that the small parameter of this expansion is $1/kl$. Within the weak disorder limit, $kl \gg 1$, it is thus legitimate to take into account only the leading order of the expansion of Σ.

Multiplying both sides of (16) by G_0^{-1} from the left and by $\overline{G}^{-1}$ from the right yields $G_0^{-1} = \overline{G}^{-1} + \Sigma$, meaning that in Fourier space $\overline{G}(\mathbf{Q}) = 1/(k^2 - Q^2 - \Sigma)$ (see (8)), and in real space

$$\overline{G}(\mathbf{R}) = -\frac{1}{4\pi}\frac{e^{iR\sqrt{k^2-\Sigma}}}{R} \simeq -\frac{1}{4\pi}\frac{e^{ikR}}{R}e^{(Im\Sigma/2k)R} \tag{17}$$

where the retarded Green function is considered. Here we have assumed that $\Sigma \ll k^2$ so that $\sqrt{k^2-\Sigma} \simeq k - \Sigma/2k$, and also have ignored the real part of Σ. It should be noted also that actually Σ depends on whether $\overline{G}$ is retarded or advanced, namely, on the sign of the exponent ikR. The imaginary part of Σ thus corresponds to an exponential decrease in the wave amplitude. This decrease is due to the scattering of the wave, which reduces its intensity while transferring it into other partial waves. We expect, thus, that $Im\Sigma$ is related to the characteristic distance (or time) traveled by the wave before it is scattered again.

The first order approximation to the self energy can be calculated to give

$$Im\Sigma_1 = -\frac{k}{l} \tag{18}$$

where l, having dimensions of length, is called the *elastic mean free path* of the wave in the medium, which is the mean distance between two successive scattering events. The first order approximation to the disorder-averaged Green function is therefore, using (17)

$$\overline{G}(\mathbf{R}) = -\frac{1}{4\pi}\frac{e^{ikR}}{R}e^{-R/2l} \tag{19}$$

expressing clearly the meaning of l.

2.2 Intensity propagation

What one usually detects and measures is not the Green function $\overline{G}$, or the amplitude, but rather the intensity of the wave at a certain time and place. In this section we will thus be concerned with the question: what is the intensity of a multiply scattered wave at a point $\mathbf{r}'$, provided it has been emitted by a point source at $\mathbf{r}$. At some given frequency of the wave, or for some frequency component of a wave packet, the quantity

$$P(\mathbf{r}, \mathbf{r}') = \frac{4\pi}{c}\overline{|G(\mathbf{r}, \mathbf{r}')|^2} \tag{20}$$

represents the intensity of the wave. As an example of this definition, consider the case of free propagation. Then, substituting (9) in (20), we find $P_0(\mathbf{r}, \mathbf{r}') = 1/4\pi cR^2$, which is the usual decrease of the intensity, as $1/R^2$, for a free spherical wave.

A first approximation (Drude-Boltzmann) to (20) is obtained by setting

$$P_{DB}(\mathbf{r}, \mathbf{r}') = \frac{4\pi}{c}|\overline{G}(\mathbf{r}, \mathbf{r}')|^2 \tag{21}$$

which from (19) yields

$$P_{DB}(\mathbf{r}, \mathbf{r}') = P_0(\mathbf{r}, \mathbf{r}')e^{-R/l} \tag{22}$$

This approximation describes the propagation of the wave intensity in between successive collisions. In other words, it is the probability that a wave, emitted at the point source $\mathbf{r}$, will not undergo any collisions until it reaches $\mathbf{r}'$. The characteristic exponential decrease $e^{-R/l}$ defines the lifetime l/c, called the *elastic mean free time*, for propagating without any collisions.

To obtain the complete multiple scattering probability, $P(\mathbf{r}, \mathbf{r}')$, we consider the structure of $G(\mathbf{r}, \mathbf{r}')$. It is a sum of all possible multiple scattering trajectories connecting the points $\mathbf{r}$ and $\mathbf{r}'$ (Figure 1), and thus can be written as

$$G(\mathbf{r}, \mathbf{r}') = \sum_i A_i(\mathbf{r}, \mathbf{r}')e^{ikL_i} \tag{23}$$

Here the index i denotes a possible multiple scattering path between $\mathbf{r}$ and $\mathbf{r}'$, A_i is its amplitude and e^{ikL_i} its phase accumulated along the scattering trajectory. In (23) we have ignored the time dependent phase since, as it will

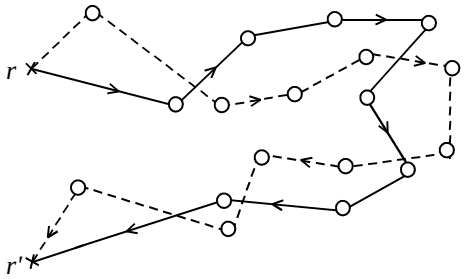

Figure 1: *An example of two possible multiple scattering trajectories between two arbitrary points* $\mathbf{r}$ *and* $\mathbf{r}'$

be seen later, it does not affect the final results. The intensity of the wave is thus

$$P(\mathbf{r},\mathbf{r}') = \frac{4\pi}{c}\sum_{i,j} A_i(\mathbf{r},\mathbf{r}')A_j^*(\mathbf{r},\mathbf{r}')e^{ik(L_i-L_j)} \tag{24}$$

Since every multiple scattering sequence is built up, on average, by "steps" of length l, the characteristic length difference between two distinct sequences i and j is at least of the order l. We therefore obtain a lower limit to the phase difference according to $|k(L_i - L_j)| \sim kl$. At this point the assumption of weak disorder, which is quantitatively written

$$kl \gg 1 \qquad \text{(weak disorder)} \ , \tag{25}$$

becomes significant. It states that the mean distance between successive scattering events is much larger than the light wavelength. It can be shown that the second correction to the self energy, Σ_2, is of the order $1/kl$ relative to the first correction Σ_1. Thus $1/kl \ll 1$ is the "small parameter" in the expansion series of Σ, and its smallness justifies taking into account only the first term Σ_1. A consequence of (25) is that each scattering event takes place in the far field of the previous one. Thus it justifies the consideration of the scattering events as being independent. The strong disorder limit is quantitatively expressed as $kl \sim 1$. In this regime, which is not considered here, the wave becomes localized, meaning that its diffusion coefficient vanishes. In particular, a metal-insulator transition is expected in 3 dimensions (Anderson transition).

The significance of (25) is however revealed when performing a disorder average. To this purpose, we first notice that the length scale over which the phase $e^{ik(L_i-L_j)}$ changes is λ, while for the amplitudes $A_i(\mathbf{r},\mathbf{r}')$ and $A_j(\mathbf{r},\mathbf{r}')$ it

is l. Since from (25) $l \gg \lambda$, and because the typical length difference between two distinct trajectories is at least l, we can finally state that cross terms involving two distinct trajectories in (24), vanish upon disorder averaging because of rapidly fluctuating phases. This is written

$$\overline{A_i(\mathbf{r},\mathbf{r}')A_j^*(\mathbf{r},\mathbf{r}')e^{ik(L_i-L_j)}} = |A_i|^2\delta_{ij} \tag{26}$$

where it is understood that $|A_i|^2$ is a disorder-averaged quantity. Therefore, the average scattered intensity is given by

$$P_d(\mathbf{r},\mathbf{r}') = \frac{4\pi}{c}\sum_i |A_i|^2 \tag{27}$$

In other words, within this approximation, called the *Diffuson* approximation (hence the subscript d), we take into account only the contributions to the intensity, which involve the coupling of two identical multiple scattering spatial trajectories (see Figure 2). When considering the multiple scattering of light, the Diffuson approximation is sometimes referred to as *radiative transfer* [21], while in the study of electronic transport, it is called the *ladder* approximation.

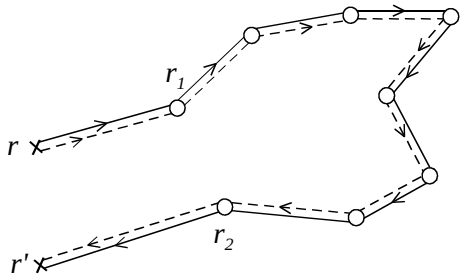

Figure 2: *A typical contribution to the Diffuson. The two multiple scattering amplitudes follow exactly the same trajectories, so that their phases exactly cancel each other.*

Expression (27), although quite intuitive, is not convenient for calculations. This is the reason why it is customary to use a continuous description, within which the scattering potential is no longer treated as being composed of discrete scatterers, but rather it is assumed to be continuous as in (11). This way, we can express the wave intensity within the Diffuson approximation, P_d, as

$$P_d(\mathbf{r},\mathbf{r}') = \frac{4\pi}{c}\int P_{DB}(\mathbf{r},\mathbf{r}_1)\mathcal{D}(\mathbf{r}_1,\mathbf{r}_2)P_{DB}(\mathbf{r}_2,\mathbf{r}')d\mathbf{r}_1 d\mathbf{r}_2 \tag{28}$$

The interpretation of the various terms in (28) is as follows. $P_d(\mathbf{r}, \mathbf{r}')$ is the intensity of a wave at $\mathbf{r}'$, given it was generated by a point source at $\mathbf{r}$, where $\mathbf{r}$ and $\mathbf{r}'$ are any points in the medium. $P_{DB}(\mathbf{r}, \mathbf{r}_1)$ is the intensity of the wave just before its first scattering event at $\mathbf{r}_1$. In other words, $P_{DB}(\mathbf{r}, \mathbf{r}_1)$ describes the first part of the path, between the creation of the wave at $\mathbf{r}$ and the first scattering event. Similarly, $P_{DB}(\mathbf{r}_2, \mathbf{r}')$ describes the last part of the path, between the last scattering event at $\mathbf{r}_2$ and the detection at $\mathbf{r}'$. The function $\mathcal{D}(\mathbf{r}_1, \mathbf{r}_2)$, also called the *Diffuson*, describes the multiple scattering sequence, from the first to the last scattering events. It is given by an iterative equation, which symbolically writes

$$\mathcal{D} = \mathcal{V} + \mathcal{V}\mathcal{W}\mathcal{V} + \cdots = \mathcal{V} + \mathcal{D}\mathcal{W}\mathcal{V} \tag{29}$$

where $\mathcal{V}$ and $\mathcal{W}$ correspond, respectively, to a single scattering event and to the propagation between two successive scattering events. In real space, (29) is written

$$\mathcal{D}(\mathbf{r}_1, \mathbf{r}_2) = \frac{4\pi}{l}\delta(\mathbf{r}_1 - \mathbf{r}_2) + \frac{c}{l}\int \mathcal{D}(\mathbf{r}_1, \mathbf{r}) P_{DB}(\mathbf{r}, \mathbf{r}_2) d\mathbf{r} \tag{30}$$

The first term on the *r.h.s* of (30) corresponds to the possibility that $\mathbf{r}_1 = \mathbf{r}_2$ and only one scattering event takes place, while the second term is the actual iteration. However, it should be remembered that (30) is a very simplified expression, since it does not take into account the polarization of the light and the internal structure of the scatterers. More realistic expressions will be developed in Chapter 5.

By considering the Diffuson approximation we retain only incoherent terms, *i.e.*, contributions to the intensity with no phase difference. There are, however, also coherent contributions to the intensity. These contributions occur when a Diffuson crosses itself and forms a "loop". The loop is built out of two counter-propagating amplitudes, which interfere in a constructive way (*Cooperon*). The probability of this loop to take place is given roughly, for a disordered medium confined in a cube of linear dimension L, as $1/g = \lambda^2/lL$. According to the weak disorder assumption, $l \gg \lambda$, and since in multiple scattering $L \gg l$, we have $g \gg 1$. When taking into account also the Cooperons, the intensity becomes an expansion of an infinite series of terms. Each term corresponds to the number of loops a Diffuson undergoes. Neglecting any loops thus amounts to the zeroth order of the expansion. The higher orders are called *weak disorder corrections* to the intensity propagation, and we do not consider them here.

2.3 The diffusion regime

In the limit of a large enough system, which we consider here, one may take (corresponding to (28) and (30))

$$|\mathbf{r}-\mathbf{r}'|, |\mathbf{r}_1-\mathbf{r}_2| \gg l \ , \tag{31}$$

meaning that we take into account only the multiple scattering sequences composed of a large number of steps of length l, *i.e.*, that includes many scattering events. This neglects short scattering sequences and constitutes the *diffusion approximation* (not the Diffuson approximation), and will be used throughout this thesis. We now show that within the diffusion approximation (or regime) the Diffuson, and also the intensity P_d, satisfy a diffusion equation.

First, we enter the time dependence of (22) by defining $t = R/c$, so that

$$P_{DB}(\mathbf{r},\mathbf{r}',t) = \frac{\delta(R-ct)e^{-t/\tau}}{4\pi R^2} \tag{32}$$

where $\tau = l/c$, with the Fourier transformed function

$$P_{DB}(\mathbf{r},\mathbf{r}',\omega) = \frac{e^{i\omega R/c - R/l}}{4\pi c R^2} \ . \tag{33}$$

In the frequency space, we now expand $\mathcal{D}(\mathbf{r}_1,\mathbf{r},\omega)$ about $\mathbf{r}=\mathbf{r}_2$ up to the second order, which gives

$$\mathcal{D}(\mathbf{r}_1,\mathbf{r},\omega) = \mathcal{D}(\mathbf{r}_1,\mathbf{r}_2,\omega) + (\mathbf{r}-\mathbf{r}_2)\cdot\nabla\mathcal{D}(\mathbf{r}_1,\mathbf{r},\omega)\mid_{\mathbf{r}_2} + \frac{1}{2}[(\mathbf{r}-\mathbf{r}_2)\cdot\nabla]^2\mathcal{D}(\mathbf{r}_1,\mathbf{r},\omega)\mid_{\mathbf{r}_2} \ . \tag{34}$$

Substituting this expansion in (30) we note that the second term on the *r.h.s* vanishes upon integration from symmetry considerations. What is left is

$$\begin{aligned}\mathcal{D}(\mathbf{r}_1,\mathbf{r}_2,\omega) = \frac{4\pi}{l}\delta(\mathbf{r}_1-\mathbf{r}_2) + \frac{c}{l}\mathcal{D}(\mathbf{r}_1,\mathbf{r}_2,\omega)\int P_{DB}(\mathbf{r},\mathbf{r}_2,\omega)d\mathbf{r} \\ + \frac{c}{6l}\Delta_{\mathbf{r}_2}\mathcal{D}(\mathbf{r}_1,\mathbf{r}_2,\omega)\int P_{DB}(\mathbf{r},\mathbf{r}_2,\omega)(\mathbf{r}-\mathbf{r}_2)^2 d\mathbf{r} \ .\end{aligned} \tag{35}$$

The calculation of the two integrals on the *r.h.s* of (35) gives $l/c + i\omega(l/c)^2$ and $2l^3/c$, respectively, so that finally

$$(-i\omega - D\Delta_{\mathbf{r}_2})\mathcal{D}(\mathbf{r}_1,\mathbf{r}_2,\omega) = \frac{4\pi c}{l^2}\delta(\mathbf{r}_1-\mathbf{r}_2) \tag{36}$$

with the diffusion coefficient $D = cl/3$. The Diffuson $\mathcal{D}$ is thus the Green function of the classical diffusion equation.

Later we will need the solution of the diffusion equation (36) in a slab geometry (Figure 3). Therefore, we devote a short discussion to the properties of this equation. We first consider the diffusion problem in an infinite and translation invariant $3d$ space. By Fourier transformations we can go from the $(\mathbf{R}, \omega)$ space to the $(\mathbf{Q}, t)$ space, where $\mathbf{Q}$ is the Fourier variable of $\mathbf{R} = \mathbf{r}_2 - \mathbf{r}_1$, and write (36) as follows

$$(\frac{\partial}{\partial t} + DQ^2)\mathcal{D}(\mathbf{Q}, t) = \frac{4\pi c}{l^2}\delta(t) \tag{37}$$

($Q = |\mathbf{Q}|$), the solution of which is

$$\mathcal{D}(\mathbf{Q}, t) = \frac{4\pi c}{l^2}\theta(t)e^{-DQ^2 t} \ . \tag{38}$$

In real space the equation is

$$(\frac{\partial}{\partial t} - D\Delta)\mathcal{D}(\mathbf{R}, t) = \frac{4\pi c}{l^2}\delta(t)\delta(\mathbf{R}) \ , \tag{39}$$

with the solution (for $t > 0$)

$$\mathcal{D}(\mathbf{R}, t) = \frac{c}{l^2\sqrt{4\pi}(Dt)^{3/2}}e^{-R^2/4Dt} \ . \tag{40}$$

An important feature of free diffusion, is that the mean square distance from the origin of motion is proportional to time, namely

$$\langle R^2(t)\rangle = 6Dt \ . \tag{41}$$

The next step is to impose boundary conditions. In this thesis we consider a slab geometry, namely a medium with sharp boundaries at $z = 0$ and $z = L$, while in the XY plane it is practically infinite. Referring to Figure 3, the diffusion along the Z axis is thus limited due to the slab boundaries. On the other hand, the diffusion in the XY plane is unlimited. Therefore, we separate these two diffusive motions and write the solution of the diffusion equation in this geometry as follows

$$\mathcal{D}(\mathbf{r}, \mathbf{r}', t) = \mathcal{D}(\mathbf{R}_\perp, z, z', t) = \frac{c}{l^2 Dt}e^{-R_\perp^2/4Dt}\mathcal{D}(z, z', t) \tag{42}$$

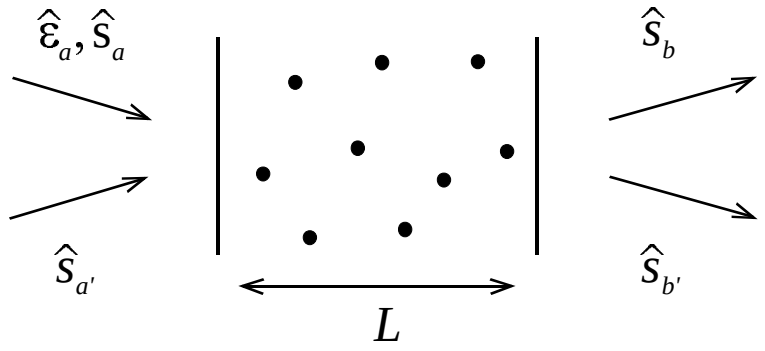

Figure 3: *The slab geometry. The sample is bounded along the Z axis between $z = 0$ and $z = L$, while in the XY plane it is practically unbounded ($\mathbf{s}_{a,a'}$ and $\mathbf{s}_{b,b'}$ denote incoming and outgoing directions of propagation, and $\hat{\varepsilon}_a$ is a polarization vector).*

where (40) for 2 dimensions has been used, $\mathbf{R}_\perp$ is the projection of $\mathbf{R} = \mathbf{r} - \mathbf{r}'$ on the XY plane, and z and z' are the components of $\mathbf{r}$ and $\mathbf{r}'$, respectively, along the Z axis. Note that in this case we no longer have translation invariance, so that $\mathcal{D}(\mathbf{r}, \mathbf{r}', t)$ does not depend on $\mathbf{R}$ only. The function $\mathcal{D}(z, z', t)$ corresponds to the diffusion only along the Z axis, and it remains to be determined. The equation to be solved is thus

$$\left(\frac{\partial}{\partial t} - D\frac{\partial^2}{\partial z'^2}\right)\mathcal{D}(z, z', t) = \frac{4\pi c}{l^2}\delta(t)\delta(z - z') \tag{43}$$

with the boundary conditions $\mathcal{D}(z, 0, t) = \mathcal{D}(z, L, t) = 0$, meaning that the diffusion probability vanishes on the boundaries. This corresponds to the case in which a wave, which impinges on the boundaries, leaves the medium and never returns. As can be easily checked, the solution of (43) is given by

$$\mathcal{D}(z, z', t) = \frac{8\pi c}{l^2 L}\sum_{n>0} e^{-\pi^2 n^2 t/\tau_D}\sin(n\pi\frac{z}{L})\sin(n\pi\frac{z'}{L}) \tag{44}$$

where the *Thouless time*, $\tau_D = L^2/D$, is the characteristic time for a diffusive particle to move from the origin of diffusion a distance comparable to the system size L.

In the next chapters we will need to describe *damped* diffusion in the slab geometry. This damping might generally occur due, *e.g.*, to absorption,

and it will be plugged in using an exponential factor $e^{-\gamma t}$, with γ being the damping rate. For convenience we use the Fourier transform

$$\mathcal{D}(\mathbf{q}, z, z', t) = \int d\mathbf{R}_\perp e^{i\mathbf{q}\cdot R_\perp} \mathcal{D}(\mathbf{R}_\perp, z, z', t) \tag{45}$$

The integral on the *r.h.s* is calculated using (40), and under the assumption that the diffusion along the Z axis and in the XY plane are independent. The result is

$$\mathcal{D}(\mathbf{q}, z, z', t) = \mathcal{D}(z, z', t) e^{-Dq^2 t} \ . \tag{46}$$

Here $\mathbf{q}$ is the Fourier variable of $\mathbf{R}_\perp$, $q = |\mathbf{q}|$. The quantity of interest is the time integral of this function, since it corresponds to the overall probability to diffuse out of the system. Including the damping and using (44), we have

$$\int_0^\infty dt \mathcal{D}(\mathbf{q}, z, z', t) e^{-\gamma t} = \frac{8\pi c}{l^2 L} \sum_{n>0} \sin(n\pi \frac{z}{L}) \sin(n\pi \frac{z'}{L}) \int_0^\infty dt e^{-t(Dq^2 + \frac{\pi^2 n^2}{\tau_D} + \gamma)} \ . \tag{47}$$

For $\gamma > 0$ we obtain

$$\int_0^\infty dt \mathcal{D}(\mathbf{q}, z, z', t) e^{-\gamma t} = \frac{8\pi c}{l^2 L} \sum_{n>0} \frac{\sin(n\pi \frac{z}{L}) \sin(n\pi \frac{z'}{L})}{Dq^2 + \pi^2 n^2 / \tau_D + \gamma} \ . \tag{48}$$

which can be found, using the identities

$$\begin{aligned} \sum_{n=1}^\infty \frac{\cos(nx)}{n^2 + a^2} &= \frac{\pi}{2a} \frac{\cosh[a(\pi - x)]}{\sinh(a\pi)} - \frac{1}{2a^2} \\ \sum_{n=1}^\infty \frac{\cos(nx)}{n^2 - a^2} &= -\frac{\pi}{2a} \frac{\cos[a(\pi - x)]}{\sin(a\pi)} + \frac{1}{2a^2} \ , \end{aligned} \tag{49}$$

to be

$$\mathcal{D}_\gamma(\mathbf{q}, z, z') = \frac{4\pi c}{l^2} \frac{L_\gamma(\mathbf{q})}{D} \frac{\sinh(z_m / L_\gamma(\mathbf{q})) \sinh((L - z_M)/L_\gamma(\mathbf{q}))}{\sinh(L/L_\gamma(\mathbf{q}))} \tag{50}$$

Here, we have used the definitions $L_\gamma(\mathbf{q}) = \sqrt{D/(\gamma + Dq^2)}$, $z_m = min(z, z')$, $z_M = max(z, z')$, and

$$\mathcal{D}_\gamma(\mathbf{q}, z, z') \equiv \int_0^\infty dt \mathcal{D}(\mathbf{q}, z, z', t) e^{-\gamma t} \ . \tag{51}$$

Moreover, since $1/\gamma$ is the characteristic damping time, and using (41), $L_\gamma(0)$ is the characteristic length over which the diffusion process is damped due to γ.

Finally, multiplying $\mathcal{D}$ by the exponential $e^{-\gamma t}$ is equivalent to inserting γ into (37), so that the modified diffusion equation becomes

$$(\gamma + \frac{\partial}{\partial t} + DQ^2)\mathcal{D}(\mathbf{Q}, t) = \frac{4\pi c}{l^2}\delta(t) \tag{52}$$

with the solution

$$\mathcal{D}(\mathbf{Q}, t) = \theta(t)e^{-DQ^2 t - \gamma t} \quad . \tag{53}$$

In the $(\mathbf{Q}, \omega)$ space, this expression is written

$$\mathcal{D}(\mathbf{Q}, \omega) = \frac{4\pi c}{l^2}\frac{1}{-i\omega + \gamma + DQ^2} \quad . \tag{54}$$

For $\gamma = 0$, the solution (54) is known as a diffusion *pole*. Later, we will see that it is closely related to the conservation of energy.

In this chapter we have developed some basic results of the multiple scattering of waves in random media, under the condition of weak disorder and within the diffusion approximation. In the next chapter we apply these concepts to find the intensity correlation of the diffusing wave, still treating it as scalar and assuming classical scatterers (no internal structure).

CHAPTER 3

The classical speckle pattern

The transmitted intensity of a light pulse, multiply scattered in a random medium, form a complex interference pattern. This pattern, called a *speckle* (Figure 4), is the result of a coherent superposition of a large number of sources. Despite its complexity, however, a speckle is essentially similar to the Young interference pattern, since they are both coherent interference pictures. The speckle is a snapshot of the instantaneous position of all scatterers in the medium, *i.e.*, of the specific spatial configuration. As is shown below, when taking the disorder average over these configurations, the transmitted intensity becomes uniform and the speckle pattern disappears.

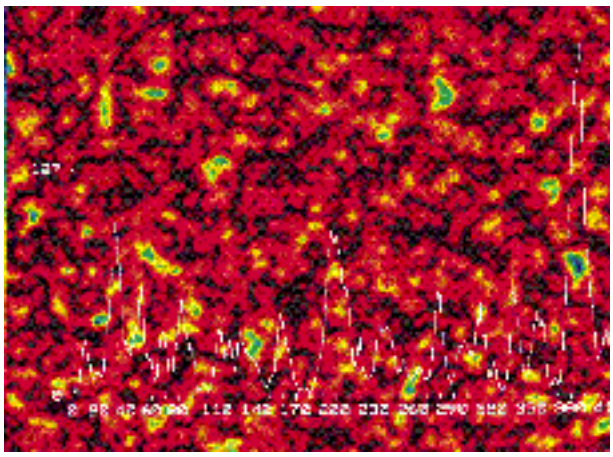

Figure 4: *A speckle pattern.*

The properties of the speckle intensity picture are studied by calculating the disorder average transmitted intensity, and various correlation functions such as the angular and temporal intensity correlation functions. The intensity fluctuations are obtained, for example, as a special case of these correlation functions. In this chapter, we apply the methods developed in the previous one, in order to find the transmitted intensity correlation of a speckle. We assume classical scatterers, namely, without internal degrees of freedom, which are treated as point-like classical objects. As stated earlier, this thesis deals with the intensity correlation of light, induced by *atomic*

scatterers. The method of calculation used for this purpose, as presented in Chapter 5, is based on the classical theory presented in the present and the previous chapters.

This chapter begins with a more detailed definition of a speckle (Section 3.1). Then, the average transmitted intensity is calculated (Section 3.2). In Section 3.3 we study the angular correlation function, while in Section 3.4 we consider the temporal correlation between the intensity transmitted at two different times.

3.1 Definition of a speckle pattern

A light beam incident on a slab of a random medium, is transmitted to the other side through many scattering paths. A "scattering path" is a sequence of scattering events, independent of each other, that the wave *may* undergo between its incidence into the slab, until its emergence out from the other side (Figure 5). These scattering sequences may be composed of any number of scattering events, and they correspond to scattering amplitudes, which one should sum and then square in order to find the transmitted intensity.

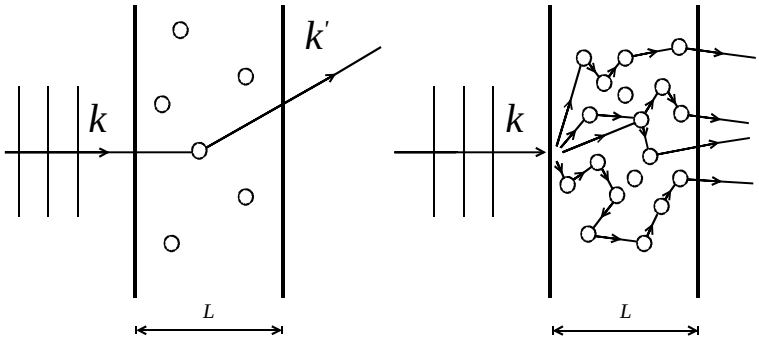

Figure 5: *The transmitted intensity in the slab geometry. A light beam is incident from the left and scattered within the slab. The transmitted intensity emerges to the right of the slab. The single scattering case is shown on the left. In the multiple scattering regime (right), there are many possible scattering trajectories for the transmitted light.*

We are interested in the transmission coefficients $\mathcal{T}_{ab}$. This notation corresponds to the direction of incidence ($\mathbf{s}_a$), and of detection ($\mathbf{s}_b$), as shown in Figure 3, where the two directions, $\mathbf{s}_a$ and $\mathbf{s}_b$, defines the *ab channel*. A

detector placed at $\rho\mathbf{s}_b$ with respect to the slab, where ρ is much larger than the dimensions of the slab, and having angular aperture $d\Omega$, captures an amount $\rho^2 I(\rho, \mathbf{s}_a, \mathbf{s}_b)$ of energy per unit time. Here

$$I(\rho, \mathbf{s}_a, \mathbf{s}_b) = \frac{4\pi}{c}|\mathcal{A}_{ab}(\rho)|^2 \tag{55}$$

is the intensity incoming along $\mathbf{s}_a$ and emerging along $\mathbf{s}_b$, at a distance ρ from the slab. $\mathcal{A}_{ab}(\rho)$ represents the sum of all possible scattering light paths, namely, the total scattering amplitude in transmission. Denoting by I_0 the incoming light intensity, the incoming power is SI_0, with S being the cross section of the slab. The corresponding transmission coefficient, defined as the light power at the detector divided by the incoming power, is thus given by

$$\mathcal{T}_{ab} = \frac{\rho^2 I(\rho, \mathbf{s}_a, \mathbf{s}_b)}{I_0 S} \tag{56}$$

$\mathcal{A}_{ab}(\rho)$ is the sum of all scattering amplitudes having the following structure. At the first stage, the incoming beam is incident along $\mathbf{s}_a$ and traveling inside the medium without being scattered until it reaches some point $\mathbf{r}$, where it undergoes the first scattering event. We denote this amplitude by $\psi_{in}(\mathbf{r})$. Then, at the second stage, a multiple scattering sequence takes place, from $\mathbf{r}$ to some other point $\mathbf{r}'$ inside the medium. This multiple scattering amplitude is given by the Green function $G(\mathbf{r}, \mathbf{r}')$ discussed in the previous chapter. In the last, third stage, the light emerges from point $\mathbf{r}'$ out of the medium, along the direction $\mathbf{s}_b$, which is represented by the amplitude $\psi_{out}(\mathbf{r}', \mathbf{r}_D)$. Here $\mathbf{r}_D = \rho\mathbf{s}_b$ is the detector position relative to the slab. Finally, to obtain the full amplitude $\mathcal{A}_{ab}(\rho)$, we have to sum over all possible endpoints, $\mathbf{r}$ and $\mathbf{r}'$, of the multiple scattering process. Therefore

$$\mathcal{A}_{ab}(\rho) = \int d\mathbf{r} d\mathbf{r}' \psi_{in}(\mathbf{r}) G(\mathbf{r}, \mathbf{r}') \psi_{out}(\mathbf{r}', \mathbf{r}_D) \tag{57}$$

The Green function $G(\mathbf{r}, \mathbf{r}')$ corresponds to the propagation of the wave between $\mathbf{r}$ and $\mathbf{r}'$, and therefore it is a sum of all possible scattering amplitudes between $\mathbf{r}$ and $\mathbf{r}'$ (see (23) in Chapter 2). Following this, we may express $\mathcal{A}_{ab}$ as a sum of amplitudes as

$$\mathcal{A}_{ab} = \sum_i A_i^{\{ab\}} e^{ikL_i} \tag{58}$$

where for convenience the argument ρ has been omitted. $A_i^{\{ab\}} e^{ikL_i}$ is the amplitude of a given multiple scattering trajectory, denoted by i. The sum over i, therefore, amounts to summing over all possible scattering paths. Each such scattering amplitude involves two parts: $A_i^{\{ab\}}$ and the phase e^{ikL_i}. This phase depends on the scatterers position via the trajectory length L_i. kL_i is the spatial phase accumulated along the trajectory i.

3.2 Average transmission coefficient

We now wish to calculate the disorder-averaged transmission coefficient $\overline{\mathcal{T}}_{ab}$. To describe its structure, we consider (55), (56), and (58), from which we obtain

$$\mathcal{T}_{ab} = \frac{4\pi\rho^2}{cI_0S} \sum_{i,j} A_i A_j^* e^{ik(L_i - L_j)} \quad . \tag{59}$$

Disorder averaging we find, as in Section 2.2 above, that all terms containing a non-vanishing phase factor average to zero. This leaves in (59) only contributions with $i = j$ leading to

$$\overline{\mathcal{T}}_{ab} = \frac{4\pi\rho^2}{cI_0S} \sum_{i} |A_i|^2 \tag{60}$$

similar to (27) of Chapter 2. We recall that this approximation, which considers only the incoherent terms $i = j$, corresponds to the Diffuson. Thus, the calculation of $\overline{\mathcal{T}}_{ab}$ is done using the Diffuson and the diffusion approximations introduced in Chapter 2. These approximations allow us to express the transmission coefficient in terms of the Diffuson function $\mathcal{D}$. Using (57), (60), and (28) of Chapter 2, we thus have

$$\overline{\mathcal{T}}_{ab} = \frac{4\pi\rho^2}{cI_0S} \int d\mathbf{r} d\mathbf{r}' |\psi_{in}(\mathbf{r})|^2 \mathcal{D}(\mathbf{r}, \mathbf{r}') |\psi_{out}(\mathbf{r}', \mathbf{r}_D)|^2 \quad . \tag{61}$$

We now wish to find $\psi_{in}(\mathbf{r})$, corresponding to the propagation of the incoming beam from its source to the point $\mathbf{r}$ inside the medium. Assuming that the incoming beam is a plane wave, ψ_{in} involves two parts: one corresponds to the incoming plane wave until it reaches the boundaries of the slab, the other is the decaying amplitude of the wave inside the medium, between the boundary of the slab and the first scattering event. This amplitude

decays, as in (19) of Chapter 2, over the length $2l$. Thus,

$$\psi_{in}(\mathbf{r}) = \sqrt{\frac{cI_0}{4\pi}} e^{-r_s/2l} e^{-ikr_f} \tag{62}$$

where r_f is the distance traveled by the wave in the free space before it impinges on the interface plane, and r_s is the distance from that interface to the location $\mathbf{r}$, of the first scattering event. The pre-factor in (62) ensures that I in (55) has dimensions of an intensity.

Next we consider $\psi_{out}(\mathbf{r}', \mathbf{r}_2)$. Again, this amplitude accounts for the propagation of the beam in two different media. First, a spherical wave that originates from the last scattering event, propagates inside the medium until it reaches the outgoing interface plane. Then, the wave emerges out of the slab along $\mathbf{s}_b$ and propagates in free space. The outgoing beam is therefore a damped spherical wave inside the medium. Using (19) in Chapter 2, $\psi_{out}(\mathbf{r}', \mathbf{r}_D)$ is

$$\psi_{out}(\mathbf{r}', \mathbf{r}_D) = \frac{e^{ik|\mathbf{r}_D - \mathbf{r}'|}}{4\pi|\mathbf{r}_D - \mathbf{r}'|} e^{-r'_s/2l} \tag{63}$$

where r'_s is the distance traveled by this wave inside the medium. Since the detector is assumed to be placed in the far field zone of the outgoing wave, then $|\mathbf{r}_D| \equiv \rho \gg |\mathbf{r}'|$, so that $k|\mathbf{r}_D - \mathbf{r}'| \simeq k\rho - k\mathbf{s}_b \cdot \mathbf{r}'$, and

$$\psi_{out}(\mathbf{r}', \mathbf{r}_D) \simeq e^{-ik\mathbf{s}_b \cdot \mathbf{r}'} \frac{e^{ik\rho}}{4\pi\rho} e^{-r'_s/2l} \quad . \tag{64}$$

We now approximate r_s and r'_s by their projections, z and $L - z'$, on the Z axis, where z and z' are respectively the projections of $\mathbf{r}$ and $\mathbf{r}'$ along Z. This approximation makes sense, provided that the directions along which the beam propagates, before the first and after the last scattering events, do not differ appreciably from the Z-direction. Therefore, using (61),

$$\overline{\mathcal{T}}_{ab} = \frac{1}{(4\pi)^2 S} \int d\mathbf{r} d\mathbf{r}' e^{-z/l} e^{-(L-z')/l} \mathcal{D}(\mathbf{r}, \mathbf{r}') \quad . \tag{65}$$

Since for the slab geometry, the system is translation invariant along the XY plane, the Diffuson $\mathcal{D}(\mathbf{r}, \mathbf{r}')$ depends only on z, z', and of the projection of $\mathbf{R} = \mathbf{r}' - \mathbf{r}$ on the XY plane, denoted by $\mathbf{R}_\perp$. Hence

$$\begin{aligned} \overline{\mathcal{T}}_{ab} &= \frac{1}{(4\pi)^2} \int dz dz' d^2\mathbf{R}_\perp e^{-z/l} e^{-(L-z')/l} \mathcal{D}(\mathbf{R}_\perp, z, z') \\ &= \frac{l^2}{(4\pi)^2} \int_S d^2\mathbf{R}_\perp \mathcal{D}(\mathbf{R}_\perp, l, L-l) \quad . \end{aligned} \tag{66}$$

But the expression on the *r.h.s* of the second equality in (66), is the Fourier transform of $\mathcal{D}(\mathbf{R}_\perp, l, L-l)$, taken for $\mathbf{q}=0$ where $\mathbf{q}$ is the Fourier variable of $\mathbf{R}_\perp$. Thus,

$$\overline{\mathcal{T}}_{ab} = \frac{l^2}{(4\pi)^2}\mathcal{D}(\mathbf{q}=0, l, L-l) \ . \tag{67}$$

The expression for $\mathcal{D}_\gamma(\mathbf{q}, z, z')$ has been given in (50) of Chapter 2. To find $\mathcal{D}(\mathbf{q}=0, l, L-l)$ we take $\gamma, \mathbf{q} \to 0$. Moreover, for $L \gg l$, we identify $z_m = l$ and $z_M = L-l$, so that

$$\mathcal{D}(\mathbf{q}=0, l, L-l) = \frac{4\pi c}{DL} \ . \tag{68}$$

Finally, since $D = cl/3$, we obtain

$$\overline{\mathcal{T}}_{ab} = \frac{3}{4\pi}\frac{l}{L} \ . \tag{69}$$

$\overline{\mathcal{T}}_{ab}$ is thus proportional to l/L. The inverse ratio L/l is called the *optical depth* and is usually denoted by b. In systems where the diffusion approximation holds, and the scatterers are structureless, b is the only parameter needed to determine the average transmitted intensity.

From (69) it is also clear that the average transmission coefficient is independent of the angles of incidence and emergence, namely, of the specific channel. However, this is valid only within the approximation we have used earlier, namely for $\mathbf{s}_a$ and $\mathbf{s}_b$ that differ only slightly from the Z-direction. Within this small angle approximation, the average transmitted intensity loses track of the direction of the incident beam. As we shall see later in this chapter, however, there is a disorder-averaged quantity, namely, the first order intensity correlation function, that "remembers" the direction of incidence.

3.3 Angular correlation of the transmitted intensity

The definition of the normalized angular intensity correlation function is

$$C_{aba'b'} = \frac{Corr(aba'b')}{\overline{\mathcal{T}}_{ab}\overline{\mathcal{T}}_{a'b'}} \tag{70}$$

with the correlation term given by

$$Corr(aba'b') = \overline{\mathcal{T}_{ab}\mathcal{T}_{a'b'}} - \overline{\mathcal{T}}_{ab}\overline{\mathcal{T}}_{a'b'} \ . \tag{71}$$

In the following, we will refer to $C_{aba'b'}$ as the angular correlation, or just the correlation. Combining (70) and (71), the angular correlation function is written as

$$C_{aba'b'} = \frac{\overline{\mathcal{T}_{ab}\mathcal{T}_{a'b'}}}{\overline{\mathcal{T}}_{ab}\overline{\mathcal{T}}_{a'b'}} - 1 \tag{72}$$

Since we have already calculated $\overline{\mathcal{T}}_{ab}$ and $\overline{\mathcal{T}}_{a'b'}$, we need now to calculate $\overline{\mathcal{T}_{ab}\mathcal{T}_{a'b'}}$. To this purpose we multiply first the non-averaged quantities $\mathcal{T}_{ab}$ and $\mathcal{T}_{a'b'}$. From (59), and using the notation

$$\mathcal{C}_i \equiv \sqrt{\frac{4\pi\rho^2}{cI_0S}} A_i e^{ikL_i} \tag{73}$$

we obtain

$$\mathcal{T}_{ab} = \sum_{i,j} \mathcal{C}_i \mathcal{C}_j^* \quad , \quad \mathcal{T}_{a'b'} = \sum_{k,l} \mathcal{C}'_k \mathcal{C}'^*_l \tag{74}$$

so that

$$\mathcal{T}_{ab}\mathcal{T}_{a'b'} = \sum_{i,j,k,l} \mathcal{C}_i \mathcal{C}_j^* \mathcal{C}'_k \mathcal{C}'^*_l \ . \tag{75}$$

$\mathcal{T}_{ab}\mathcal{T}_{a'b'}$ is thus the sum of all combinations coupling two amplitudes of the ab channel and two of the $a'b'$ channel. Figure 6 shows a typical term of the sum (75). In the figure, two amplitudes ($\mathcal{C}_1$ and $\mathcal{C}_2$) that belong to the ab channel, are coupled to two amplitudes ($\mathcal{C}_3$ and $\mathcal{C}_4$) of the $a'b'$ channel. These four amplitudes have no further restrictions so far.

We now use the more explicit form of the amplitudes and have

$$\mathcal{T}_{ab}\mathcal{T}_{a'b'} = \frac{4\pi\rho^2}{cI_0S} \sum_{i,j,k,l} A_i A_j^* A'_k A'^*_l e^{ik(L_i - L_j + L_k - L_l)} \ . \tag{76}$$

Upon disorder-averaging, all terms in (76) containing non-vanishing phase factors average to zero, as explained previously. This leaves two kinds of terms contributing to $\overline{\mathcal{T}_{ab}\mathcal{T}_{a'b'}}$, that survive the disorder averaging. The first kind couples amplitudes of the *same* channel to cancel the phase factors in (76), namely, $i = j$ and $k = l$ (Figure 7(a)). This possibility of amplitudes coupling includes, therefore, the set of all terms like $|\mathcal{C}_i|^2|\mathcal{C}'_k|^2$. But from (60), this is just the product of the two averaged transmission coefficients. Written in terms of the amplitudes $\mathcal{C}$ we thus have

$$\overline{\mathcal{T}}_{ab}\overline{\mathcal{T}}_{a'b'} = \sum_{i,k} |\mathcal{C}_i|^2 |\mathcal{C}'_k|^2 \ . \tag{77}$$

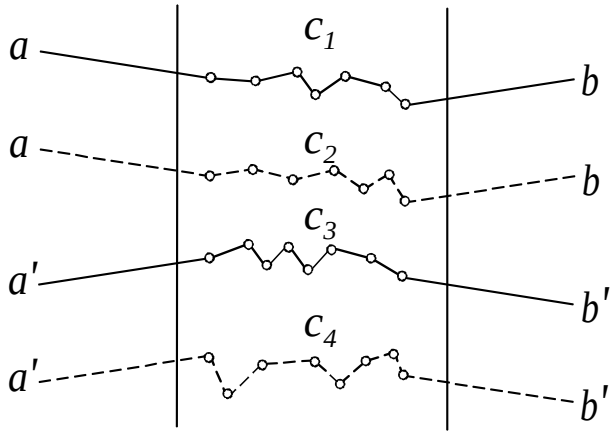

Figure 6: *A typical contribution to $\mathcal{T}_{ab}\mathcal{T}_{a'b'}$. The figure shows two arbitrary amplitudes of the ab channel, coupled to two arbitrary amplitudes of the $a'b'$ channel. The solid and dashed lines correspond, respectively, to direct and conjugate amplitudes.*

The other possibility of amplitudes coupling, that survives the disorder average in (76), is $i = l$ and $j = k$, which also sets the phase difference to 0. From (77) and the definition (71) it thus follows that,

$$Corr(aba'b') = \sum_{i,k} (\mathcal{C}_i \mathcal{C}_i'^*)(\mathcal{C}_k^* \mathcal{C}_k') \ . \tag{78}$$

The contributions to the correlation function are therefore products of pairs of amplitudes, where one of them belongs to one channel and the other belongs to the second channel, coupled in such a way that the total phase of each pair is zero. This coupling scheme is shown in Figure 7(b). The figure shows also that the contribution denoted symbolically as, *e.g.*, $\mathcal{C}_i \mathcal{C}_i'^*$, consists of three parts: (i) before the first scattering event, (ii) between the first and the last scattering events, and (iii) after the last scattering event. In parts (i) and (iii), one can distinguish between amplitudes belonging to two different channels, since they propagate along different directions. In part (ii), on the other hand, if the scatterers are classical one cannot tell which amplitude belongs to which channel. The mathematical description of part (ii) of the propagation path is, therefore, the same as for the intensity $\overline{\mathcal{T}}$, but where the two amplitudes belong to different channels. It corresponds to the propagation between the first and the last scattering events, and is

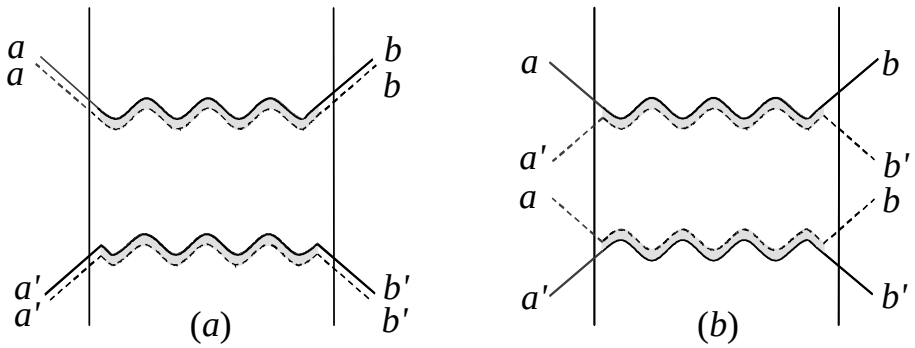

Figure 7: *(a) A typical contribution to* $\overline{\mathcal{T}}_{ab}\overline{\mathcal{T}}_{a'b'}$*. Two amplitudes of the ab channel are coupled together, as well as two amplitudes of the* $a'b'$ *channel. (b) A typical contribution to the correlation function* $\overline{\mathcal{T}_{ab}\mathcal{T}_{a'b'}} - \overline{\mathcal{T}}_{ab}\overline{\mathcal{T}}_{a'b'}$*. The coupling scheme involves one amplitude of the ab channel with one of the* $a'b'$ *channel.*

represented by the Diffuson. For the correlation we are thus allowed to use the same Diffuson function built for the average intensity in the previous section. We emphasize, that when the scatterers have internal degrees of freedom interacting with light (*e.g.* atoms), the two amplitudes are generally *distinguishable* even in part (ii), where the directions of incidence and emergence are irrelevant. This is because light, when interacting with the scatterers, changes their internal state. Therefore, two amplitudes belonging to different channels experience generally different internal states of scatterers, even if they correspond to the same scattering path. This point is crucial when atomic scatterers will be discussed in Chapter 5.

We now write (78) as

$$Corr(aba'b') = \left(\sum_i \mathcal{C}_i \mathcal{C}_i'^* \right)^2 \tag{79}$$

which states that this function may be expressed as the square of a term, similar in form to the average transmission coefficient, which is defined as

$$\overline{\mathcal{T}}^{(c)}_{aba'b'} = \sum_i \mathcal{C}_i \mathcal{C}_i'^* \tag{80}$$

where the superscript c denotes the fact, that it is related to the correlation and not to the usual intensity. $\overline{\mathcal{T}}^{(c)}_{aba'b'}$ is almost formally identical to $\overline{\mathcal{T}}_{ab}$ or

$\overline{\overline{\mathcal{T}}}_{a'b'}$, except that it should contain an additional phase factor due to the fact that a and a', as well as b and b', correspond to generally different directions. Since we have assumed the incoming beam to be a plane wave, and using the form (64), this phase factor is $\exp[ik(\mathbf{a}\cdot\mathbf{r}-\mathbf{b}\cdot\mathbf{r}')]$, where $\mathbf{a}$ ($\mathbf{b}$) is defined as the vector difference $\mathbf{s}_a-\mathbf{s}_{a'}$ ($\mathbf{s}_b-\mathbf{s}_{b'}$). Apart from this phase, $\overline{\overline{\mathcal{T}}}^{(c)}_{aba'b'}$ is described similarly to $\overline{\overline{\mathcal{T}}}_{ab}$ and $\overline{\overline{\mathcal{T}}}_{a'b'}$. Thus, following (65)

$$Corr(aba'b') = \left(\frac{1}{(4\pi)^2 S}\int d\mathbf{r}d\mathbf{r}' e^{ik(\mathbf{a}\cdot\mathbf{r}-\mathbf{b}\cdot\mathbf{r}')}e^{-z/l}e^{-(L-z')/l}\mathcal{D}(\mathbf{r},\mathbf{r}')\right)^2 \quad . \quad (81)$$

As for the average transmission, because of the translation invariance in the XY plane, $\mathcal{D}(\mathbf{r},\mathbf{r}')$ depends actually only on $\mathbf{R}_\perp$, z, and z'. Integrating over z and z' yields (see (66))

$$Corr(aba'b') = \left(\frac{l^2}{(4\pi)^2}\delta_{\mathbf{a},\mathbf{b}}\int_S d\mathbf{R}_\perp e^{ik\mathbf{R}_\perp\cdot\mathbf{a}}\mathcal{D}(\mathbf{R}_\perp,l,L-l)\right)^2 \quad (82)$$

or

$$Corr(aba'b') = \left(\frac{l^2}{(4\pi)^2}\delta_{\mathbf{a},\mathbf{b}}\mathcal{D}(\mathbf{q},l,L-l)\right)^2 \quad (83)$$

where the Fourier variable $\mathbf{q}$ is equal to $k\mathbf{a}$. From (50) of Chapter 2 we have ($\gamma=0, q=|\mathbf{q}|$)

$$\mathcal{D}(\mathbf{q},l,L-l) = \frac{4\pi c}{Dl^2}\frac{\sinh^2(ql)}{q\sinh(qL)} \quad . \quad (84)$$

As before, we assume that the angles of incidence and emergence of the beams do not differ appreciably from the Z axis. Quantitatively we set $ql \ll 1$, leading to

$$\mathcal{D}(\mathbf{q},l,L-l) = \frac{4\pi c}{D}\frac{q}{\sinh(qL)} \qquad (ql \ll 1) \quad (85)$$

from which

$$Corr(aba'b') = \delta_{\mathbf{a},\mathbf{b}}\left(\frac{3}{4\pi}\frac{ql}{\sinh(qL)}\right)^2 \quad (86)$$

Finally, using (69) and the definition (70) we obtain

$$C_{aba'b'} = \delta_{\mathbf{a},\mathbf{b}}\left(\frac{qL}{\sinh(qL)}\right)^2 \quad (87)$$

We have thus found the transmitted intensity correlation function of a speckle. It is seen from the δ-function on the *r.h.s* of (87), that the correlation is nonzero only when the relative angle of incidence is equal to the relative angle of emergence. This is the *memory effect* [22], and it means that the outgoing beams "remember" the incoming beams directions, even though each of them underwent many scattering events. Consequently, if one keeps fixed the direction of incidence of one beam (say of the ab channel), while altering slowly the direction of incidence corresponding to the other channel, the speckle pattern of the transmitted light will be also changed accordingly.

For $q = 0$, that is for $\mathbf{s}_a = \mathbf{s}_{a'}$ and $\mathbf{s}_b = \mathbf{s}_{b'}$, we obtain the transmitted intensity *fluctuation*

$$C_{abab} = 1 \tag{88}$$

or, with the help of (72),

$$\overline{\mathcal{T}_{ab}^2} = 2\overline{\mathcal{T}}_{ab}^2 \tag{89}$$

The result (89) (or (88)) is the *Rayleigh law* fluctuation. It states that the root mean square fluctuation is of the same order as the average transmitted intensity.

As discussed previously, the correlation function $C_{aba'b'}$ calculated above is actually only the zeroth order of a perturbation series. The next orders correspond to the number of times the two Diffusons are allowed to cross each other. In the literature, the above correlation function is often denoted by $C^{(1)}$. The correlation function that takes into account up to one crossing is denoted by $C^{(2)}$, up to two crossings by $C^{(3)}$, *etc.* When one is interested only in the correlation between single channels, as for $C_{aba'b'}$, the zeroth order dominates and the contributions of $C^{(2)}$, $C^{(3)}$ *etc.* are negligible.

3.4 Temporal correlation of the transmitted intensity

The temporal intensity correlation of the transmitted intensity, is defined and calculated in complete analogy with the angular correlation. Instead of (70) we now have the definition

$$C(T) = \frac{Corr(T)}{\overline{\mathcal{T}}(t)\overline{\mathcal{T}}(t+T)} \tag{90}$$

with

$$Corr(T) = \overline{\mathcal{T}(t)\mathcal{T}(t+T)} - \overline{\mathcal{T}}(t)\overline{\mathcal{T}}(t+T) \tag{91}$$

where $\overline{\cdots}$ denotes an average over the initial time t. In (90), the transmission coefficients at two different times, t and $t+T$, are playing the role of the two different channels, ab and $a'b'$, in the angular correlation function. Due to the ergodic theorem, which is assumed to be applicable here, we can replace the average over the time t by a disorder average. It will moreover be assumed that the average transmitted intensity does not depend on time. Therefore, (90) becomes

$$C(T) = \frac{\overline{\mathcal{T}(0)\mathcal{T}(T)}}{\overline{\mathcal{T}}^2} - 1 \tag{92}$$

since $Corr(T) = \overline{\mathcal{T}(0)\mathcal{T}(T)} - \overline{\mathcal{T}}^2$. Here $\overline{\mathcal{T}}$ is the average transmitted intensity at any time. In the literature, one uses also the *degree of second order coherence*, $g^{(2)}(T)$, which is defined as

$$g^{(2)}(T) \equiv \frac{\overline{\mathcal{T}(0)\mathcal{T}(T)}}{\overline{\mathcal{T}}^2} = C(T) + 1 \tag{93}$$

The value $g^{(2)}(T \to 0)$ (and thus of $C(T \to 0)$) is the fluctuation of the light intensity at a certain observation point. In the case of angular correlation, this is analogous to setting $a = a'$ and $b = b'$, which will be discussed extensively later in this work.

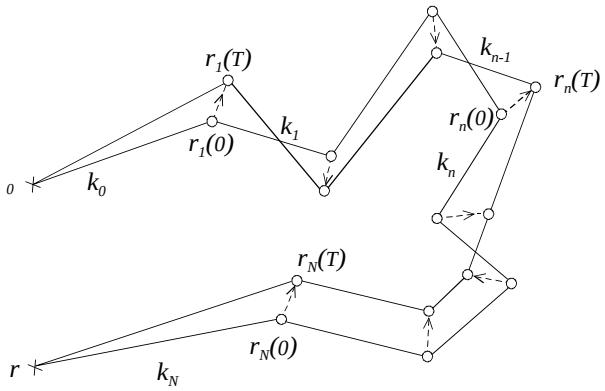

Figure 8: *Dephasing due to the motion of scatterers. Between* $t = 0$ *and* $t = T$ *the scatterers move randomly, and move from* $\mathbf{r}_i(0)$ *to* $\mathbf{r}_i(T)$*. The amplitudes at* $t = 0$ *and at* $t = T$*, although corresponding to the same scatterers, have a random phase difference between them.*

When the multiply scattered light can be treated within the diffusion approximation, the temporal correlation function can be a direct measure of

the motion of the scatterers, a method known as diffusing wave spectroscopy [14]. To understand why it is so, we first note that, as in (78)

$$Corr(T) = \sum_{i,k} \left(\mathcal{C}_i(0)\mathcal{C}_i(T)^*\right)\left(\mathcal{C}_k(0)^*\mathcal{C}_k(T)\right) \tag{94}$$

where the amplitudes $\mathcal{C}_i$ are defined in (73). In other words, the contributions to the temporal correlation are made of pairs of coupled amplitudes, each belongs to a different time (0 or T). These contributions are maximal when the phase difference between pairs like $\mathcal{C}_i(0)\mathcal{C}_i(T)$ is zero (constructive interference). But, when the motion of scatterers is taken into account, and if T is larger than 0, a *random* phase difference occurs between two such coupled amplitudes (see Figure 8), because the motion of the scatterers is random. It is a source of dephasing, namely a randomization of the phase difference between amplitudes like $\mathcal{C}_i(0)$ and $\mathcal{C}_i(T)$. When this random phase difference becomes comparable to π, the products $\mathcal{C}_i(0)\mathcal{C}_i(T)$ vanish upon disorder average. The rate of decrease of $C(T)$ depends, therefore, on the following factors: first, the mean free path of the light inside the medium, l, and the size of the slab, L, both determine the order of magnitude of the number of scattering events the light undergoes; and second, the time scale τ_b, over which the scatterers move from their original position a distance comparable to the light wavelength $\lambda = 2\pi/k$. Assuming that the motion of scatterers is Brownian, with a diffusion coefficient D_b, this time scale can be evaluated using the relation (see (41) of Chapter 2) $\lambda^2 \sim 6D_b\tau_b$, leading to $\tau_b \sim 1/D_bk^2$. A more careful calculation, however, gives the value

$$\tau_b = \frac{1}{4D_bk^2} \tag{95}$$

In experiments such as [11, 23], where the scatterers were classical submicron spheres in suspensions, τ_b was of the order of $10^{-3}s$, much longer than the typical time for a multiple scattering path (about $10^{-11}s$).

The temporal correlation is calculated in exactly the same manner as the angular correlation, the only difference between them is the fact that one labels the two "channels" by 0 and T instead of ab and $a'b'$. The result is

$$C(T) = \left(\frac{L/L_\gamma(T)}{\sinh(L/L_\gamma(T))}\right)^2 \tag{96}$$

with

$$L_\gamma(T) = \sqrt{\frac{2Dl\tau_b}{cT}} \tag{97}$$

Taking the limit $T \to 0$ we obtain for the intensity fluctuation, again, the Rayleigh law

$$C(0) = 1 \tag{98}$$

In terms of the degree of second order coherence, the Rayleigh law is given by

$$g^{(2)}(0) = 2 \ . \tag{99}$$

Note that the incoming beam is assumed to be a plane wave, for which it is well known [24] that $g^{(2)}(0) = 1$. The transmission through the disordered medium thus increases the fluctuations of the light. In terms of photon statistics, if the incoming plane wave was to fall onto a detector before passing through the random medium, the photons would be counted randomly, with no correlation between two photon counts. This is a property of a coherent plane wave when described quantum mechanically. On the other hand, after being transmitted through the random medium, the fact that $g^{(2)}(0) > 1$ indicates that the photons are *bunched*. This means that there is a positive correlation among photon arrivals: counting a photon increases the probability to count another photon immediately afterwards. The photon bunching, or more explicitly the fluctuation value $g^{(2)}(0) = 2$, is a characteristic of the so-called *chaotic* light, an example of which is the light coming from the sun. The fact that the disorder of the scattering medium increases the transmitted light fluctuations was experimentally observed (*i.e.* [11]). It raises the following question: if we somehow increase the disorder, will the fluctuations be enhanced? As we shall see, if one adds additional random degrees of freedom to the system, *e.g.* if the scatterers possess internal structure, the transmitted intensity fluctuations indeed become larger than the Rayleigh law.

Finally, in the definition (90) it was assumed that the light at all times corresponds to one channel, *i.e.*, to certain directions of incidence and emergence that do not change with time. Rather, one may define a combined version of the angular and temporal correlation functions, allowing for the light at $t = 0$ and at $t = T$ to belong to different channels, namely

$$C_{aba'b'}(T) = \frac{\overline{\mathcal{T}_{ab}(0)\mathcal{T}_{a'b'}(T)}}{\overline{\mathcal{T}}_{ab}(0)\overline{\mathcal{T}}_{a'b'}(T)} - 1 \ . \tag{100}$$

This is the correlation between two different channels at two different times. Again, the calculation is formally identical to that presented in Section 3.3,

and gives

$$C_{aba'b'}(T) = \delta_{\mathbf{a},\mathbf{b}} \left(\frac{L/\mathcal{L}}{\sinh(L/\mathcal{L})} \right)^2 \tag{101}$$

with $\mathcal{L}^{-1} = \sqrt{q^2 + 1/L_\gamma^2}$ and q, $\mathbf{a}$, and $\mathbf{b}$ defined as in Section 3.3. This result is indeed a combination of (87) and (96).

In this chapter we have obtained the angular and temporal correlation functions for the case of classical scatterers, which will be referred to as the *classical case*. We have seen that both correlation functions have a maximal value (for $q = 0$ and for $T = 0$) which corresponds to the Rayleigh law. This result is due to the existence of certain cross terms that contribute to the correlation, but not to the average intensity. In the following we show, that for scatterers with internal degrees of freedom, there are much more such cross terms, and the correlation is enhanced relative to the classical case.

.

CHAPTER 4

Scattering of photons by atoms

The purpose of this chapter is to survey some characteristics of the scattering of photons by atoms. This is a wide field, and we do not present here a comprehensive description. Rather, we describe only the essential theory and results, needed for later purposes.

We begin by discussing the Hamiltonian describing the interaction between light and matter. Then, in Section 4.2, a general quantum mechanical expression for the scattering cross section of light by atoms is given. In Section 4.3, the important case of resonant scattering is addressed, and in Section 4.4 the Wigner-Eckart theorem is discussed. Finally, in Section 4.5 we dwell on the question of "which path" information.

4.1 The Hamiltonian

The Hamiltonian of a spinless particle of charge e and mass μ, interacting with an electromagnetic field, is given by [25]

$$H = \frac{1}{2\mu}(\mathbf{P} - e\mathbf{A})^2 + e\phi + \Phi \tag{102}$$

where $\mathbf{P}$ is the quantum mechanical operator of the particle momentum, $\mathbf{A}$ and ϕ are, respectively, the vector and scalar potentials of the electromagnetic field, and Φ is any other potential to which the particle is subjected. These quantities generally depend on time and position which, for convenience, are not explicitly shown. Because of the gauge invariance of the field, one can always choose the vector potential such that [26]

$$\nabla \cdot \mathbf{A} = 0 \tag{103}$$

When this property is satisfied, the field is said to be in the Coulomb gauge. It can be easily shown [27] that within the Coulomb gauge, $\mathbf{P}$ and $\mathbf{A}$ commute, namely

$$[\mathbf{P}, \mathbf{A}] = 0 \qquad \text{(Coulomb gauge)} \tag{104}$$

which makes it possible to write the Hamiltonian as

$$H = \frac{1}{2\mu}\mathbf{P}^2 + \frac{e}{\mu}\mathbf{P} \cdot \mathbf{A} + \frac{e^2}{2\mu}\mathbf{A}^2 + e\phi + \Phi \equiv H_0 + V \tag{105}$$

Here the unperturbed Hamiltonian is $H_0 = \mathbf{P}^2/2m + \Phi$, and $V = \frac{e}{\mu}\mathbf{P}\cdot\mathbf{A} + \frac{e^2}{2\mu}\mathbf{A}^2$ is the interaction term.

Another important property of the Coulomb gauge [24], is that the vector potential is solely responsible for the transverse fields, which correspond to the electromagnetic waves. In the Coulomb gauge, the scalar potential describes only the electrostatic part of the fields, and thus does not contribute to the radiation of electromagnetic energy. Since we are interested in the interaction of the particle with the electromagnetic radiation, and not with the electric charges that create it, it can be assumed that the particle described by the Hamiltonian (105) is far enough from these charges, so that the term $e\phi$ is negligible. Moreover, in the limit of weak electromagnetic field, it is legitimate to retain only the first order term in the vector potential, and thus the interaction Hamiltonian between the particle and the field, V, is reduced to

$$V = \frac{e}{\mu}\mathbf{P}\cdot\mathbf{A} \ . \tag{106}$$

In the interaction process of light with atoms, the particle (atomic electron) is bound to some region of space of dimension comparable to the Bohr radius $a_0 = \hbar/me^2 \simeq 0.5\times 10^{-10}m$. In the *long wavelength approximation*, one assumes that the wavelength λ of the electromagnetic wave is much larger than a_0. This is the case, for example, for visible light where $\lambda/a_0 \sim 10^3$. Within this approximation, one can neglect the spatial variation of the field felt by the atomic electron, and consider it as being spatially uniform but still time dependent. Under these conditions, one can transform the interaction Hamiltonian (106) into the equivalent form

$$V = -\mathbf{d}\cdot\mathbf{E} \qquad \text{(long wavelength)} \ . \tag{107}$$

Here $\mathbf{E} = -\partial\mathbf{A}/\partial t$ is the electric field of the radiation, and $\mathbf{d} = e\mathbf{r}$ is the electric dipole operator of the atomic electron ($\mathbf{r}$ is its position). The equivalence of (106) and (107), within the long wavelength approximation, is shown [27] using the unitary transformation $T = e^{-(i/\hbar)(\mathbf{d}\cdot\mathbf{A}_\perp(0))}$, where and $\mathbf{A}_\perp$ is the transverse part of the vector potential $\mathbf{A}$.

The total Hamiltonian becomes

$$H = H_0 - \mathbf{d}\cdot\mathbf{E} \tag{108}$$

This Hamiltonian, sometimes called the *electric dipole* Hamiltonian, is useful in many cases where light and atoms interact. It is noted that to this

approximation, the magnetic field corresponding to the radiation does not appear. This is the reason for the neglect of the electron spin.

4.2 The quantum mechanical description of light scattering

When the electromagnetic field is quantized, the electric field operator is given by [28]

$$\mathbf{E}(\mathbf{r},t)=\sum_j i\sqrt{\frac{\hbar\omega_j}{2\varepsilon_0 L^3}}\left(a_j\mathbf{e}_j e^{i(\mathbf{k}_j\cdot\mathbf{r}-\omega_j t)}-a_j^\dagger\mathbf{e}_j^* e^{-i(\mathbf{k}_j\cdot\mathbf{r}-\omega_j t)}\right)\ . \tag{109}$$

Here j denotes an eigenmode of the quantized field, a_j and $a_j^\dagger$ are, respectively, the destruction and creation operators of the mode j, $\mathbf{e}_j$ is the unit polarization vector of the mode j, $\mathbf{k}_j$ is its wave vector, and L^3 is the quantization volume. The quantization of the electromagnetic field appears in (109) through the operators a_j and $a_j^\dagger$ which, when operate on a number state of the field, destroys and creates, respectively, one photon of the corresponding mode j.

The scattering of a photon in the mode i by an atom, is described as a transition from some initial state of the system "atom+photons"

$$|I\rangle=|1,n_i=1,0\rangle \tag{110}$$

to some final state

$$|F\rangle=|2,n_s=1,0\rangle\ . \tag{111}$$

This notation expresses that in the state $|I\rangle$, the atom is in its level $|1\rangle$, while the radiation field contains one photon in mode i, and zero photons in any other mode. In the state $|F\rangle$, the atom has moved to the level $|2\rangle$ as a result of the interaction with the radiation, the initial photon of the mode i has disappeared, and a new scattered photon, of some mode s, has appeared. The scattering is therefore said to be a two-photon process. This transition is caused by the interaction (107). Energy conservation imposes the constraint

$$E_I\equiv E_1+\hbar\omega_i=E_2+\hbar\omega_s\equiv E_F \tag{112}$$

where E_1 and E_2 are, respectively, the energy of the atom in levels $|1\rangle$ and $|2\rangle$.

We are interested in the transition amplitude between $|I\rangle$ and $|F\rangle$. From (107) and (109) we see, however, that to first order in the interaction V one obtains

$$T_1 \equiv \langle F|V|I\rangle = 0 \ . \tag{113}$$

This result is due to the fact, that the transition $|I\rangle \to |F\rangle$ involves one photon that is destroyed, and another one which is created. Mathematically, we thus need the combination $a_s^\dagger a_i$ to appear in between the ket $|I\rangle$ and the bra $\langle F|$, in order to make the transition amplitude nonzero. However, this combination of creation and destruction operators is not possible to first order in V, hence (113).

In order to describe a scattering process to the lowest order in V, we therefore have to consider the second order, for which the transition amplitude is given by [27]

$$T_2 \equiv \sum_M \frac{\langle F|V|M\rangle\langle M|V|I\rangle}{E_I - E_M} \tag{114}$$

where $|M\rangle$ accounts for any state in the relevant space of the "atom+radiation" system, $E_I = E_1 + \hbar\omega_i$, and E_M is the energy of the state $|M\rangle$. Concerning the photons, two kinds of intermediate states are possible, for which $\langle F|V|M\rangle\langle M|V|I\rangle$ is nonzero: one is $|M\rangle \equiv |m, 0, 0\rangle$, the second one is $|M'\rangle \equiv |m', 1, 1\rangle$. The first possibility corresponds to an initially absorbed photon of the mode i, inducing an atomic transition to the state $|m\rangle$, and then emission of a scattered photon of the mode s. The second possibility describes the emission of a photon of the mode s, leaving the atom in the state $|m'\rangle$, followed by the absorption of the photon from the mode i. The energies of these intermediate states are E_m for the first kind, and $E_{m'} + \hbar\omega_i + \hbar\omega_s$ for the second kind, where E_m and $E_{m'}$ are the energies of the atom in the states $|m\rangle$ and $|m'\rangle$, respectively. The total transition amplitude is obtained by adding these two contributions, namely,

$$T_2 = \sum_M \frac{\langle F|V|M\rangle\langle M|V|I\rangle}{E_1 - E_m + \hbar\omega_i} + \sum_{M'} \frac{\langle F|V|M'\rangle\langle M'|V|I\rangle}{E_2 - E_m - \hbar\omega_i} \tag{115}$$

where (112) has been used in the denominator of the last term on the *r.h.s.* This is the total transition amplitude, up to second order, between $|I\rangle$ and $|F\rangle$. Using the Fermi golden rule

$$W_{FI} = \frac{2\pi}{\hbar}|T_2|^2\rho(\hbar\omega_s) \tag{116}$$

we obtain the transition *rate* W_{FI}, *i.e.*, the transition probability per unit time between the two states $|I\rangle$ and $|F\rangle$. $\rho(E)$ is the density of states at the energy E of the scattered photon. It is given by [27]

$$\rho(E) = E^2 \left(\frac{L}{2\pi\hbar c} \right)^3 \quad . \tag{117}$$

The *differential scattering cross section*, $d\sigma/d\Omega$, is defined by the ratio of the transition rate W_{FI} to the incident flux of photons $f = c/L^3$ so that

$$\frac{d\sigma}{d\Omega} \equiv \frac{W_{FI}}{f} = \frac{L^6 \omega_s^2}{(2\pi\hbar)^2 c^4} |T_2|^2 \quad . \tag{118}$$

Using in (115) the explicit form of V, with the help of (107) and (109), and substituting in (118), yields the *Kramers-Heisenberg cross section* [28]

$$\frac{d\sigma}{d\Omega} = r_0^2 \omega_i \omega_s^3 \mu^2 \left| \sum_m \left[\frac{\langle 2|\mathbf{r}\cdot\mathbf{e}_s|m\rangle\langle m|\mathbf{r}\cdot\mathbf{e}_i|1\rangle}{E_1 - E_m + \hbar\omega_i} + \frac{\langle 2|\mathbf{r}\cdot\mathbf{e}_i|m\rangle\langle m|\mathbf{r}\cdot\mathbf{e}_s|1\rangle}{E_2 - E_m - \hbar\omega_i} \right] \right|^2 \tag{119}$$

with the classical radius of the electron $r_0 = e^2/4\pi\varepsilon_0\mu c^2$, and where $|m\rangle$ denotes any internal atomic level with energy E_m. The Kramers-Heisenberg formula (119) is the general quantum mechanical expression, to lowest order in V, for the differential scattering cross section of a photon by an atom.

We now consider a very important limiting case of (119), in which the incoming photon energy is resonant with some atomic transition.

4.3 Resonant scattering

From now on, atoms will be modeled as degenerate two level systems, so that (Figure 9) there are only two possible atomic energy states, a ground state $|g\rangle$ of energy E_g, and an excited state $|e\rangle$ of energy E_e, where $E_e > E_g$. These states may be Zeeman degenerate. Hereafter we shall use the term "state" for a set of Zeeman levels corresponding to the same energy in the absence of an external magnetic field. These states are characterized by some definite value of total angular momentum, that we denote by j_g and j_e for the ground and excited states, respectively, where the total angular momenta of the two states are $\hbar\sqrt{j_g(j_g+1)}$ and $\hbar\sqrt{j_e(j_e+1)}$. The quantum numbers j_g and j_e may generally correspond to a merely orbital angular momenta, orbital

+ electronic spin angular momenta (fine structure), or orbital + electronic and nuclear spin angular momenta (hyperfine structure). We will usually assume that $j_e = j_g + 1$, which is an allowed electric dipole transition [25]. The ground and excited energy states are therefore composed of $2j_g + 1$ and $2j_e + 1$ Zeeman sublevels, respectively, which will be often referred to as just "levels". These levels are characterized by a magnetic quantum numbers, which correspond to the Z component of the total angular momentum. In the following we will use the notation $|m_i\rangle$ and $|m_i'\rangle$ to denote the ground state Zeeman levels, where $-j_g \leq m_i, m_i' \leq j_g$, and $|M_i\rangle$ and $|M_i'\rangle$ for the excited state Zeeman levels with $-j_e \leq M_i, M_i' \leq j_e$ $(i = 1, 2, ...)$. In reality, the atom have additional energy states with energies other than E_g and E_e. However, for an incoming light that is resonant with the transition $|g\rangle \leftrightarrow |e\rangle$, and when other possible atomic transitions are far from resonance with the light, the atom is well approximated by such a two states system.

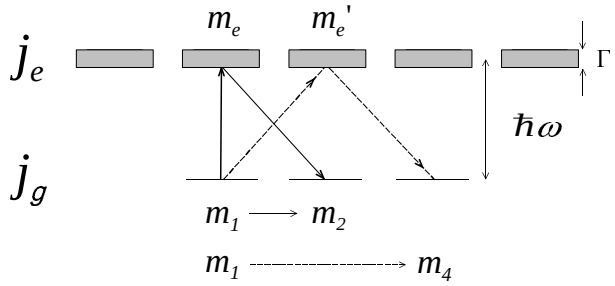

Figure 9: *A two level atom. j_g and j_e are, respectively, the total angular momentum quantum numbers of the ground and the excited atomic states (in this picture $j_g = 1$ and $j_e = 2$). m_i and m_e, m_e' are the Zeeman magnetic quantum numbers of the two states. Γ is the natural width of the excited state, while the ground state is assumed to be stable. The energy difference $\hbar\omega$ between the two states is resonant with the incident photon. In this figure two Raman processes are shown.*

With the above description of the atom, the scattering process occurs as follows. An atom is initially in a ground level $|m_1\rangle$. From the electric dipole selection rules we know that the intermediate levels are excited states $|M_i\rangle$. This is because the quantum numbers, j_g and j_e, correspond to a certain value of the orbital angular momentum l. Since the electric dipole selection rules impose $\Delta l = \pm 1$ (to have nonzero matrix elements in (119)), the intermediate levels $|m\rangle$ must be an excited state sublevels, given that $|1\rangle$

and $|2\rangle$ belong to the ground state. Assuming the atom is in the ground level $|m_2\rangle$ after scattering, two kinds of processes are considered. If $|m_1\rangle = |m_2\rangle$ the process is called *Rayleigh* scattering. For a degenerate ground state, however, a *Raman* scattering, for which $|m_1\rangle \neq |m_2\rangle$, may take place. For a two states atom, thus, the Kramers-Heisenberg cross section becomes

$$\frac{d\sigma}{d\Omega} = r_0^2 \omega_i \omega_s^3 \mu^2 \left| \sum_i \left[\frac{\langle m_2|\mathbf{r}\cdot\mathbf{e}_s|M_i\rangle\langle M_i|\mathbf{r}\cdot\mathbf{e}_i|m_1\rangle}{E_g - E_e + \hbar\omega_i} + \frac{\langle m_2|\mathbf{r}\cdot\mathbf{e}_i|M_i\rangle\langle M_i|\mathbf{r}\cdot\mathbf{e}_s|m_1\rangle}{E_g - E_e - \hbar\omega_i} \right] \right|^2 . \tag{120}$$

We note that the notation used here is a shorthand. For example, what is meant by $\langle m_2|\mathbf{r}\cdot\mathbf{e}_s|M_i\rangle$, is actually $\langle j_g, m_2|\mathbf{r}\cdot\mathbf{e}_s|j_e, M_i\rangle$. As already mentioned, the notation $|m_i\rangle$ will always mean $|j_g, m_i\rangle$, and $|M_i\rangle \equiv |j_e, M_i\rangle$

In a resonant scattering process, considered hereafter, $\hbar\omega_i \simeq E_e - E_g$. One can see immediately that in this case, the second term in the *r.h.s* of (120) becomes negligible compared to the first one, because of the values of their denominators. Then, we can approximate the differential scattering cross section by

$$\frac{d\sigma}{d\Omega} = r_0^2 \omega_i \omega_s^3 \mu^2 \left| \sum_i \frac{\langle m_2|\mathbf{r}\cdot\mathbf{e}_s|M_i\rangle\langle M_i|\mathbf{r}\cdot\mathbf{e}_i|m_1\rangle}{E_g - E_e + \hbar\omega_i} \right|^2 \quad \text{(near resonance)} \ . \tag{121}$$

Thus, the process that contributes to the resonant cross section is the one, in which the incoming photon is first absorbed in the atom, initially in a ground level, and then the scattered photon is emitted, leaving the atom in another ground level.

A problem occurs, however, in the case of exact resonance $\hbar\omega_i = E_e - E_g$, where it seems that the cross section (121) diverges. This spurious divergence is due to our neglect of spontaneous emission from $|e\rangle$ to $|g\rangle$. Such a divergence occurs also in the classical description of the interaction between an "atom" and electromagnetic radiation [26]. In this case, the atomic electron is bound to the atomic nucleus by a harmonic force. An electromagnetic wave of frequency ω then forces the electron to oscillate in this frequency. If ω is equal to the natural oscillator frequency of the electron due to the nucleus, the "atom" absorbs more and more energy from the field. The amount of energy that can be absorbed is unlimited, leading to a divergence. To remedy this, one should take into account damping processes of the atom's energy. Still in the classical picture, this damping exists because the oscillat-

ing electron radiates as a result of its electric charge, a process which reduces its energy and thus balances the energy absorption.

In the quantum picture, the role of the damping mechanism is played by the spontaneous emission from $|e\rangle$ to $|g\rangle$, which also makes the atom to lose energy. Due to the spontaneous emission, the excited state $|e\rangle$ has some lifetime $1/\Gamma$, where Γ is the natural width of this state. The physical meaning of this lifetime is that the probability of finding the atom in the state $|e\rangle$, assuming it was excited at $t = 0$, decreases as $e^{-\Gamma t}$, according to the well known Wigner-Weisskopf model. Generally, the ground state $|g\rangle$ might also possess a lifetime, $1/\Gamma_g$, due to spontaneous emission toward lower energy states. We will however assume, throughout this work, that $1/\Gamma_g \to \infty$, meaning that $|g\rangle$ is stable.

Such an exponential decrease is equivalent to modifying the energy E_e by adding to it the imaginary value $-i\hbar\Gamma/2$, namely

$$E_e \to E_e - i\frac{\hbar\Gamma}{2} \quad . \tag{122}$$

Then, the time evolution of $|e\rangle$ is governed by the exponential $e^{-iE_e t/\hbar - \Gamma t/2}$, and the probability to find the atom in the excited state $|e\rangle$ at time t behaves like

$$|e^{-iE_e t/\hbar - \Gamma t/2}|^2 = e^{-\Gamma t} \quad . \tag{123}$$

The cross section (121) then becomes

$$\frac{d\sigma}{d\Omega} = r_0^2 \omega_i \omega_s^3 \mu^2 \left| \sum_i \frac{\langle m_2|\mathbf{r}\cdot\mathbf{e}_s|M_i\rangle\langle M_i|\mathbf{r}\cdot\mathbf{e}_i|m_1\rangle}{E_g - E_e + \hbar\omega_i + i\hbar\Gamma/2} \right|^2 \quad . \tag{124}$$

To obtain this result in a more rigorous way, one should take into account all orders in the perturbation V. As a result, the intermediate states are no longer separated into atomic levels and photon states, but rather become a continuum of combined states, that include all possible virtual emission-absorption processes. This calculation is done, *e.g.*, in [27]. The final result is, however, the same as (124).

The properties of the scattered light, called *resonance fluorescence*, depend upon the incoming beam. When the incoming wave is monochromatic, as is assumed here, the scattered light is also monochromatic with the same frequency [27], that is $\omega_i = \omega_s \equiv \omega$. Moreover, it can be shown [29] that the emitted radiation is coherent with the incident radiation. This means that

there is a definite, *i.e.* non-random, phase difference between the incoming and scattered beams. In this sense, therefore, resonant scattering cannot be viewed as a simple two-photon case, in which one photon is absorbed and then another one is emitted. This is because in the latter case, the phase difference between the incoming and the scattered light would be random due to the uncertainty in the exact instant of emission.

There are cases in which we do not know what are the initial and final sublevels, $|m_1\rangle$ and $|m_2\rangle$, of the atom. According to quantum mechanics, one has then to sum over all possible final states and to average over the initial states. The averaging procedure requires information about the distribution of initial sublevels in the atom. In other words, we have to know the quantum state of the atom before the scattering has taken place. Often, the atom is not in a pure state but in some statistical mixture, so that what is needed is its initial density matrix. In the case we consider, there are no pumping mechanisms that can affect this density matrix. Therefore, we assume equipartition of all initial sublevels, namely, a scalar density matrix. Since the number of possible initial levels is $J \equiv 2j_g + 1$, the probability of each sublevel to be occupied before the atom has interacted with the light, is $1/J$. At resonance $\hbar\omega = E_e - E_g$, therefore, the differential scattering cross section (124) is

$$\frac{d\sigma}{d\Omega} = \frac{\mathcal{F}}{J} \sum_{j,k} \left| \sum_i \langle m_k | \mathbf{d} \cdot \mathbf{e}_s | M_i \rangle \langle M_i | \mathbf{d} \cdot \mathbf{e}_i | m_j \rangle \right|^2 \tag{125}$$

with $\mathbf{d} = e\mathbf{r}$ and $\mathcal{F} = (2\omega^2/4\pi\varepsilon_0 c^2 \hbar\Gamma)^2$

We may calculate from (125) the averaged total cross section toward all scattering directions and polarizations. The word "averaged" corresponds to the averaging over initial sublevels of the atom. For exact resonance $\hbar\omega_i = E_e - E_g$, the result is [2]

$$\langle \sigma \rangle = \frac{3\lambda^2}{2\pi} a_{j_g j_e} \tag{126}$$

with

$$a_{j_g j_e} \equiv \frac{1}{3} \frac{2j_e + 1}{2j_g + 1} \quad . \tag{127}$$

4.4 The Wigner-Eckart theorem

A useful relation for the calculation of matrix elements like in (125), is the Wigner-Eckart theorem, which states that [30]

$$\langle j_g m|v_p|j_e M\rangle = (-)^{j_g-m}\langle j_g||\mathbf{v}||j_e\rangle \begin{pmatrix} j_g & 1 & j_e \\ -m & p & M \end{pmatrix} . \tag{128}$$

Here $\mathbf{v}$ is some vector and the v_p's ($p=-1,0,1$) are its spherical components defined as

$$v_0 = v_z \ , \quad v_{\pm 1} = \mp\frac{1}{\sqrt{2}}(v_x \pm i v_y) \tag{129}$$

with v_x, v_y, v_z being the cartesean components of $\mathbf{v}$. As before, (j_g,m) and (j_e,M) are the quantum numbers corresponding to the total angular momentum and its Z component, related to the ground and excited states, respectively. The scalar $\langle j_g||\mathbf{v}||j_e\rangle$ depends only on $\mathbf{v}$, j_g, and j_e, and is called a *reduced matrix element*. It corresponds to the radial (as opposed to the angular) part of the spatial integration in $\langle j_g m|v_p|j_e M\rangle$. Since, given j_g, j_e, and $\mathbf{v}$, the reduced matrix element is constant, it is not essential in our case, in which j_g and j_e are some given parameters. It will cancel out in the expression for the normalized correlation. The last term in the *r.h.s* of (128) is a *3j symbol*, related to Clebsch-Gordan coefficients by definition as

$$\begin{pmatrix} j_g & k & j_e \\ -m & p & M \end{pmatrix} = \frac{(-)^{j_g-k-M}}{\sqrt{2j_e+1}}\langle j_g, k, -m, p|j_e, -M\rangle \tag{130}$$

where $\langle j_g, k, -m, p|j_e, -M\rangle$ is the Clebsch-Gordan coefficient corresponding to the addition of two angular momenta, given by the quantum numbers j_g and k. It is the coefficient of the vector state $|j_e, -M\rangle$, in the expansion of the separate angular momenta vector state $|j_g, k, -m, p\rangle$ (p is the Z-component quantum number that corresponds to k), in the total angular momentum basis. The $3j$-symbol describes the angular part of the matrix element $\langle j_g m|v_p|j_e M\rangle$, and as such it corresponds to the polarization properties of the incoming and outgoing radiation. In particular, the $3j$-symbol in (130) is zero, unless

$$M = m - p \ . \tag{131}$$

This selection rule constitutes the interplay between photons polarization and atomic angular momenta. To show this, we now apply the Wigner-Eckart

theorem to the matrix elements in (125). But first, we define the spherical basis unit vectors according to

$$\sigma_0 = \hat{z} \ , \quad \sigma_{\pm 1} = \mp \frac{1}{\sqrt{2}} (\hat{x} \pm i\hat{y}) \tag{132}$$

where $\hat{x}$, $\hat{y}$, and $\hat{z}$ are the unit vectors along the X, Y, and Z axis, respectively. $\sigma_{\pm 1}$ are the left and right circular polarization unit vectors in the XY plane, while σ_0 is a Z-directed linear polarization unit vector.

Suppose now that $\mathbf{e}_i = \sigma_1$, namely, that the incoming beam is left circularly polarized. Then, referring to the matrix element in (125) and using (128) we find

$$\langle M_i | \mathbf{d} \cdot \mathbf{e}_i | m_j \rangle = \langle M_i | d_1 | m_j \rangle = (-)^{j_e - M_i} \langle j_e || \mathbf{v} || j_g \rangle \begin{pmatrix} j_e & 1 & j_g \\ -M_i & 1 & m_j \end{pmatrix} \ . \tag{133}$$

This matrix element describes the absorption part of the scattering process, namely, a photon which is σ_1 polarized is absorbed by the atom initially in the $|m_j\rangle$ level of the ground state. The absorption of the photon excites the atom to the $|M_i\rangle$ sublevel. The selection rule (131) then gives

$$M_i = m_j + 1 \ . \tag{134}$$

Since a photon with a circular polarization σ_1 carries one unit ($\hbar$) of angular momentum along the Z-axis [31], the last relation is readily interpreted as follows: before the scattering process, the Z-component angular momentum of the atom was $m_j\hbar$, while for the photon it was $\hbar$. After the photon has been absorbed, it gave its angular momentum to the atom, which is then left with an angular momentum $\hbar M_i$ along Z. (134) therefore simply expresses conservation of angular momentum along the quantization-axis Z. It exhibits the connection between the incoming and scattered photons polarization, and the corresponding atomic transition. The conservation of total angular momentum requires that

$$|j_g - 1| \leq j_e \leq j_g + 1 \tag{135}$$

which complies with our default choice $j_e = j_g + 1$.

Other properties of the $3j$-symbols are [32]:

$$\begin{pmatrix} j_1 & j_2 & j_3 \\ m_1 & m_2 & m_3 \end{pmatrix} \tag{136}$$

is:

(i) invariant in a circular permutation of the three columns;

(ii) multiplied by $(-)^{j_1+j_2+j_3}$ in a permutation of two columns;

(iii) multiplied by $(-)^{j_1+j_2+j_3}$ when changing simultaneously the signs of m_1, m_2, and m_3.

(iv) Orthogonality:

$$\sum_{m_1=-j_1}^{j_1}\sum_{m_2=-j_2}^{j_2}\begin{pmatrix} j_1 & j_2 & j_3 \\ m_1 & m_2 & m_3 \end{pmatrix}\begin{pmatrix} j_1 & j_2 & j_3' \\ m_1 & m_2 & m_3' \end{pmatrix} = \frac{1}{2j_3+1}\delta_{j_3 j_3'}\delta_{m_3 m_3'}$$

$$\sum_{j_3=|j_1-j_2|}^{j_1+j_2}\sum_{m_3=-j_3}^{j_3}(2j_3+1)\begin{pmatrix} j_1 & j_2 & j_3 \\ m_1 & m_2 & m_3 \end{pmatrix}\begin{pmatrix} j_1 & j_2 & j_3 \\ m_1' & m_2' & m_3 \end{pmatrix} = \delta_{m_1 m_1'}\delta_{m_2 m_2'} \quad (137)$$

4.5 "Which path" information

Interference effects play an important role in this work, because a speckle is an interference picture. Interference occurs when a system evolves between some initial state and some final state through several possible intermediate states, provided that one cannot detect the specific intermediate state of the system. As a result, the system evolves through several intermediate states simultaneously, giving rise to a superposition of a few "paths". A knowledge about the intermediate state of a system is termed *"which path" information*, and is expected to reduce, and/or eliminate, the interference pattern.

The simplest example of interference is the Young interferometer which consists of a coherent light beam, shined on an opaque screen having two slits. The light then falls on a second screen and forms a fringe pattern. In the classical version of this experiment, in which the light is scattered merely by the two slits and no additional detectors are present, apart from the one used for measuring the intensity pattern on the second screen, there is no "which path" information and the interference effect is maximal. A measure for the "amount of interference" in the fringes pattern is given by the *visibility* at the center of the second screen, defined as $(I_{max} - I_{min})/(I_{max} + I_{min})$. Here I_{max} is the intensity at the center of the brightest fringe, and I_{min} is the intensity at the center of the closest dark fringe. If there is no "which path" information, the visibility v equals 1, disregarding experimental imperfections and technical limitations.

Itano *et.al.* [33] have performed a Young-like experiment with two atoms instead of the original two slits. The intensity pattern of the light scattered by the two atoms has been measured. In the experiment, two Mercury atoms (actually ions) have been placed using a trap built out of a combination of static and rf electric fields (Paul trap). These ions were illuminated by a linearly polarized CW beam, nearly resonant with the $194nm$ transition between the levels $^2S_{1/2}$ and $^2P_{1/2}$ of the $n = 6$ atomic shell. The relevant transition is thus Zeeman degenerate, since both the ground and excited states possess a total angular momentum $j_g, j_e = 1/2$ and therefore are both two-fold degenerate. Assuming that the ions are initially in their ground state, the light scattering induces transitions during which the ions are excited and then relax back to their ground states. Some of these transitions leave the ion in the *same* ground state sublevel as the initial one before the scattering (π transitions), while in the others the initial and final states of the ion are *different* (σ transitions). Suppose that only one photon is scattered by the system of two ions. Then, measuring the initial and final states of the ions can provide information about the transitions that have actually took place. If one finds that the ions stay in the same ground sublevels after scattering (π case), then no information about the path of the light can be obtained and a full interference effect (maximal visibility) is expected. However, if the final state of one of the ions is found to be different than the initial (σ case), it can be concluded that the photon has gone through that ion in his way to the screen. If there is only one photon, and in the limit of a single scattering (namely, the photon is assumed to be scattered only once), then one can be sure that the photon has *not* interacted with the other ion in his way to the screen. In this case, therefore, the interference pattern is expected to vanish.

The vanishing of the interference effect in the σ case is expected not only when there is just one photon in the incoming light beam, but whenever the incoming intensity is sufficiently weak so that the possibility of both ions to be excited simultaneously is negligible. In other words, the photons are assumed to be scattered one by one. In [33] this is specifically emphasized: *"The preceding analysis is valid only in the limit of low laser intensity, so that the probability of both ions being excited at the same time is negligible..."*. This is readily understood in terms of "which path" information. Suppose, for example, that two photons are simultaneously scattered by the ions, and that one measures their initial and final states. Then, no matter what are these states, the observer cannot determine which photon has gone through which ion, because the photons are indistinguishable. To be more precise,

let us assume that ion 1 has made the transition $m_{1i} = 1/2 \rightarrow m_{1f} = -1/2$ (σ transition), and ion 2 has undergone the π transition $m_{2i} = 1/2 \rightarrow m_{2f} = 1/2$. In the case of only one scattered photon, there is only one possible path that connects the initial and final states, namely:

The photon was scattered by ion 1.

If, however, two photons (say a and b) are scattered simultaneously, the same initial and final states may correspond to several different paths, such as

(1) Photon a was scattered by ion 1 and photon b by ion 2.
(2) Photon b was scattered by ion 1 and photon a by ion 2.
(3) Both photons were scattered by ion 1.

etc. In the experiment [33], the low intensity limit has been considered. The results clearly show that interference occurs in the π case, while in the σ case it disappears.

In what follows we consider a classical light (*e.g.* a laser beam) that is scattered in an atomic gas. In this case, many photons are being scattered simultaneously within the cloud of atoms, and there is thus no "which path" information, as is demonstrated in the above simple example. As a result, there is an interference effect even in σ cases. In Chapters 5 and 6 it is shown, that this interference effect plays a central role in the scattered intensity correlation.

In this chapter we have considered the elementary theory of the interaction between photons and atoms. We have obtained the general quantum mechanical scattering cross section of a photon by an atom, and also the cross section for the specific case of resonant scattering. Finally, the subject of "which path" information has been addressed, and we explained why it is not relevant in our situation.

CHAPTER 5

Intensity correlations of the multiply scattered light in an atomic gas

In this chapter we calculate the transmitted intensity correlation of a speckle pattern, obtained from scattering by atoms. Atoms will be assumed to be degenerate two level systems as described in Section 4.3. The main difference between classical and atomic scatterers is the internal structure, namely, the possibility of a Zeeman degeneracy of the atomic levels. In this sense, as we shall see, atoms heaving a non-degenerate ($j_g = 0$) ground state may be interpreted as if they were classical scatterers. Thus, what distinguishes quantum from classical scatterers *in this context*, is the degeneracy of the atomic ground state: if it is degenerate - the scatterers are quantum, if it is not - they are classical. The experimental reference setup is the same as in Chapter 3.

The exact species of atoms used in the experiment is not important to the following analysis, as long as a few general assumptions are fulfilled:

(i) The atoms are cold enough so that the theory presented in Chapters 2 and 3 is valid.

(ii) There is one atomic transition that is resonant with the incident light, the other transitions are far from this resonance. This allows us to treat the atoms as two level systems.

(iii) The wavelength of the light is long compared to the atomic size, so that the long wavelength approximation mentioned in Chapter 4 can be used.

These conditions are quite standard in experiments, involving the multiple scattering of light in an atomic sample. In [18], for example, Rubidium atoms have been used. The light wavelength is $\lambda = 780nm$, and the total angular momenta of the only two states resonant with the light (criterion (ii)) are $j_g = 3$ and $j_e = 4$. The temperature of the sample is below 0.25K, corresponding to an average atomic velocity of about $v \simeq 0.1m/s$. The elastic mean free path is about $l \simeq 0.7mm$ and the optical depth $b \simeq 6$. Criterion (i) is thus fulfilled, using the following simple argument: the typical time a

photon stays within the sample is $b^2 l/c \sim 10^{-10} s$. During this time the atoms move a distance of about $10^{-11} m$, which is much smaller than λ. Criterion (iii) is immediately seen to be satisfied since λ is much larger than the Bohr radius.

We begin in Section 5.1 with presenting our ideas, at a general level, using a simplified situation where only two atoms are present, and where photons are scattered only once. In Section 5.2 we apply, still on a general ground, these ideas to the multiple scattering regime. Section 5.3 deals with the method used for actually calculating the correlation, and in Section 5.4 we focus on the development of the single scattering contribution, from which the multiple scattering series is built up. The results for the intensity correlation, obtained using the methods of Sections 5.3 and 5.4, are presented in Section 5.5. Finally, in Section 5.6 we show that our predictions are valid in any physical system satisfying some basic conditions.

5.1 Single scattering

It is instructive to begin with the simple example of two atoms in the gas "cloud", and an incident "beam" containing only two photons of wave vector $\mathbf{k}_a$. These two photons are scattered by the system of two atoms, and this scattering is assumed to be simultaneous, meaning that there is no way by which one can obtain the intermediate state of the system between individual scattering events. This point is crucial, since it distinguishes our case from others, in which the low intensity limit is assumed, thus excluding the situation of two photons scattered simultaneously off the atoms, as discussed in Section 4.5. Regarding the atoms, one can only obtain their initial and final states, *i.e.* the internal quantum states (in addition to the positions) before and after the "beam" has interacted with them. Suppose that at $t = 0$, before scattering has taken place, the atoms were in the Zeeman sublevels $|m_1\rangle$ and $|m_3\rangle$, and after scattering they were in the $|m_2\rangle$ and $|m_4\rangle$ sublevels, respectively. Since the scattering of the two photons happens simultaneously, there is no way by which we could assign a given transition (say $|m_1\rangle \to |m_2\rangle$ of atom 1) to a certain photon. In other words, the fact that the two photons are indistinguishable and that they were scattered simultaneously, makes any "which path" information unavailable.

The mean number of photons scattered along $\mathbf{k}_b$ is proportional to the mean intensity scattered along this direction. In the case of only two photons and two atoms, this quantity can be calculated explicitly using identical

particles [25]. However, our main concern here is in the case where there are very large numbers of photons and atoms, so that the exact calculation is not possible. Therefore, we shall ask the following question: "if we had picked one of the photons incoming along $\mathbf{k}_a$, what is the probability, $\mathcal{T}_{ab}$, for this photon to be scattered along $\mathbf{k}_b$ after scattering?". Assuming a slab geometry, the average scattered intensity along $\mathbf{k}_b$ would be then $I_{ab} = I_0\mathcal{T}_{ab}$, where I_0 is the incident intensity, and $\mathcal{T}_{ab}$ is the corresponding transmission coefficient. Because there is no way by which one can tell whether the picked photon has been scattered off one atom or another, we have to sum over both scattering amplitudes, corresponding to the scattering off the two atoms, and then square the sum to obtain $\mathcal{T}_{ab}$. This is correct provided we consider the single scattering case, for which each atom scatters, at most, one photon. Following the description of Chapter 4 we thus write

$$\mathcal{T}_{ab} = \mathcal{G}|\langle m_2|U_1|m_1\rangle e^{-i\mathbf{Q}\cdot\mathbf{R}_1} + \langle m_4|U_2|m_3\rangle e^{-i\mathbf{Q}\cdot\mathbf{R}_2}|^2 \tag{138}$$

where $\mathcal{G} = \mathcal{F}/S$, S is the slab cross section and $\mathcal{F}$ has been defined after (125) in Chapter 4. We have defined the operators $U_i = \sum_M (\mathbf{d}_i\cdot\mathbf{e}_b^*)|M\rangle\langle M|(\mathbf{d}_i\cdot\mathbf{e}_a)$, M being the Zeeman quantum numbers of the atomic excited state, $\mathbf{R}_i$ is the position and $\mathbf{d}_i$ is the electric dipole moment of atom i, and $\mathbf{Q} = \mathbf{k}_b - \mathbf{k}_a$. We have also defined $\mathbf{e}_a$ ($\mathbf{e}_b$) to be the incoming (scattered) photon's polarization unit vector, and assumed a purely resonant scattering.

If the atomic initial and final sublevels are unknown, and their positions are random, the average transmission coefficient $\overline{\mathcal{T}}_{ab}$ is found by averaging (138) both over the positions $\mathbf{R}_{1,2}$ and the initial quantum states $|m_1\rangle$, $|m_3\rangle$. The summation over undetected final quantum states must also be performed. Assuming $k|\mathbf{R}_2 - \mathbf{R}_1| \gg 1$, the cross terms involving products like $e^{-i\mathbf{Q}\cdot\mathbf{R}_1}e^{i\mathbf{Q}\cdot\mathbf{R}_2}$ vanish upon averaging over the positions of the atoms (disorder average) because of the rapidly fluctuating phase difference. Thus, with $J = 2j_g + 1$, we obtain

$$\overline{\mathcal{T}}_{ab} = \frac{\mathcal{G}}{J}\sum_{m_{1,2}} |\langle m_2|U_1|m_1\rangle|^2 + \frac{\mathcal{G}}{J}\sum_{m_{3,4}} |\langle m_4|U_2|m_3\rangle|^2 \ . \tag{139}$$

We now wish to find the (not normalized) correlation function between $\mathcal{T}_{ab}$ and $\mathcal{T}_{a'b'}$, namely

$$Corr(aba'b') = \overline{\mathcal{T}_{ab}\mathcal{T}_{a'b'}} - \overline{\mathcal{T}}_{ab}\overline{\mathcal{T}}_{a'b'} \ . \tag{140}$$

Denoting $A_i^{\{mm'\}} = \sqrt{\mathcal{G}}\langle m'|U_i|m\rangle e^{-i\mathbf{Q}\cdot\mathbf{R}_i}$, we have

$$\overline{\mathcal{T}}_{ab} = \frac{1}{J}\sum_{m_{1,2}} \left|A_1^{\{m_1 m_2\}}\right|^2 + \frac{1}{J}\sum_{m_{3,4}} \left|A_2^{\{m_3 m_4\}}\right|^2 \quad . \tag{141}$$

The expression for $\overline{\mathcal{T}}_{a'b'}$ is similar to (141), except that the internal atomic states are generally different, so that

$$\overline{\mathcal{T}}_{a'b'} = \frac{1}{J}\sum_{m'_{1,2}} \left|A_1^{\{m'_1 m'_2\}}\right|^2 + \frac{1}{J}\sum_{m'_{3,4}} \left|A_2^{\{m'_3 m'_4\}}\right|^2 \quad . \tag{142}$$

Note that the primes designate only the internal quantum numbers m_i. This is because the other degrees of freedom, namely the positions $\mathbf{R}_i$, are assumed to be the same for $\mathcal{T}_{ab}$ and $\mathcal{T}_{a'b'}$.

We may thus write

$$\mathcal{T}_{ab}\mathcal{T}_{a'b'} = \left|A_1^{\{m_1 m_2\}} + A_2^{\{m_3 m_4\}}\right|^2 \ \left|A_1^{\{m'_1 m'_2\}} + A_2^{\{m'_3 m'_4\}}\right|^2 \tag{143}$$

which we now average to find $Corr(aba'b')$. We first notice that (143) contains products of four amplitudes corresponding to all possible combinations of internal and external degrees of freedom. Only products involving zero phase difference survive the disorder average, the others, having rapidly fluctuating phases, vanish on average leaving in the *r.h.s* of (143)

$$\left(|A_1^{\{m_1 m_2\}}|^2 + |A_2^{*\{m_3 m_4\}}|^2\right)\left(|A_1^{\{m'_1 m'_2\}}|^2 + |A_2^{*\{m'_3 m'_4\}}|^2\right) + \left(A_1^{\{m_1 m_2\}} A_2^{*\{m_3 m_4\}} A_1^{*\{m'_1 m'_2\}} A_2^{\{m'_3 m'_4\}} + \text{c.c.}\right) \quad . \tag{144}$$

By averaging the first term of (144) over internal quantum numbers, we see from (141) and (142) that it amounts to the product $\overline{\mathcal{T}}_{ab}\overline{\mathcal{T}}_{a'b'}$. Therefore, using the definition (140) we find that

$$Corr(aba'b') = \frac{1}{J^4}\sum_{m_i,m'_i} A_1^{\{m_1 m_2\}} A_1^{*\{m'_1 m'_2\}} \sum_{m_i,m'_i} A_2^{*\{m_3 m_4\}} A_2^{\{m'_3 m'_4\}} + \text{c.c.} \tag{145}$$

where the pre-factor $1/J^4$ results from averaging over initial internal states of the atoms.

We now write (145) in its explicit form, which is

$$Corr(aba'b') = \frac{\mathcal{G}^2}{J^4} \sum_{m_i,m_i'} \langle m_2|U_1|m_1\rangle\langle m_2'|U_1|m_1'\rangle \sum_{m_i,m_i'} \langle m_4|U_2|m_3\rangle\langle m_4'|U_2|m_3'\rangle + \text{c.c.} \quad (146)$$

Looking at (139) and (146), we see that these quantities are composed of certain building blocks, which we term *vertices*. For the average intensity (139), this vertex is written as

$$\mathcal{V}^{(i)} = \frac{\mathcal{G}}{J} \sum_{m_{1,2}} |\langle m_2|U|m_1\rangle|^2 \ , \quad (147)$$

while for the correlation (146) it is

$$\mathcal{V}^{(c)} = \frac{\mathcal{G}}{J^2} \sum_{m_{1,2,3,4}} \langle m_2|U|m_1\rangle\langle m_4|U|m_3\rangle^* \ . \quad (148)$$

The vertex $\mathcal{V}^{(i)}$, up to the factor $1/S$, is identical to the differential cross section (125) of Chapter 4, and thus have the same physical meaning. Similarly, we interpret the correlation vertex $\mathcal{V}^{(c)}$ as the analog of the intensity cross section in the case of correlation. It is clearly not a real cross section, but however it plays exactly the same formal role. What distinguishes these two vertices, is that $\mathcal{V}^{(c)}$ involves the coupling of two scattering amplitudes that correspond to generally *different* Zeeman quantum numbers, while in the intensity cross section $\mathcal{V}^{(i)}$, these quantum numbers are identical for both coupled amplitudes. These two kinds of vertices give rise to two different Diffuson functions, as discussed in the next section.

For non-degenerate atomic states we have $J = 1$, and the two vertices coincide. Therefore, focusing on the case $a = a'$, $b = b'$, we find

$$Corr(abab) = 2|A_1|^2|A_2|^2 \qquad \text{(non-degenerate)} \quad (149)$$

using (145). Since the two atoms are identical, we have $|A_1|^2 = |A_2|^2 \equiv |A|^2$ so that from (141)

$$\overline{\mathcal{T}}_{ab} = 2|A|^2 \qquad \text{(non-degenerate)} \quad (150)$$

and

$$C_{abab} = \frac{Corr(abab)}{\overline{\mathcal{T}}_{ab}^2} = \frac{1}{2} \qquad \text{(non-degenerate).} \quad (151)$$

This is the Rayleigh law for two scattering atoms (the result $C_{abab} = 1$ is the Rayleigh law in the limit of many atoms). Comparing (151) to (145) and (139) we notice that the correlation in the degenerate ($J > 1$) case generally differs significantly from that of the non-degenerate case. An upper bound of the correlation in the degenerate case is obtained by taking in (145) all the amplitudes $A_i^{\{mm'\}}$ to be equal. This leads to $C_{abab} = J^2/2$, a much larger value than $1/2$ obtained for non-degenerate atomic levels.

In the non-degenerate case, $J = 1$, it is simple to generalize (150) and (151) for N atoms. We have

$$\mathcal{T}_{ab} = |A|^2 \left| \sum_i e^{-i\mathbf{q}\cdot\mathbf{R}_i} \right|^2 = |A|^2 \left[N + 2 \sum_{i>j} \cos(\mathbf{q} \cdot \mathbf{R}_{ij}) \right] \tag{152}$$

with $\mathbf{R}_{ij} = \mathbf{R}_i - \mathbf{R}_j$. Because the disorder averaged quantity $\overline{\cos(\mathbf{q} \cdot \mathbf{R}_{ij})}$ is 0 for $i \neq j$, we thus obtain

$$\overline{\mathcal{T}}_{ab} = N|A|^2 \ . \tag{153}$$

The generalization of the correlation is also straightforward. We first observe that

$$\overline{\mathcal{T}^2}_{ab} = |A|^4 \left[N^2 + 4N \sum_{i>j} \overline{\cos(\mathbf{q} \cdot \mathbf{R}_{ij})} + 4 \sum_{i>j} \sum_{k>l} \overline{\cos(\mathbf{q} \cdot \mathbf{R}_{ij}) \cos(\mathbf{q} \cdot \mathbf{R}_{kl})} \right] \tag{154}$$

Because $i \neq j$, the second term in the *r.h.s* of (154) vanishes. Moreover, using that $i > j$ and $k > l$, and that $\overline{\cos(\mathbf{q} \cdot \mathbf{R}_{ij}) \cos(\mathbf{q} \cdot \mathbf{R}_{kl})} = 1/2$ for $i = k, j = l$, the third term on the *r.h.s* of (154) equals $N^2 - N$. Therefore

$$\overline{\mathcal{T}^2}_{ab} = |A|^4[N^2 + N^2 - N] \tag{155}$$

so that the normalized correlation function $C_{abab} = (\overline{\mathcal{T}^2}_{ab} - \overline{\mathcal{T}}^2_{ab})/\overline{\mathcal{T}}^2_{ab}$ gives

$$C_{abab} = 1 - \frac{1}{N} \ . \tag{156}$$

For $N \gg 1$, we obtain the usual form of the Rayleigh law, $C_{abab} = 1$, which characterizes the intensity fluctuations of light scattered by a cloud of classical scatterers.

5.2 Multiple scattering

We now come back to the case of a large number of atoms, where the photon is multiply scattered in the medium. The experimental reference setup, designed for the purpose of measuring $C_{aba'b'}$, is presented in Figure 10. The first pulse of light is incident along $\mathbf{s}_a$ and detected along $\mathbf{s}_b$. A time τ later, a second pulse incomes along $\mathbf{s}_{a'}$ and measured along $\mathbf{s}_{b'}$. During the time period τ the scatterers are taken to be of fixed positions. Multiplying the transmitted intensity of the first pulse, along $\mathbf{s}_b$, by that of the second pulse along $\mathbf{s}_{b'}$, gives rise to a single measurement of $\mathcal{T}_{ab}\mathcal{T}_{a'b'}$. To find the disorder averaged quantity $\overline{\mathcal{T}_{ab}\mathcal{T}_{a'b'}}$, a similar procedure is then repeated, as shown in the figure, after a time T taken to be long enough to allow the scatterers to move appreciably between the two measurements. By repeating these measurements a sufficient number of times, the disorder average is realized.

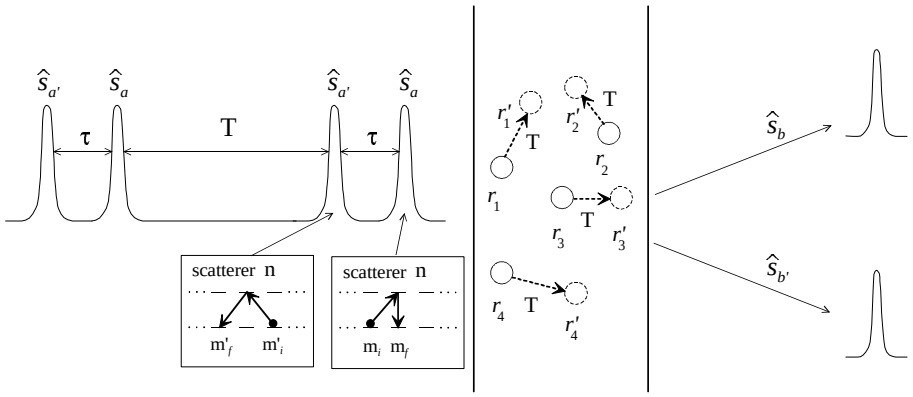

Figure 10: *A suggested setup for measuring $C_{aba'b'}$. A pulse of light is shined along $\mathbf{s}_a$ and being measured along $\mathbf{s}_b$. A time τ later, which is very short so that the atoms do not move, a second pulse is shined along $\mathbf{s}_{a'}$ and being measured along $\mathbf{s}_{b'}$. The internal states of atoms, that "representative" photons of the two pulses experience, are different and practically uncorrelated, as shown in the insets. $\mathbf{r}_i$ and $\mathbf{r}'_i$ denote the position of atoms at times 0 and T, respectively. After a time T, long enough so that the atoms move during it, this process is repeated. Taking the average of a sufficient number of such measurements, gives the angular correlation function between channels ab and $a'b'$.*

As before, the transmission coefficient $\mathcal{T}_{ab}$ ($\mathcal{T}_{a'b'}$) is calculated by consid-

ering some "representative" photon of the first (second) pulse in Figure 10, and summing all its possible scattering paths. Consider a photon, denoted by 1, of the first pulse. When this photon is incoming, the sample is in some spatial configuration denoted by $\{R\}$, the set of all scatterers positions, and every atom is at some internal state. After the photon is multiply scattered, the sample is still in the spatial configuration $\{R\}$, but the internal state of the atoms might be changed due to the interaction with the light. The configuration of the scatterers in the sample, corresponding to this photon, is therefore characterized by (1) a set of external degrees of freedom, $\{R\}$, which corresponds to the position vectors of all the atoms, and (2) by a set of internal degrees of freedom, $\{m\}$, which denotes the quantum levels of all atoms, before and after pulse 1 has been scattered. Now consider another photon, which we shall denote by 2, of the second ($\mathbf{s}_{a'} \rightarrow \mathbf{s}_{b'}$) pulse. According to our setup, the external configuration that photon 2 experiences is also $\{R\}$. However, between the arrivals of photon 1 and photon 2, many other photons have been scattered in the sample. As a result, the quantum states of the atoms between the scattering of photons 1 and 2 are randomly changed, so that the internal configuration $\{m\}$ that photon 1 experiences and that of photon 2, $\{m'\}$, are generally different and uncorrelated. Disregarding any pumping mechanisms, it is not possible experimentally to know $\{m\}$ and $\{m'\}$. Therefore, the average transmitted intensity and the correlation should be averaged both over all possible internal and external configurations.

The transmission coefficients before averaging are

$$\mathcal{T}_{ab} = \sum_{ij} A_i^{\{R,m\}} A_j^{*\{R,m\}} \tag{157}$$

and

$$\mathcal{T}_{a'b'} = \sum_{ij} A_i^{\{R,m'\}} A_j^{*\{R,m'\}} \tag{158}$$

where $A_i^{\{R,m\}}$ denotes the amplitude of the scattering trajectory i, corresponding to the sample external and internal configurations $\{R\}$ and $\{m\}$, respectively. In this expression and in the following ones, we do not distinguish explicitly between amplitudes of the first pulse and those of the second pulse apart from the difference between $\{m\}$ and $\{m'\}$. They however do not describe exactly the same processes. For example, A_i that corresponds to the first pulse describes the process in which an incoming photon along $\mathbf{s}_a$ is scattered toward $\mathbf{s}_b$, while the same notation A_i for the second pulse,

describes different directions of incidence and emergence. In most of the following analysis this distinction is not important. For the case $a = a'$ and $b = b'$, the two processes are identical. We first average (157) and (158) over $\{R\}$, according to the prescription of Chapters 2 and 3: all cross terms, $i \neq j$, vanish on average due to fluctuating phase differences. Thus we find

$$\overline{\mathcal{T}}_{ab} = \sum_i \overline{|A_i^{\{m\}}|^2}^{\{m\}} \tag{159}$$

and

$$\overline{\mathcal{T}}_{a'b'} = \sum_i \overline{|A_i^{\{m'\}}|^2}^{\{m'\}} \tag{160}$$

where $\overline{\cdots}^{\{m\}}$ denotes an internal configuration average.

To find the correlation, we first multiply the transmission coefficients

$$\mathcal{T}_{ab}\mathcal{T}_{a'b'} = \sum_{ij}\sum_{kl} A_i^{\{R,m\}} A_j^{*\{R,m\}} A_k^{\{R,m'\}} A_l^{*\{R,m'\}} \quad . \tag{161}$$

The configuration average leaves only terms with zero total phase. Two kinds of terms in (161) fulfill this requirement: (1) terms with $i = j$, $k = l$, and (2) terms with $i = l$, $j = k$, namely

$$\begin{aligned}\overline{\mathcal{T}_{ab}\mathcal{T}_{a'b'}} &= \sum_{ik} \overline{|A_i^{\{m\}}|^2\,|A_k^{\{m'\}}|^2}^{\{m,m'\}} + \sum_{ik} \overline{(A_i^{\{m\}} A_i^{*\{m'\}})(A_k^{\{m'\}} A_k^{*\{m\}})}^{\{m,m'\}} \\ &= \overline{\mathcal{T}}_{ab}\overline{\mathcal{T}}_{a'b'} + \sum_{ik} \overline{(A_i^{\{m\}} A_i^{*\{m'\}})(A_k^{\{m'\}} A_k^{*\{m\}})}^{\{m,m'\}}\end{aligned} \tag{162}$$

where (159) and (160) have been used. Finally, the unnormalized correlation function becomes

$$Corr(aba'b') = \sum_{ik} \overline{(A_i^{\{m\}} A_i^{*\{m'\}})(A_k^{\{m'\}} A_k^{*\{m\}})}^{\{m,m'\}} \quad . \tag{163}$$

The *r.h.s* of (163) is composed of pairs of multiple scattering sequences i and k. For a large number of atoms, the sequences i and k hardly share any scatterers. To illustrate this point, we consider a path of n scattering events, assumed to be smaller than the number of scatterers in the sample, namely, $n \ll N$. The total number of trajectories involving n scattering events is

$$S = \left(\begin{array}{c} N \\ n \end{array} \right) n! \ . \tag{164}$$

Given two sets (A and B) containing S trajectories each, there are

$$P = S^2 = \left(\begin{array}{c} N \\ n \end{array} \right)^2 (n!)^2 \ . \tag{165}$$

possibilities to pair one trajectory from set A with another one from set B. The number of trajectory pairs, out of this total number, that share exactly z scatterers, is

$$P_z = \left(\begin{array}{c} N-z \\ n-z \end{array} \right)^2 [(n-z)!]^2 \left(\begin{array}{c} N \\ z \end{array} \right) \ . \tag{166}$$

It is obtained as follows: we pick z scatterers, and find the number of trajectory pairs of length n that share them. Then, we multiply this quantity by the number of possibilities to choose z scatterers out of N. From (165) and (166) we find

$$\frac{P_z}{P} = \frac{(N-z)!}{z!N!} \ . \tag{167}$$

Summing (167) over z gives the ratio of the number of trajectory (of length n) pairs that share at least one scatterer, to the total number of pairs. We obtain

$$\sum_{z=1}^{n} \frac{P_z}{P} = \frac{1}{N!} \sum_{z=1}^{n} \frac{(N-z)!}{z!} \leq \frac{1}{N!} \sum_{z=1}^{n} (N-1)! = \frac{n}{N} \ll 1 \ .$$

It is thus legitimate to ignore the case for which i and k share scatterers, and perform separately the averaging in (163), which gives

$$Corr(aba'b') = \left| \sum_i \overline{A_i^{\{m\}} A_i^{\{m'\}*}}^{\{m,m'\}} \right|^2 \ . \tag{168}$$

The internal configuration averaging is performed as in the previous section. We average over initial atomic sublevels assuming they are equiprobable, and in addition we sum over final atomic sublevels. This yields for (159) and (160), to

$$\overline{\mathcal{T}}_{ab} = \sum_i \sum_{\{m_i\}} \frac{|A_i^{\{m_i\}}|^2}{J^{n_i}} \tag{169}$$

and

$$\overline{\mathcal{T}}_{a'b'} = \sum_i \sum_{\{m_i'\}} \frac{|A_i^{\{m_i'\}}|^2}{J^{n_i}} \tag{170}$$

where $\{m_i\}$ is the internal configuration of the n_i atoms in the sequence i. For (168), and assuming the specific case $a = a'$ and $b = b'$ we obtain, using the definition (70) in Chapter 3,

$$\sqrt{C_{abab}} = \frac{\sum_i \sum_{\{m_i\},\{m_i'\}} A_i^{\{m_i\}} A_i^{*\{m_i'\}} / J^{2n_i}}{\sum_i \sum_{\{m_i\}} |A_i^{\{m_i\}}|^2 / J^{n_i}} \ . \tag{171}$$

We note that in the correlation (the numerator on the *r.h.s* of (171)), averaging over internal quantum numbers involves a factor $1/J^{2n_i}$ instead of $1/J^{n_i}$ for the intensity. This is because in the correlation we average over two sets of initial sublevels, that correspond to $\{m\}$ and to $\{m'\}$.

Here again, like the single scattering case discussed previously, we see that the average transmitted intensity ($\overline{\mathcal{T}}_{ab}$ and $\overline{\mathcal{T}}_{a'b'}$), and the correlation ($Corr(aba'b')$) are essentially different. The contributions to the intensity involve two coupled amplitudes corresponding to the same scattering sequence and to the same internal configurations. On the other hand, the contributions to the correlation are pairs of amplitudes with the same scattering sequence, but generally *different* internal configurations of atomic Zeeman sublevels. In the previous section we have defined the vertices $\mathcal{V}^{(i)}$ and $\mathcal{V}^{(c)}$ which were described, respectively, as the building blocks of the average intensity and of the correlation. These vertices play the same role here. Consider the average intensity. From (169), (170), and the definition of the amplitudes A, it contains terms like

$$|A_i^{\{m\}}|^2 \propto |\langle m_{1I}|U|m_{1F}\rangle|^2 \, |\langle m_{2I}|U|m_{2F}\rangle|^2 \cdots |\langle m_{n_iI}|U|m_{n_iF}\rangle|^2 \tag{172}$$

where the operator U has been defined in the previous section, and the subscripts I and F denote initial and final Zeeman sublevels, respectively. Averaging (172) over the internal quantum numbers m_{iI}, summing over m_{iF}, and using the definition (147) lead to

$$\overline{|A_i^{\{m\}}|^2}^{\{m\}} \propto \underbrace{\mathcal{V}^{(i)}\mathcal{V}^{(i)} \cdots \mathcal{V}^{(i)}}_{n_i \text{ times}} \ . \tag{173}$$

Similarly, using (148) and the numerator of (171), it can be easily verified that the typical contribution to the correlation is

$$\overline{A_i^{\{m\}} A_i^{\{m'\}}}^{\{m,m'\}} \propto \underbrace{\mathcal{V}^{(c)}\mathcal{V}^{(c)}\ldots\mathcal{V}^{(c)}}_{n_i \text{ times}} . \tag{174}$$

The two vertices, $\mathcal{V}^{(i)}$ and $\mathcal{V}^{(c)}$, thus account for single scattering events that build the whole multiple scattering path. Such a scattering event corresponds to a real physical quantity (cross section) in the case of intensity. For the correlation, on the other hand, it can be said to be virtual because no process occurs, in which two photons are actually scattered simultaneously by an atom. Formally, as already mentioned, the two quantities $\mathcal{V}^{(i)}$ and $\mathcal{V}^{(c)}$ play the same role. The vertices characterize exclusively the interaction between the light and the scatterers.

Another point which was already discussed earlier, concerns the non-degenerate ground state, $J = 1$. In this case there is only one internal configuration, so that $\{m\} = \{m'\}$ and there is no meaning for the averaging over internal degrees of freedom. It is straightforward to show that for non-degenerate scatterers the Rayleigh law $C_{abab} = 1$ is obtained in (171). For degenerate scatterers with $J > 1$, the correlation can in principle exceed the Rayleigh law. To illustrate this, let us assume that all amplitudes are equal. This gives $\sqrt{C_{abab}} = \sum_i J^{2n_i} / \sum_i J^{n_i}$ which, for $n_i \gg 1$ and $J > 1$, is much larger than 1. Note that this upper bound expression coincides with the one obtained previously for the two atoms-single scattering case, up to a factor of $1/2$ which results from the fact, that in the latter case it is not legitimate to neglect pairs of trajectories that share scatterers. In what follows we present an explicit calculation which indeed shows an enhancement of the correlation above the Rayleigh limit, provided that the scatterers are such that $J > 1$. The effect of the internal structure is, therefore, important only for atoms having a degenerate ground state.

5.3 The method of calculation

In Chapters 2 and 3 we have surveyed the method of calculating the quantities of interest, such as the average transmitted intensity and the function $Corr(aba'b')$. The method involves essentially a continuous limit description of the problem, where diffusion theory accounts for the light propagation within the medium. This is done by means of the Diffuson function (see (28)

of Chapter 2) that corresponds, in the real space, to all multiple scattering sequences between two given scatterers. In particular, we have obtained for the slab geometry the expression (66) (see Chapter 3)

$$\overline{\mathcal{T}}_{ab} = \frac{l^2}{(4\pi)^2}\int_S d^2\mathbf{R}_\perp \mathcal{D}(\mathbf{R}_\perp, l, L-l) \tag{175}$$

for the average intensity, and (82) in Chapter 3

$$Corr(aba'b') = \left(\frac{l^2}{(4\pi)^2}\int_S d\mathbf{R}_\perp e^{ik\mathbf{R}_\perp\cdot\mathbf{a}}\mathcal{D}(\mathbf{R}_\perp, l, L-l)\right)^2 \tag{176}$$

for the correlation. Here it was assumed that $\mathbf{a} = \mathbf{b}$, explaining the absence of the δ-function appearing in (82).

As described in Chapter 2, the Diffusons $\mathcal{D}$ account for the propagation of the scattered intensity between two endpoints inside the sample, and are thus built out of the iteration of (i) the single scattering vertex, and (ii) the propagation of the photon between two scattering events, denoted by $\mathcal{W}$. In Fourier space, the Diffuson is given by (see (29) of Chapter 2)

$$\mathcal{D} = \mathcal{V} + \mathcal{V}\mathcal{W}\mathcal{V} + \cdots = \mathcal{V} + \mathcal{D}\mathcal{W}\mathcal{V} \ . \tag{177}$$

In this iterative equation $\mathcal{D}$ and $\mathcal{W}$ are functions of $\mathbf{Q}$, which is the Fourier variable of $\mathbf{R} = \mathbf{r}' - \mathbf{r}$, where $\mathbf{r}$ and $\mathbf{r}'$ are the positions of two scatterers. All quantities in (177) are dimensionless. Conventionally, the cross section $\mathcal{V}$ is normalized by $3\langle\sigma\rangle_{cl}/2$, where the averaged cross section for classical scatterers is found by substituting in (126) of Chapter 4, $j_g = 0$ and $j_e = 1$, giving $\langle\sigma\rangle_{cl} = 3\lambda^2/2\pi$. As a result, the total cross section obtained from $\mathcal{V}^{(i)}$ is $\langle\sigma\rangle/(3\langle\sigma\rangle_{cl}/2) = 2a_{j_g j_e}/3$.

There are, however, two essential differences between the results of the previous chapters and that of the present case. First, the intensity Diffuson, $\mathcal{D}^{(i)}$, obtained from the iteration of $\mathcal{V}^{(i)}$, is generally different from $\mathcal{D}^{(c)}$, the correlation Diffuson, which is obtained from the vertex $\mathcal{V}^{(c)}$. Second, as opposed to the scalar description of light in Chapters 2 and 3, here the photons polarization is important. This can be seen clearly if we rewrite the expressions for the vertices in the more explicit form

$$\begin{aligned}\mathcal{V}^{(i)}(\mathbf{e}_1, \mathbf{e}_2) = \frac{\mathcal{G}}{J}\sum_{m_{1,2}}\sum_{MM'}&\langle m_2|\mathbf{d}\cdot\mathbf{e}_2^*|M\rangle\langle M|\mathbf{d}\cdot\mathbf{e}_1|m_1\rangle \\ &\times\langle m_1|\mathbf{d}\cdot\mathbf{e}_1^*|M'\rangle\langle M'|\mathbf{d}\cdot\mathbf{e}_2|m_2\rangle\end{aligned} \tag{178}$$

and

$$\mathcal{V}^{(c)}(\mathbf{e}_1,\mathbf{e}_2,\mathbf{e}_3,\mathbf{e}_4)=\frac{\mathcal{G}}{J^2}\sum_{m_{1,\ldots,4}}\sum_{MM'}\langle m_2|\mathbf{d}\cdot\mathbf{e}_2^*|M\rangle\langle M|\mathbf{d}\cdot\mathbf{e}_1|m_1\rangle \\ \times\langle m_3|\mathbf{d}\cdot\mathbf{e}_3^*|M'\rangle\langle M'|\mathbf{d}\cdot\mathbf{e}_4|m_4\rangle \qquad (179)$$

using (147), (148), and the definition of the operator U in Section 5.1. We note that the correlation vertex, because it is a product of two amplitudes corresponding to distinct photons, depends on two incoming and two outgoing polarization vectors. Moreover, $\mathcal{V}^{(i)}$ is obtained as a special case of $\mathcal{V}^{(c)}$ by setting $m_1=m_3$, $m_2=m_4$, $\mathbf{e}_1=\mathbf{e}_3$, $\mathbf{e}_2=\mathbf{e}_4$, and multiplying it by J.

The decomposition of a vector $\mathbf{A}$ into the spherical components is [34]

$$\mathbf{A}=\sum_{\mu=-1}^{1}(-)^{\mu}A_{\mu}\sigma_{-\mu} \qquad (180)$$

where the spherical basis vectors σ_μ ($\mu=-1,+1,0$) are defined in Section 4.4. From (180) it also follows that

$$A_\mu=\mathbf{A}\cdot\sigma_\mu \qquad (181)$$

and

$$\mathbf{A}\cdot\mathbf{B}=\sum_{\mu}(-)^{\mu}A_{\mu}B_{-\mu}\ . \qquad (182)$$

From the definition of the spherical basis vectors we notice that

$$\sigma_\mu^*=(-)^{\mu}\sigma_{-\mu}\ ,\ \ \sigma_\mu\cdot\sigma_\nu=(-)^{\mu}\delta_{\mu,-\nu}\ . \qquad (183)$$

Thus

$$\mathbf{e}_1=\sum_{\mu}(-)^{\mu}(e_1)_{\mu}\sigma_{-\mu}\ ,\ \ \mathbf{e}_2^*=\sum_{\mu}(e_2)_{\mu}^*\sigma_\mu \qquad (184)$$

so that

$$\mathbf{d}\cdot\mathbf{e}_1=\sum_{\mu=-1}^{1}(-)^{\mu}d_{\mu}(e_1)_{-\mu} \qquad (185)$$

and

$$\mathbf{d}\cdot\mathbf{e}_2^*=\sum_{\mu=-1}^{1}d_{\mu}(e_2)_{\mu}^*\ . \qquad (186)$$

It is useful to decompose the vertices into their spherical components, namely

$$\begin{aligned}\mathcal{V}^{(i)}_{\alpha\beta\gamma\delta} &= \frac{\mathcal{G}}{J}\sum_{m_{1,2}}\sum_{MM'}\langle m_2|\mathbf{d}\cdot\sigma^*_\gamma|M\rangle\langle M|\mathbf{d}\cdot\sigma_\alpha|m_1\rangle\langle m_1|\mathbf{d}\cdot\sigma^*_\beta|M'\rangle\langle M'|\mathbf{d}\cdot\sigma_\delta|m_2\rangle \\ &= \frac{\mathcal{G}}{J}\sum_{m_{1,2}}\sum_{MM'}(-)^{\beta+\gamma}\langle m_2|d_{-\gamma}|M\rangle\langle M|d_\alpha|m_1\rangle\langle m_1|d_{-\beta}|M'\rangle\langle M'|d_\delta|m_2\rangle \quad (187)\end{aligned}$$

and

$$\begin{aligned}\mathcal{V}^{(c)}_{\alpha\beta\gamma\delta} &= \frac{\mathcal{G}}{J^2}\sum_{m_{1,\ldots,4}}\sum_{MM'}\langle m_2|\mathbf{d}\cdot\sigma^*_\gamma|M\rangle\langle M|\mathbf{d}\cdot\sigma_\alpha|m_1\rangle\langle m_3|\mathbf{d}\cdot\sigma^*_\beta|M'\rangle\langle M'|\mathbf{d}\cdot\sigma_\delta|m_4\rangle \\ &= \frac{\mathcal{G}}{J^2}\sum_{m_{1,\ldots,4}}\sum_{MM'}(-)^{\beta+\gamma}\langle m_2|d_{-\gamma}|M\rangle\langle M|d_\alpha|m_1\rangle\langle m_3|d_{-\beta}|M'\rangle\langle M'|d_\delta|m_4\rangle \quad (188)\end{aligned}$$

where $\alpha,\beta,\gamma,\delta = -1,+1,0$. Here d_λ denotes the $\lambda = -1,+1$,or 0 spherical component of the electric dipole vector $\mathbf{d}$. We have also used the fact that $\sigma^*_\lambda \cdot \mathbf{d} = (-)^\lambda d_{-\lambda}$. In the next section, we will calculate further these expressions.

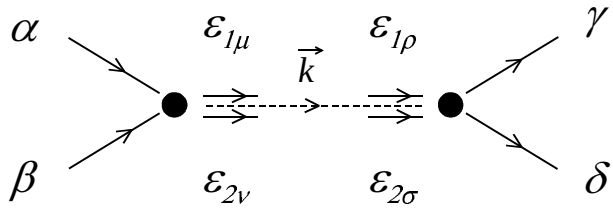

Figure 11: *The structure of the tensor $\mathcal{P}$. Between the two successive scattering events, represented by the black circles, the propagation is free of any other scatterings. The quantity $\mathcal{P}_{\mu\nu\rho\sigma}$, built of two amplitudes having polarization vectors $\hat{\varepsilon}_1$ and $\hat{\varepsilon}_2$, corresponds to the μ and ν components of the polarization vectors at the beginning of the propagation, and to the ρ and σ components of the polarizations just before the next scattering.*

To find the term $\mathcal{W}$, which corresponds to the free intensity propagation between two scattering events, we first write it as $\mathcal{W} = W\mathcal{P}$. W is the scalar part, *i.e.* the polarization-independent part, of the free propagator, which in Fourier space is given by (see Appendix A)

$$W(\mathbf{Q}) = \frac{3}{2a_{j_g j_e}}\left(1 - \frac{DQ^2 l}{c}\right) \quad (189)$$

where c is the velocity of light, $Q = |\mathbf{Q}|$, and $D = cl/3$ is the photon diffusion coefficient. $\mathcal{P}$ is the polarization dependent part of $\mathcal{W}$, and it is decomposed into spherical components in a way similar to (187) and (188), to form a rank four tensor $\mathcal{P}_{\mu\nu\rho\sigma}$. This tensor can be found as follows (see Figure 11). We consider a pair of amplitudes that correspond to the same scattering sequence, and look at two successive scattering events. After the first scattering, the two amplitudes proceed with random but identical wave vector $\hat{\mathbf{s}} = \mathbf{k}/k$ towards the next scatterer. In between the two scatterings, the direct amplitude (the upper one in Figure 11) can have two independent polarizations $\hat{\varepsilon}$ and $\hat{\varepsilon}'$. To obtain $\mathcal{P}_{\mu\nu\rho\sigma}$ we must project $\hat{\varepsilon}$ and $\hat{\varepsilon}'$ onto their μ and ρ components. The direct amplitude should be multiplied, therefore, by $\hat{\varepsilon}^*_\mu \hat{\varepsilon}_\rho + \hat{\varepsilon'}^*_\mu \hat{\varepsilon}'_\rho = \delta_{\mu,-\rho}(-1)^\mu - \hat{s}_\mu \hat{s}_\rho$, where we have used the orthonormality of $\hat{\varepsilon}$, $\hat{\varepsilon}'$, and $\mathbf{s}$. The complex conjugation results from the μ component that belongs to an outgoing photon. The second, conjugate amplitude (the lower one in Figure 11) is multiplied by a similar expression for the components ν and σ. Finally, since the vector $\mathbf{s}$ in between scatterings is random and unknown, we average over its direction so that

$$\mathcal{P}_{\mu\nu\rho\sigma} = \langle (\delta_{\mu,-\rho}(-1)^\mu - \hat{s}_\mu \hat{s}_\rho)(\delta_{\nu,-\sigma}(-1)^\nu - \hat{s}_\nu \hat{s}_\sigma) \rangle_{\hat{\mathbf{s}}} \ . \tag{190}$$

The iteration (177) can be now written in the tensorial form

$$\mathcal{D}^{(i,c)}_{\alpha\beta\gamma\delta} = \mathcal{V}^{(i,c)}_{\alpha\beta\gamma\delta} + W \sum_{\mu\nu\rho\sigma} \mathcal{D}^{(i,c)}_{\alpha\beta\mu\nu} \mathcal{P}_{\mu\nu\rho\sigma} \mathcal{V}^{(i,c)}_{\rho\sigma\gamma\delta} \ . \tag{191}$$

We now wish to find an analytic expression for $\mathcal{D}^{(i,c)}$ in terms of $\mathcal{V}^{(i,c)}$ and $\mathcal{W}$. As a first step, we note that the rank four tensors $\mathcal{D}$, $\mathcal{V}$, and $\mathcal{W}$ have 81 components each and can be arranged as 9×9 matrices, as explained later on. We thus write (191), in matrix form, as

$$\mathcal{D} = (I + W\mathcal{V}\mathcal{P} + (W\mathcal{V}\mathcal{P})^2 + \cdots)\mathcal{V} \tag{192}$$

where I is the unit matrix. For the simplicity of notation, we do not differentiate here between the two cases of intensity and correlation. Our method consists in using the spectral decomposition theorem [35] (see Appendix B), which allows to decompose a matrix into a sum of projectors. Applying the theorem to $\mathcal{V}\mathcal{P}$ we have

$$\mathcal{V}\mathcal{P} = \sum_K u_K T_K \tag{193}$$

with the u_K's being the *different* eigenvalues of $\mathcal{VP}$, and the T_K's constitute an orthonormal set of matrices with the properties

$$T_i T_j = \delta_{ij} T_i \quad , \quad \sum_i T_i = I \quad . \tag{194}$$

Substituting (193) in (192), and using the properties of the T_K's, we find

$$\begin{aligned} \mathcal{D} &= \left(\sum_K T_K + W \sum_K u_K T_K + W^2 \sum_K u_K^2 T_K + \cdots \right) \mathcal{V} \\ &= \sum_K \left(\sum_{n=0}^{\infty} (W u_K)^n \right) T_K \mathcal{V} \end{aligned} \tag{195}$$

so that the Diffuson may be written as

$$\mathcal{D} = \sum_K U_K \mathcal{V}_K \tag{196}$$

with

$$U_K = \frac{1}{1 - W u_K} \tag{197}$$

and the matrices $\mathcal{V}_K = \mathcal{V} T_K$. Taking into account (189) we obtain

$$U_K(\mathbf{Q}) = \frac{2c}{3l} a_{j_g j_e} \frac{1/u_K}{\gamma_K + DQ^2} \tag{198}$$

The quantities γ_K are given by

$$\gamma_K = \frac{c}{l} \left(\frac{2 a_{j_g j_e}}{3 u_K} - 1 \right) \tag{199}$$

and are the damping rates of the *mode* K. To see this, let us write (198) in real space

$$U_K(\mathbf{R}, t) = \frac{1}{u_K} \mathcal{D}_0(\mathbf{R}, t) e^{-\gamma_K t} \tag{200}$$

where $\mathbf{R} = \mathbf{r}' - \mathbf{r}$ is the Fourier variable of $\mathbf{Q}$, $\mathbf{r}$ and $\mathbf{r}'$ are the two endpoints of the diffusion process, and $\mathcal{D}_0$, denoted by just $\mathcal{D}$ in Chapters 2 and 3, is the infinite space Diffuson for the case of classical scatterers and scalar light. We have thus separated the diffusion mode K into a classical part, $\mathcal{D}_0$,

and another part that accounts for the internal structure of the scatterers, namely, $e^{-\gamma_K t}/u_K$.

The Diffuson tensors are thus found, using (196) and (200), to be

$$\mathcal{D}^{(i,c)}_{\alpha\beta\gamma\delta}(\mathbf{R},t) = \sum_K \frac{1}{u_K^{(i,c)}} (\mathcal{V}_K^{(i,c)})_{\alpha\beta\gamma\delta} \mathcal{D}_0(\mathbf{R},t) e^{-\gamma_K^{(i,c)} t} \quad . \tag{201}$$

where we now distinguish between the two cases of intensity and correlation. The Diffuson, since it describes the propagation of intensity, is a sum of pairs of amplitudes that correspond to all possible multiple scattering paths, from the first to the last scattering events. $\mathcal{D}^{(i,c)}_{\alpha\beta\gamma\delta}$ thus appears as the decomposition of the Diffuson function into the α and β components of the incoming light polarization, one component for each of the two amplitudes, and the γ and δ components of the outgoing polarization. To restore the Diffuson function that corresponds to the slab geometry and for determined incoming and outgoing polarizations, we have to (i) substitute the expression for the Diffuson in a slab (Section 2.3), and (ii) compose all the $\alpha\beta\gamma\delta$ projections back together. Moreover, since we are interested in the total transmitted intensity, (201) must be integrated over all scattering times t. We finally obtain for the Diffuson, in real space and using the notation of Section 2.3, the expression

$$\mathcal{D}^{(i,c)}(\mathbf{r},\mathbf{r}') = \sum_K Y_K^{(i,c)} \int_0^\infty dt \;\; \mathcal{D}_0(\mathbf{R}_\perp, z, z', t) \;\; e^{-\gamma_K^{(i,c)} t} \tag{202}$$

with

$$Y_K^{(i)} = \frac{1}{u_K^{(i)}} \sum_{\alpha\beta\gamma\delta} (-)^{\alpha+\delta} (\mathbf{e}_a)_{-\alpha} (\mathbf{e}_b)^*_{\gamma} (\mathbf{e}_a)^*_{-\beta} (\mathbf{e}_b)_\delta \left(\mathcal{V}_K^{(i)}\right)_{\alpha\beta\gamma\delta} , \tag{203}$$

and

$$Y_K^{(c)} = \frac{1}{u_K^{(c)}} \sum_{\alpha\beta\gamma\delta} (-)^{\alpha+\delta} (\mathbf{e}_a)_{-\alpha} (\mathbf{e}_b)^*_{\gamma} (\mathbf{e}_{a'})^*_{-\beta} (\mathbf{e}_{b'})_\delta \left(\mathcal{V}_K^{(c)}\right)_{\alpha\beta\gamma\delta} . \tag{204}$$

Here $\mathbf{e}_{a,a'}$ and $\mathbf{e}_{b,b'}$ are respectively the incoming and outgoing light polarization vectors. We note that for the correlation, there are generally two incoming and two outgoing directions in (204), respective to the two channels ab and $a'b'$. On the other hand, for the intensity $a = a'$ and $b = b'$, since $\mathcal{D}^{(i)}$ corresponds to a single channel.

The meaning of the γ_K's appears clearly in (202). For $\gamma_K = 0$ the mode K behaves as a vector wave diffusing in a medium composed of classical scatterers. In particular, it is infinite range (no damping), which expresses energy conservation. If $\gamma_K > 0$ the mode K is damped with the characteristic time $1/\gamma_K$. From (199), $1/\gamma_K$ is given in units of l/c, which is the elastic mean free time. The ratio $(c/l)/\gamma_K$ thus gives the number of scattering events over which the mode K is damped. Therefore, if $(c/l)/\gamma_K$ is small enough (on the order of 1), the mode K is rapidly damped and its contribution to $\mathcal{D}$ is negligible. On the other hand, if $(c/l)/\gamma_K$ is greater than the (normalized) Thouless time $3b^2$, where $b = L/l$ is the optical depth of the sample, the damping is too weak to eliminate the contribution of the mode K. The third possibility $\gamma_K < 0$ seems peculiar, since it means an amplification of the mode K. However, we shall see in the following that this amplification is found for the correlation Diffuson $\mathcal{D}^{(c)}$ in the case of degenerate atomic scatterers. This enhancement effect has been explained previously in this chapter, on a more general ground than the present diffusion model.

It follows from (199), that the characteristic number of scattering events for damping (or amplification), $(c/l)/\gamma_K$, depends only on the interaction between the light and a single scatterer, that is, on the vertices $\mathcal{V}^{(i,c)}$. As discussed previously, the quantity $2a_{j_g j_e}/3$ corresponds to the total scattering cross section related to the transition $j_g \to j_e$. Therefore, the existence of a $\gamma_K = 0$ mode is equivalent to the existence of at least one u_K that is exactly equal to the total normalized cross section. An eigenvalue u_K that is smaller or larger than the total normalized cross section amounts, respectively, to a decaying mode ($\gamma_K > 0$) or an enhanced ($\gamma_K < 0$) mode.

Finally, distinguishing between the two kinds of Diffuson functions, the expressions for the average intensity and the correlation, (175) and (176), becomes

$$\overline{\mathcal{T}}_{ab} = \frac{l^2}{(4\pi)^2} \sum_K Y_K^{(i)} \int_S d^2\mathbf{R}_\perp \int_0^\infty dt \mathcal{D}_0(\mathbf{R}_\perp, l, L-l) e^{-\gamma_K^{(i)} t} \tag{205}$$

and

$$Corr(aba'b') = \left(\frac{l^2}{(4\pi)^2} \sum_K Y_K^{(c)} \int_S d\mathbf{R}_\perp \int_0^\infty dt e^{ik\mathbf{R}_\perp \cdot \mathbf{a}} \mathcal{D}_0(\mathbf{R}_\perp, l, L-l) e^{-\gamma_K^{(c)} t} \right)^2 \tag{206}$$

where we have also used the results of Section 2.3.

5.4 The vertex

The tensorial forms $\mathcal{V}^{(i,c)}_{\alpha\beta\gamma\delta}$ of the vertices $\mathcal{V}^{(i,c)}$, contain all information about the interaction between light and scatterers in (191), from which the Diffusons are obtained. Therefore, most of the physics of the problem is in the vertices. Also the difference, when it exists, between the intensity ($\mathcal{D}^{(i)}$) and the correlation ($\mathcal{D}^{(c)}$) Diffusons resides in the difference between $\mathcal{V}^{(i)}$ and $\mathcal{V}^{(c)}$. From (147) and (148) we notice that for classical scatterers, namely $J = 1$, there is no difference between the two vertices, which leads to the Rayleigh law. On the other hand, for $J > 1$ the difference between $\mathcal{V}^{(i)}$ and $\mathcal{V}^{(c)}$ is clear. For $\mathcal{V}^{(c)}$, shown schematically in Figure 12, the two scattering amplitudes (on the *same* atom), correspond to two distinct events, *i.e.* to two distinct photons, and thus to generally two pairs of initial and final atomic internal states. In the case of $\mathcal{V}^{(i)}$, the two coupled amplitudes participating in the scattering, belong to the same photon and thus find the atom in the same quantum number m_1 before the scattering, and leave it after the scattering in the same quantum number m_2.

Our aim in this section is to develop an expression for the interaction vertex. We focus on $\mathcal{V}^{(c)}$, the correlation vertex which we shall denote in this section by $\mathcal{V}$. As was mentioned, $\mathcal{V}^{(i)}$ is obtained as a limiting case of $\mathcal{V}^{(c)}$ by setting $m_1 = m_3$, $m_2 = m_4$, $\mathbf{e}_1 = \mathbf{e}_3$, and $\mathbf{e}_2 = \mathbf{e}_4$.

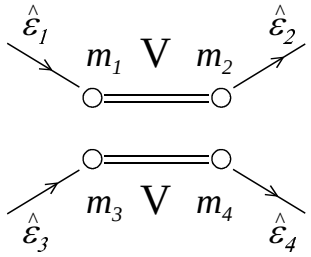

Figure 12: *The vertex $\mathcal{V}^{(c)}$. m_i are the various Zeeman quantum numbers. $\hat{\varepsilon}_i$ are the polarization vectors. V denotes an electric dipole interaction Hamiltonian.*

With the help of the Wigner-Eckart theorem (Section 4.4) we obtain for

the second matrix element on the *r.h.s* of (188)

$$\langle j_e M|d_\alpha|j_g m_1\rangle = (-)^{j_e-M}\langle j_e||\mathbf{d}||j_g\rangle \begin{pmatrix} j_e & 1 & j_g \\ -M & \alpha & m_1 \end{pmatrix} \tag{207}$$

The first matrix element on the *r.h.s* of (188) becomes

$$\langle j_g m_2|d_{-\gamma}|j_e M\rangle = (-)^{j_g-m_2}\langle j_g||\mathbf{d}||j_e\rangle \begin{pmatrix} j_g & 1 & j_e \\ -m_2 & -\gamma & M \end{pmatrix} \tag{208}$$

Using the properties of the $3j$-symbols defined in Section 4.4, we simultaneously multiply, in the last expression, the second row by -1 and make a permutation of the first and third columns. This gives

$$\langle j_g m_2|d_{-\gamma}|j_e M\rangle = (-)^{j_g-m_2}\langle j_g||\mathbf{d}||j_e\rangle \begin{pmatrix} j_e & 1 & j_g \\ -M & \gamma & m_2 \end{pmatrix} \tag{209}$$

Expressing in a similar way the two other matrix elements in (188), the tensorial form of the vertex becomes

$$\mathcal{V}_{\alpha\beta\gamma\delta} = \mathcal{C} \sum_{m_1,\ldots,m_4} \sum_{M,M'} (-)^{2j_e-M-M'}(-)^{2j_g-m_2-m_3}(-)^{\beta+\gamma}$$
$$\times \begin{pmatrix} j_e & 1 & j_g \\ -M & \alpha & m_1 \end{pmatrix} \begin{pmatrix} j_e & 1 & j_g \\ -M & \gamma & m_2 \end{pmatrix} \begin{pmatrix} j_e & 1 & j_g \\ -M' & \beta & m_3 \end{pmatrix} \begin{pmatrix} j_e & 1 & j_g \\ -M' & \delta & m_4 \end{pmatrix} \tag{210}$$

with $\mathcal{C} = (\mathcal{G}/J^2)|\langle j_g||\mathbf{d}||j_e\rangle\langle j_e||\mathbf{d}||j_g\rangle|^2$. Expression (210) can be evaluated numerically to give the elements of $\mathcal{V}_{\alpha\beta\gamma\delta}$.

More information about the vertices can be gained from the following analysis. Using the operator (previously defined)

$$U(\mathbf{e},\mathbf{e}') = \sum_M \mathbf{e}'^* \cdot \mathbf{d}|M\rangle\langle M|\mathbf{e}\cdot\mathbf{d} \tag{211}$$

the vertex rewrites (see (179))

$$\mathcal{V}(\mathbf{e}_1,\mathbf{e}_2,\mathbf{e}_3,\mathbf{e}_4) = \frac{\mathcal{G}}{J^2} \sum_{m_1,\ldots,m_4} \langle m_2|U(\mathbf{e}_1,\mathbf{e}_2)|m_1\rangle\langle m_3|U^\dagger(\mathbf{e}_3,\mathbf{e}_4)|m_4\rangle \tag{212}$$

Using the closure relation we have

$$U(\mathbf{e},\mathbf{e}') = \sum_{m_g m_g'} \sum_M |m_g'\rangle\langle m_g'|\mathbf{e}'^*\cdot\mathbf{d}|M\rangle\langle M|\mathbf{e}\cdot\mathbf{d}|m_g\rangle\langle m_g| \tag{213}$$

where $|m_g\rangle$ and $|m'_g\rangle$ denote any atomic ground state sublevel. With the help of the Wigner-Eckart theorem we can then write

$$U(\mathbf{e},\mathbf{e}') = \langle j_g||\mathbf{d}||j_e\rangle\langle j_e||\mathbf{d}||j_g\rangle \sum_{pp'}\sum_{m_g m'_g}\sum_{M} |m'_g\rangle\langle m_g|(-)^{j_g-m_g+j_e-M} \times \begin{pmatrix} j_g & 1 & j_e \\ -m_g & p & M \end{pmatrix}\begin{pmatrix} j_e & 1 & j_g \\ -M & p' & m'_g \end{pmatrix} e_{-p}e'^{*}_{-p'}(-)^{p+p'} \quad (214)$$

Summing over M one obtains [32]

$$U(\mathbf{e},\mathbf{e}') = \langle j_g||\mathbf{d}||j_e\rangle\langle j_e||\mathbf{d}||j_g\rangle \sum_{kq}\sum_{pp'}\sum_{m_g} |m_g - q\rangle\langle m_g|(-)^{1-m_g+j_e+k}(2k+1) \times \begin{Bmatrix} 1 & 1 & k \\ j_g & j_g & j_e \end{Bmatrix}\begin{pmatrix} 1 & 1 & k \\ p & p' & -q \end{pmatrix}\begin{pmatrix} j_g & j_g & k \\ -m_g & m_g-q & q \end{pmatrix} e_{-p}e'^{*}_{-p'} \quad (215)$$

where $k = 0, 1, 2$ and $|q| \leq k$. The $6j$-symbol (the quantity with the curly brackets on the *r.h.s*) is defined in Appendix C. We now decompose $U(\mathbf{e},\mathbf{e}')$ by means of a set of irreducible tensor operators [36]

$$Q^k_q \equiv \sum_{m_g} |m_g - q\rangle\langle m_g|(-)^{m_g-j_g}\begin{pmatrix} j_g & j_g & k \\ -m_g & m_g-q & q \end{pmatrix}\sqrt{2k+1} \quad (216)$$

so that

$$U(\mathbf{e},\mathbf{e}') = \sum_{k=0}^{2}\sum_{q=-k}^{k} U_{kq}(\mathbf{e},\mathbf{e}')Q^k_q \quad (217)$$

with

$$U_{kq}(\mathbf{e},\mathbf{e}') = \langle j_g||\mathbf{d}||j_e\rangle\langle j_e||\mathbf{d}||j_g\rangle \sum_{pp'}(-)^{1+j_g+k}\sqrt{2k+1} \times \begin{Bmatrix} 1 & 1 & k \\ j_g & j_g & j_e \end{Bmatrix}\begin{pmatrix} 1 & 1 & k \\ p & p' & -q \end{pmatrix} e_{-p}e'^{*}_{-p'} \quad (218)$$

$\mathcal{V}$ can be now expressed in the form

$$\mathcal{V}(\mathbf{e}_1,\mathbf{e}_2,\mathbf{e}_3,\mathbf{e}_4) = \mathcal{C}\sum_{kq}\sum_{\tilde{k}\tilde{q}}\sum_{pp'}\sum_{\tilde{p}\tilde{p}'}\sqrt{(2k+1)(2\tilde{k}+1)}\begin{Bmatrix} 1 & 1 & k \\ j_g & j_g & j_e \end{Bmatrix}\times \times\begin{pmatrix} 1 & 1 & k \\ p & p' & -q \end{pmatrix}\begin{Bmatrix} 1 & 1 & \tilde{k} \\ j_g & j_g & j_e \end{Bmatrix}\begin{pmatrix} 1 & 1 & \tilde{k} \\ \tilde{p} & \tilde{p}' & -\tilde{q} \end{pmatrix}(\mathbf{e}_1)_{-p}(\mathbf{e}^*_2)_{-p'}(\mathbf{e}^*_4)_{\tilde{p}'}(\mathbf{e}_3)_{\tilde{p}}(-)^{\tilde{p}+\tilde{p}'} \times \sum_{m_1\ldots m_4}\langle m_2|Q^k_q|m_1\rangle\langle m_3|Q^{\tilde{k}}_{-\tilde{q}}|m_4\rangle(-)^{-\tilde{q}} \quad (219)$$

We further define

$$S_q^k \equiv \sqrt{2k+1}\sum_m \sigma_m(\sigma_{m-q})^*(-)^{m-1}\begin{pmatrix} 1 & 1 & k \\ m & q-m & -q \end{pmatrix} \tag{220}$$

where the σ_m's are the spherical basis unit vectors defined in Section 4.4, so that

$$\begin{aligned}
&\sqrt{2k+1}\sum_{pp'}\begin{pmatrix} 1 & 1 & k \\ p & p' & -q \end{pmatrix} e_{-p}e'^*_{-p'} \\
&= \sqrt{2k+1}\sum_p \begin{pmatrix} 1 & 1 & k \\ p & q-p & -q \end{pmatrix} e_{-p}(e'_{q-p})^*(-)^{q-p} \\
&= \mathbf{e}\cdot\left(\sqrt{2k+1}\sum_p \begin{pmatrix} 1 & 1 & k \\ p & q-p & -q \end{pmatrix} e_{-p}(e_{q-p})^*(-)^{q-p}\right)\cdot\mathbf{e}'^* \\
&= \mathbf{e}\cdot S^k_{-q}\cdot\mathbf{e}'^*(-)^{q+1}
\end{aligned} \tag{221}$$

Taking into account that

$$\begin{aligned}
\sum_{m_g m'_g}\langle m'_g|Q^k_q|m_g\rangle &= \sum_{m_g m'_g}(-)^{m_g-j_g}\begin{pmatrix} k & j_g & j_g \\ q & m'_g & -m_g \end{pmatrix} \\
&= \sum_{m_g}(-)^{m_g-j_g}\begin{pmatrix} k & j_g & j_g \\ q & m_g-q & -m_g \end{pmatrix} \equiv f_{j_g}(k,q)
\end{aligned} \tag{222}$$

we find finally

$$\mathcal{V}(\mathbf{e}_1,\mathbf{e}_2,\mathbf{e}_3,\mathbf{e}_4) = \mathcal{C}\sum_{k\tilde{k}} s_k s_{\tilde{k}} \sum_{q\tilde{q}} f_{j_g}(k,q)f_{j_g}(\tilde{k},-\tilde{q})(\mathbf{e}_1\cdot S^k_{-q}\cdot\mathbf{e}^*_2)(\mathbf{e}_4\cdot S^{\tilde{k}}_{\tilde{q}}\cdot\mathbf{e}^*_3)(-)^{q+\tilde{q}}(-)^{\tilde{k}-\tilde{q}} \tag{223}$$

with

$$s_k \equiv \begin{Bmatrix} 1 & 1 & k \\ j_g & j_g & j_e \end{Bmatrix} \tag{224}$$

The tensor $\mathcal{V}_{\alpha\beta\gamma\delta}$ is obtained by setting

$$\begin{aligned}
&\mathcal{V}_{\alpha\beta\gamma\delta} = \mathcal{V}(\mathbf{e}_1=\sigma_\alpha,\mathbf{e}_3=\sigma_\beta,\mathbf{e}_2=\sigma_\gamma,\mathbf{e}_4=\sigma_\delta) = \\
&\mathcal{C}\sum_{k\tilde{k}}\sqrt{s_k s_{\tilde{k}}}\sum_{q\tilde{q}} f_{j_g}(k,q)f_{j_g}(\tilde{k},-\tilde{q})(\sigma_\alpha\cdot S^k_{-q}\cdot\sigma^*_\beta)(\sigma_\delta\cdot S^{\tilde{k}}_{\tilde{q}}\cdot\sigma^*_\gamma)(-)^{q+\tilde{q}}(-)^{\tilde{k}-\tilde{q}}
\end{aligned} \tag{225}$$

Since $k, \tilde{k} = 0, 1, 2$, there are generally nine combinations $k\tilde{k}$ in (225) that describe the change of photon polarization due to scattering.

For the specific case of the intensity vertex $\mathcal{V}^{(i)}_{\alpha\beta\gamma\delta}$ we have $m_1 = m_3$ and $m_2 = m_4$. In this case [37]

$$\sum_{m_1=m_3} \sum_{m_2=m_4} \langle m_2|Q^k_q|m_1\rangle\langle m_3|Q^{\tilde{k}}_{-\tilde{q}}|m_4\rangle = Tr[Q^k_q Q^{\tilde{k}}_{-\tilde{q}}] = \delta_{k,\tilde{k}}\delta_{q,\tilde{q}}(-)^q \quad (226)$$

Therefore, there are only three combinations $k\tilde{k}$ for the intensity vertex $\mathcal{V}^{(i)}$, and only three different eigenvalues.

The condition $k = \tilde{k}$, which holds for $\mathcal{V}^{(i)}$ (226), is related to angular momentum conservation. From (219) and the properties of the $6j$-symbols (Appendix C), it follows that $k, \tilde{k} = 0$, 1, and 2, as if they were the sum of two angular momenta of magnitude 1. Each of the two $6j$-symbols in (219) refers to a different amplitude. In the case of the intensity vertex, $\mathcal{V}^{(i)}$ corresponds to the cross section of a real process, for which the two coupled amplitudes belong to the same photon, and thus to the same physical process. Angular momentum must then be conserved. Mathematically, this fact is reflected in that $k = \tilde{k}$, so that there are only three $k\tilde{k}$ combinations, corresponding to the values 0,1, and 2 as for the addition of two angular momenta of magnitude 1. In contrast, the two amplitudes involved in the correlation vertex $\mathcal{V}^{(c)}$ belong to two different photons. This is a virtual process, in which angular momentum needs not to be conserved. As a result, k and $\tilde{k}$ are generally different, and the product $k\tilde{k}$ has generally nine different values, which is the upper limit. As already mentioned earlier, the distinction between $\mathcal{V}^{(c)}$ and $\mathcal{V}^{(i)}$ exists only if the lower atomic level is degenerate, namely for $j_g > 0$. For the classical case $j_g = 0$, condition (226) always holds.

5.5 Amplified correlation

To find the angular correlation function, what is left to do is to solve for (202), and to substitute in (205) and (206). But to this purpose, we need to find the damping rates γ_K. This is done by numerically calculating the $u^{(i,c)}_K$'s, *i.e.*, the eigenvalues of $\mathcal{V}^{(i,c)}\mathcal{P}$, and then using (199). The results are two sets of damping rates, one that corresponds to the intensity ($\gamma^{(i)}_K$) and one for the correlation ($\gamma^{(c)}_K$).

The matrices that correspond to $\mathcal{V}^{(i)}\mathcal{P}$ and $\mathcal{V}^{(c)}\mathcal{P}$, for the transition $j_g =$

$1 \to j_e = 2$, are found to be

$$\mathcal{V}^{(i)}\mathcal{P}_{(1\to 2)} = \begin{pmatrix} \frac{337}{1620} & 0 & 0 & 0 & \frac{151}{1620} & 0 & 0 & 0 & \frac{28}{405} \\ 0 & \frac{31}{270} & 0 & 0 & 0 & \frac{13}{540} & 0 & 0 & 0 \\ 0 & 0 & \frac{49}{540} & 0 & 0 & 0 & 0 & 0 & 0 \\ 0 & 0 & 0 & \frac{31}{270} & 0 & 0 & 0 & \frac{13}{540} & 0 \\ \frac{151}{1620} & 0 & 0 & 0 & \frac{149}{810} & 0 & 0 & 0 & \frac{151}{1620} \\ 0 & \frac{13}{540} & 0 & 0 & 0 & \frac{31}{270} & 0 & 0 & 0 \\ 0 & 0 & 0 & 0 & 0 & 0 & \frac{49}{540} & 0 & 0 \\ 0 & 0 & 0 & \frac{13}{540} & 0 & 0 & 0 & \frac{31}{270} & 0 \\ \frac{28}{405} & 0 & 0 & 0 & \frac{151}{1620} & 0 & 0 & 0 & \frac{337}{1620} \end{pmatrix} \tag{227}$$

and

$$\mathcal{V}^{(c)}\mathcal{P}_{(1\to 2)} = \begin{pmatrix} \frac{727}{4860} & \frac{59}{972} & \frac{7}{486} & \frac{59}{972} & \frac{301}{4860} & -\frac{1}{243} & \frac{7}{486} & -\frac{1}{243} & \frac{58}{1215} \\ \frac{41}{486} & \frac{115}{972} & \frac{35}{486} & \frac{7}{243} & \frac{91}{972} & \frac{5}{486} & \frac{7}{972} & \frac{7}{972} & \frac{37}{972} \\ \frac{23}{972} & \frac{25}{486} & \frac{35}{243} & \frac{5}{972} & \frac{11}{243} & \frac{25}{486} & \frac{7}{4860} & \frac{5}{972} & \frac{23}{972} \\ \frac{41}{486} & \frac{7}{243} & \frac{7}{972} & \frac{115}{972} & \frac{91}{972} & \frac{7}{972} & \frac{35}{486} & \frac{5}{486} & \frac{37}{972} \\ \frac{65}{972} & \frac{25}{486} & \frac{35}{972} & \frac{25}{486} & \frac{85}{486} & \frac{25}{486} & \frac{35}{972} & \frac{25}{486} & \frac{65}{972} \\ \frac{37}{972} & \frac{5}{486} & \frac{35}{486} & \frac{7}{972} & \frac{91}{972} & \frac{115}{972} & \frac{7}{972} & \frac{7}{243} & \frac{41}{486} \\ \frac{23}{972} & \frac{5}{972} & \frac{7}{4860} & \frac{25}{486} & \frac{11}{243} & \frac{5}{972} & \frac{35}{243} & \frac{25}{486} & \frac{23}{972} \\ \frac{37}{972} & \frac{7}{972} & \frac{7}{972} & \frac{5}{486} & \frac{91}{972} & \frac{7}{243} & \frac{35}{486} & \frac{115}{972} & \frac{41}{486} \\ \frac{58}{1215} & -\frac{1}{243} & \frac{7}{486} & -\frac{1}{243} & \frac{301}{4860} & \frac{59}{972} & \frac{7}{486} & \frac{59}{972} & \frac{727}{4860} \end{pmatrix} \tag{228}$$

Each row (column) in the matrices (227) and (228) corresponds to some combination of two incoming (outgoing) spherical basis components of the polarizations. The first row (column) denote the combination -1-1, the second ones denote -10, and so on: -11 for the third, 0-1 for the fourth, 00 for the fifth, 01 for the sixth, 1-1 for the seventh, 10 for the eighth, and 11 for the last (ninth). Thus, for example, the matrix element (1,1) (first row, first column) corresponds to the element $\mathcal{VP}_{-1-1-1-1}$, the (1,2) matrix element is $\mathcal{VP}_{-1-1-10}$, the (1,3) is $\mathcal{VP}_{-1-1-11}$, the (5,5) is $\mathcal{VP}_{0000}$ *etc.*

The eigenvalues of $\mathcal{V}^{(i)}\mathcal{P}$ in (227) are $u_0^{(i)} = 10/27$ (non-degenerate), $u_1^{(i)} = 0.14$ (3-fold degenerate), and $u_2^{(i)} = 0.09$ (5-fold degenerate), corresponding to $\gamma_0^{(i)} = 0$ (since $2a_{12}/3 = 10/27$), $\gamma_1^{(i)} = 0.6c/l$, and $\gamma_2^{(i)} = 1.1c/l$, where (199) has been used. The mode denoted by 0 is infinite ranged, while the other two decay on time scales of the order of two scattering events, namely, l/c.

The eigenvalues of $\mathcal{V}^{(c)}\mathcal{P}$ in (228) have been also calculated numerically, and the corresponding decay rates are shown in Table 1 (the values are rounded).

$\gamma_0^{(c)}$	$\gamma_1^{(c)}$	$\gamma_2^{(c)}$	$\gamma_3^{(c)}$	$\gamma_4^{(c)}$	$\gamma_5^{(c)}$	$\gamma_6^{(c)}$	$\gamma_7^{(c)}$	$\gamma_8^{(c)}$
-0.18	0.85	0.95	1.85	3.11	3.35	9.00	9.27	23.66

Table 1. Decay rates for the correlation (in units of c/l). These values correspond to the transition $j_g = 1 \to j_e = 2$

The mode 0 corresponds to the condition $u_0^{(c)} > 2a_{12}/3 = 10/27$, leading to a negative decay rate. The remaining eight modes have positive decay rates, and are damped on the time scale of l/c and less. For example, $1/\gamma_1^{(c)} \simeq 1.17l/c$, meaning that this contribution to the diffusion process decays on a length scale of about 1.17 times the mean free path l. $1/\gamma_3^{(c)}, ..., 1/\gamma_8^{(c)} < l/c$, so that these contributions decay before even one scattering event has been taken place. Since any multiple scattering process is at least l-long, it is clear that modes 1 to 8 contribute very negligibly to the correlation function.

In all transitions we have considered, namely, $j_g = 0 \to j_e = 1$, $j_g = 1 \to j_e = 2$, $j_g = 2 \to j_e = 3$, and $j_g = 3 \to j_e = 4$, a similar situation occurs: there are only three $\gamma_K^{(i)}$'s, one of them is zero ($\gamma_0^{(i)} = 0$), and the other two are finite and positive $\gamma_{1,2}^{(i)} > 0$, both of them are on the order of c/l. According to (202) and the discussion that follows it, $\gamma_0^{(i)} = 0$ is related to energy conservation due to the infinite-ranged propagation of the average intensity. It ensures that the incoming energy eventually also leaves. The infinite-ranged mode $\gamma_0^{(i)} = 0$ corresponds to the free diffusion $\mathcal{D}^{(i)} \propto 1/Dq^2$ as discussed in Section 2.3. The other two modes decay very fast, on a time scale of one or two scattering events (l/c). These two modes are thus negligible in multiple scattering, *i.e.*, when the size of the medium L satisfies $L \gg l$, so that the typical scattering path involves many scattering events. A similar behaviour with one infinite-ranged and two rapidly decaying modes,

is obtained for vector light wave and classical scatterers [2]. In the following table, the decay rates of the intensity modes for some atomic transitions are shown.

$j_g \to j_e$	$\gamma_0^{(i)}$	$\gamma_1^{(i)}$	$\gamma_2^{(i)}$
$0 \to 1$	0	0.28	0.67
$1 \to 2$	0	0.62	1.14
$2 \to 3$	0	1.12	3.24
$3 \to 4$	0	1.88	5.37

Table 2. Decay rates for the intensity (in units of c/l).

For the correlation Diffuson with *degenerate* atomic scatterers we obtain a different result. As in Table 1, among the nine modes $\gamma_K^{(c)}$, for $j_g > 0$ we obtain at least one mode with a *negative* damping rate $\gamma_0^{(c)} < 0$, which corresponds to amplification and thus to an enhancement of the correlation function as can be verified from (202). The remaining $\gamma_K^{(c)}$'s are finite, positive, and usually on the order of a few c/l, so that they decay rapidly and have a negligible contribution to $\mathcal{D}^{(c)}$. There is no infinite-ranged mode for correlation. The negative $\gamma_0^{(c)}$ can be explained as follows: from (147) and (148), it turns out that every possible transition that contribute to $\mathcal{V}^{(i)}$, contribute also to $\mathcal{V}^{(c)}$. However, there are contributions to $\mathcal{V}^{(c)}$ that do not appear in $\mathcal{V}^{(i)}$ (see Figure 13). These are cross terms between two coupled

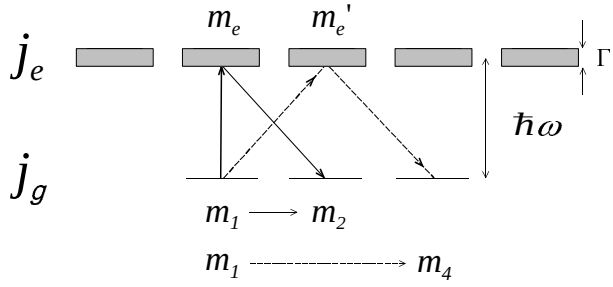

Figure 13: *A process that contributes to $\mathcal{V}^{(c)}$ but not to $\mathcal{V}^{(i)}$, because the final states corresponding to the two amplitudes are not the same.*

amplitudes that do not belong to the same process, as previously explained. As a result, the largest eigenvalue of $\mathcal{V}^{(c)}\mathcal{P}$, denoted by $u_0^{(c)}$, exceeds the largest eigenvalue of $\mathcal{V}^{(i)}\mathcal{P}$, namely $u_0^{(i)} = 2a_{j_g j_e}/3$, thus leading to a negative

damping rate according to (199). In other words, since we take into account more terms in $\mathcal{V}^{(c)}$ than in $\mathcal{V}^{(i)}$, the correlation cross section is larger than the intensity cross section. On the other hand, the mean free path l is the same for both cases of intensity and correlation (it is a measurable quantity characteristic of the transport of real photons in the medium). Thus, each amplitude, whether it is used for the intensity or the correlation vertices, describes a multiple scattering path characterized by the mean free path l. But, l is by definition the characteristic length for a free diffusion without scattering. More precisely, the probability to diffuse freely without scattering decays as $e^{-l/R}$, where R is the distance between the two endpoints of the path. Therefore, increasing the cross section inevitably amounts, in real processes, to a decrease in l [2]. In the case of the correlation Diffuson, the cross section $\mathcal{V}^{(c)}$ becomes larger than $\mathcal{V}^{(i)}$ while l, obtained from the intensity cross section, remains constant. Within the diffusive limit of multiple scattering, therefore, it is as if the correlation diffusion is amplified by the medium. This is reflected in the occurrence of the negative $\gamma_K^{(i)}$. We will return to this argument in the next chapter. For classical scatterers, *i.e.* for $j_g = 0$, there is no difference between the intensity and the correlation vertices, so that both diffusion processes are identical, leading to one infinite-ranged mode $\gamma_0^{(i,c)} = 0$ and to two decaying modes. In Table 3 we list the negative damping rates of the correlation vertex for some examples of atomic transitions.

$j_g \to j_e$	$\gamma_0^{(c)}$
$0 \to 1$	0
$1 \to 2$	-0.18
$2 \to 3$	-0.23
$3 \to 4$	-0.27

Table 3. Negative decay rates of the correlation diffusion (in units of c/l) for some atomic transitions. The absolute value of these rates becomes larger, and thus the amplification effect becomes stronger, as the atomic levels get more and more degenerate.

The average transmitted intensity is now readily found using (68) in Chapter 3 and the fact that the infinite-ranged mode $\gamma_0^{(i)} = 0$ is dominant. From (205)

$$\overline{\mathcal{T}}_{ab} = \frac{Y_0^{(i)} l^2}{(4\pi)^2} \int_S d^2\mathbf{R}_\perp \int_0^\infty dt\, \mathcal{D}_0(\mathbf{R}_\perp, l, L-l) = Y_0^{(i)} \frac{3}{4\pi} \frac{1}{b} \tag{229}$$

where $b = L/l$ is the optical depth.

What is left is to calculate the correlation $Corr(aba'b')$. This is done neglecting all the contributions except for that of the amplified mode $\gamma_0^{(c)} < 0$. Using (206) we may write

$$\sqrt{Corr(aba'b')} = \frac{Y_0^{(c)} l^2}{(4\pi)^2} \int_S d\mathbf{R}_\perp \int_0^\infty dt\, e^{ik\mathbf{R}_\perp \cdot \mathbf{a}}\, \mathcal{D}_0(\mathbf{R}_\perp, l, L-l)\, e^{\gamma_c t} \quad (230)$$

with $\gamma_c = |\gamma_0^{(c)}|$. Following Section 3.3, we notice that the integral over $\mathbf{R}_\perp$ is the Fourier transform of $\mathcal{D}_0(\mathbf{R}_\perp, l, L-l)$, so that

$$\sqrt{Corr(aba'b')} = \frac{Y_0^{(c)} l^2}{(4\pi)^2} \int_0^\infty dt\, \mathcal{D}_0(\mathbf{q}, l, L-l, t)\, e^{\gamma_c t} \quad (231)$$

where $\mathbf{q} = k\mathbf{a}$ is the Fourier variable of $\mathbf{R}_\perp$, and $q = |\mathbf{q}|$ equals k times the angle θ between the directions of the two incoming (and outgoing) beams. The integral in (231) diverges. However, the upper bound is actually not infinite, but bounded by the Thouless time $\tau_D = L^2/D$, which corresponds to the typical diffusion path in a sample of linear dimension L. According to diffusion theory, trajectories which are significantly longer, can be neglected. To calculate the correlation (231) we need to evaluate the integral (47) of Chapter 2, where the decay rate is now negative and the integration upper bound is τ_D. Thus

$$\int_0^{\tau_D} dt \mathcal{D}(\mathbf{q}, l, L-l, t) e^{\gamma_c t} = \frac{8\pi c}{Ll^2} \sum_{n=1}^{\infty} \sin\left(\frac{n\pi}{b}\right) \sin\left(n\pi - \frac{n\pi}{b}\right) \int_0^{\tau_D} dt e^{-t(Dq^2 + \frac{\pi^2 n^2}{\tau_D} - \gamma_c)} \quad . \quad (232)$$

Implementing the integration on the *r.h.s* we find

$$\frac{Ll^2}{4\pi c} \int_0^{\tau_D} dt \mathcal{D}(\mathbf{q}, l, L-l, t) e^{\gamma_c t} = \sum_{n=1}^{\infty} \frac{\cos\left(n\pi(1-2/b)\right) - \cos(n\pi)}{Dq^2 + \frac{\pi^2 n^2}{\tau_D} - \gamma_c} - \sum_{n=1}^{\infty} \left[\cos\left(n\pi(1-2/b)\right) - \cos(n\pi)\right] \frac{e^{-\tau_D(Dq^2 + \pi^2 n^2/\tau_D - \gamma_c)}}{Dq^2 + \frac{\pi^2 n^2}{\tau_D} - \gamma_c} \quad . \quad (233)$$

The term containing the exponent $e^{-\tau_D(Dq^2 + \pi^2 n^2/\tau_D - \gamma_c)}$ on the *r.h.s* corresponds to the correlation amplification. We notice now that a negative

decay rate is not enough to obtain amplification. Rather, the amplification condition is

$$\tau_D D q^2 + \pi^2 n^2 - \tau_D \gamma_c < 0 \qquad \rightarrow \qquad \text{amplification}$$

$$\tau_D D q^2 + \pi^2 n^2 - \tau_D \gamma_c > 0 \qquad \rightarrow \qquad \text{no amplification} \ . \tag{234}$$

As we have seen above (Table 3), γ_c is on the order of $0.2c/l$. Moreover, in multiple scattering experiments usually b does not exceed 7, so that $\tau_D = 3b^2 l/c \sim 150 l/c$ at most, meaning that $\tau_D \gamma_c$ is usually not larger than 30. According to condition (234), this means that correlation amplification is obtained only if (i) q is small, and (ii) $n = 1$, since for $n \geq 2$ $\pi^2 n^2 \geq 40$. If (i) and (ii) does not hold, $\tau_D D q^2 + \pi^2 n^2 - \tau_D \gamma_c > 0$ and the exponent on the *r.h.s* of (233) is negligible. Therefore, rather than summing over n in the second term on the *r.h.s* of (233), we impose $n = 1$. In summing over n in the first term on the *r.h.s* of (233), we use results (49) of Chapter 2. Defining $X(q)^2 = \tau_D \gamma_c - (Lq)^2$ we thus find

$$\frac{Ll^2}{4\pi c} \int_0^{\tau_D} dt \mathcal{D}(\mathbf{q}, l, L-l, t) e^{\gamma_c t} = \tau_D \frac{1 - \cos\left(2X(q)/b\right)}{2X(q)\sin(X(q))} - \tau_D \left[\cos(\pi(1-2/b)) + 1\right] \frac{e^{-\pi^2 + X(q)^2}}{\pi^2 - X(q)^2} \ . \tag{235}$$

Using (231) we finally obtain

$$\sqrt{Corr(aba'b')} = \frac{3bY_0^{(c)}}{4\pi} \left(\frac{\sin^2(\frac{X(q)}{b})}{X(q)\sin X(q)} - 2\sin^2(\frac{\pi}{b}) \frac{e^{-\pi^2 + X(q)^2}}{\pi^2 - X(q)^2} \right) \ . \tag{236}$$

It is instructive to study the classical limit of this expression, namely, the case for which $\gamma_c = 0$, meaning that there is no correlation amplification. As already discussed, this happens for a non-degenerate atomic ground state. In this case $X(q)^2 = -(Lq)^2$ and the second term on the *r.h.s* of (236) becomes negligible. Furthermore, since $X(q)$ is now pure complex we have $\sin(X(q)) = \sinh(Lq)$, and if b is large (multiple scattering) and q is small enough, we may set $\sinh(Lq/b) \simeq lq$. We obtain thus

$$Corr(aba'b') = \left| \sqrt{Corr(aba'b')} \right|^2 = \left(Y_0^{(c)} \frac{3}{4\pi} \frac{lq}{\sinh(Lq)} \right)^2 \quad (\text{for } \gamma_c = 0) \tag{237}$$

which agrees with the classical result (86) of Chapter 3. The factor $Y_0^{(c)}$ accounts for the effect of light polarization, which has not been taken into account in Chapter 3.

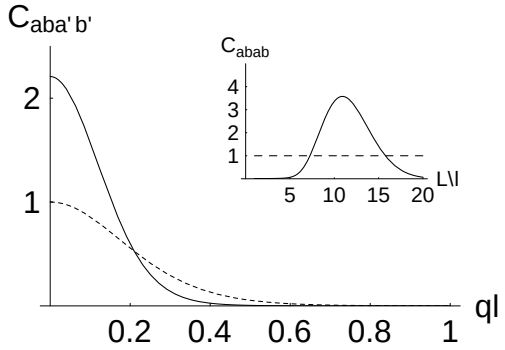

Figure 14: *The angular correlation function for $j_g = 1$ and $j_e = 2$ (solid line). q is equal to k times the angle between $\mathbf{s}_a$ and $\mathbf{s}_{a'}$. Here $b = 7$ and $\Lambda = 60l/c$. Also shown is the classical correlation function (dashed line), obtained for $j_g = 0$ and $j_e = 1$, which gives the Rayleigh law for $q \simeq 0$. The above Rayleigh correlation for the degenerate transition in this region is clearly seen. The inset shows the dependence of the fluctuation C_{abab} on the optical depth.*

The transmitted intensity correlation (236) thus diverges with L. This is not a very physical behavior, since other mechanisms of dephasing, such as Doppler shifts, the motion of scatterers *etc.*, need to be taken into account. These mechanisms are expected to limit the diffusion processes of the intensity and the correlation. To include these mechanisms, we introduce phenomenologically a cutoff Λ as an upper bound for the integral (231). Result (236) now becomes

$$\sqrt{Corr(aba'b')} = \frac{3bY_0^{(c)}}{4\pi}\left(\frac{\sin^2(\frac{X(q)}{b})}{X(q)\sin X(q)} - 2\sin^2(\frac{\pi}{b})\frac{e^{-\frac{\Lambda D}{L^2}(\pi^2 - X(q)^2)}}{\pi^2 - X(q)^2}\right) . \tag{238}$$

The two expressions (236) and (238) coincide for $\Lambda = \tau_D$. Expression (238), divided by $\overline{T}_{ab}$, gives $\sqrt{C_{aba'b'}}$, which is displayed in Figure 14 as a function of $lq = lk\theta$, and for $\Lambda = 60l/c$. Also shown in this figure is a plot of $\sqrt{Corr(aba'b')}$ for non-degenerate atoms with $j_g = 0, j_e = 1$. The non-degenerate curve shows the expected value 1 at $q = 0$, which is the Rayleigh

law ($C_{abab} = 1$). On the other hand, in the degenerate case we see a steep decrease and a large intensity correlation near $q = 0$, as compared to the Rayleigh law obtained for classical scatterers and atoms with a non-degenerate ground state.

The intensity correlation for $q = 0$ (C_{abab}) is depicted in the inset of Figure 14 as a function of the optical depth $b = L/l$. The degenerate fluctuation (solid line) shows a very different behaviour relative to the non-degenerate case (dashed line). While in the non-degenerate case the correlation is independent of L/l, for degenerate scatterers it is peaked at some value of L/l. The maximal value of the correlation is much larger that the Rayleigh value of the classical case. When γ_c tends to 0, and $\Lambda \to \infty$, C_{abab} becomes independent of L and converges to the Rayleigh law $C_{abab} = 1$, as expected.

5.6 Amplified correlation in the general case

In this section we show that the amplified correlation is not restricted to the case of photon-atom interactions. Rather, it appears when additional degrees of freedom are added to the system and enhance the disorder.

Consider a system that can take a few possible paths, connecting its initial and final states. If each path is denoted by C_k, the probability to find the system in the final state is

$$I = \left| \sum_k C_k \right|^2 \tag{239}$$

Consider *two* such systems, denoted by a and b, that are absolutely independent of each other, but however have exactly the same ensemble of states. We would like to find the correlation between I_a and I_b, namely,

$$Corr(I_a, I_b) = \langle I_a I_b \rangle - \langle I_a \rangle \langle I_b \rangle \tag{240}$$

where $\langle \cdots \rangle$ denotes here any relevant ensemble average. Therefore

$$Corr(I_a, I_b) = \left| \sum_{k_a} C_{k_a} \right|^2 \left| \sum_{k_b} C_{k_b} \right|^2 - \left| \sum_{k_a} C_{k_a} \right|^2 \left| \sum_{k_b} C_{k_b} \right|^2 = 0 \tag{241}$$

In this case, there are no degrees of freedom to average on.

We now disorder the system. It will be plugged into the problem by a phase $\phi_k(R)$, which characterizes each of the paths C_k. It is assumed that

if the system evolves through the path C_{k_0}, say, by the time it reaches the final states, it acquires a phase $\phi_{k_0}(R)$. This phase, as it is written, depends on the degree of freedom R. Each value of R corresponds to certain values of the phases $\phi_k(R)$. However, we do *not* know the value of R, so that every physical quantity of interest should be disorder (or R) averaged. In the case of light multiply scattered inside a medium, for which the positions of scatterers are not known and random in nature, R corresponds to a certain scatterers configuration, while the C_k's represent the various possible scattering trajectories of the light inside the medium.

Consider first the average probabilities $\langle I_a \rangle$ and $\langle I_b \rangle$, where the average $\langle \cdots \rangle$ is over R. From (239), each of the two probabilities is a sum of terms like $C_{k_1} C_{k_2}$. The cross terms, for which $k_1 \neq k_2$, represent interference between different paths C_{k_1} and C_{k_2}. The resulting phase $\phi(R) = \phi_{k_1}(R) - \phi_{k_2}(R)$ is in general nonzero and fluctuates as R changes. We now assume that the order of magnitude of the fluctuations of $\phi(R)$ (for $k_1 \neq k_2$) is typically larger than π, so that on average $\langle e^{i\phi(R)} \rangle = 0$. This means actually two requirements: first, that the two paths C_{k_1} and C_{k_2} are not too close to each other, and second, that the dependence of the phases ϕ_k on R is strong enough. Under these conditions we have

$$\langle e^{i\phi_{k_1}(R) - i\phi_{k_2}(R)} \rangle = \delta_{k_1, k_2} \tag{242}$$

meaning that the interference terms do not contribute to the average probability. Thus

$$\langle I_a \rangle = \sum_{k_a} |C_{k_a}|^2 \tag{243}$$

with a similar expression for $\langle I_b \rangle$, from which

$$\langle I_a \rangle \langle I_b \rangle = \sum_{k_a, k_b} |C_{k_a}|^2 |C_{k_b}|^2 \tag{244}$$

On the other hand, we have

$$\langle I_a I_b \rangle = \sum_{k_{a1}, k_{b1}} \sum_{k_{a2}, k_{b2}} C_{k_{a1}} C^*_{k_{a2}} C_{k_{b1}} C^*_{k_{b2}} \langle e^{i\phi_{k_{a1}}(R) - i\phi_{k_{a2}}(R) + i\phi_{k_{b1}}(R) - i\phi_{k_{b2}}(R)} \rangle$$

Due to the disorder average, only two kinds of terms contribute to $\langle I_a I_b \rangle$, namely those in which either (i) $k_{a1} = k_{a2}$ and $k_{b1} = k_{b2}$, or (ii) $k_{a1} = k_{b2}$ and $k_{b1} = k_{a2}$. Possibility (i) yields just $\langle I_a \rangle \langle I_b \rangle$, while possibility (ii) involves

cross terms between a and b. These cross terms, however, do not describe interference, because they result from a product of *probabilities* and not of *amplitudes*. Only these cross terms contribute to the correlation function, which is written

$$Corr(I_a, I_b) = \sum_{k,k'} \left(C_k C_k^*\right) \left(C_{k'}^* C_{k'}\right) = \langle I_a \rangle \langle I_b \rangle \tag{245}$$

where for the last equality we have used (243). This result corresponds to the Rayleigh law, since for $a = b$ one obtains

$$\langle I_a^2 \rangle = 2 \langle I_a \rangle^2 \tag{246}$$

The correlation (245) is enhanced relative to (241). This enhancement results from the presence of the disorder. We emphasize that in (245), the pairs of amplitudes characterized by the parameters k and k', contain one amplitude that belongs to the system a, and another amplitude that belongs to system b.

Now suppose that we add to the disorder another degree of freedom, $\alpha(k)$, that characterizes every path. Each path will be denoted thus by $C_k^{\alpha(k)}$. We shall assume that α is random, meaning that it may change from one system to another, thus "enhancing" the previous disorder that depends only on R. Because α is not known, we average the possible paths over it. Then, for example

$$\langle I_a \rangle = \sum_{k_a} \sum_{\alpha(k_a)} |C_{k_a}^{\alpha(k_a)}|^2 \tag{247}$$

where the summation over $\alpha(k_a)$ results from the averaging, and the probabilities of the different values of α are assumed to be implicit in C_k^α. Also, the parameter α depends on the certain path k, as explicitly shown. Repeating the steps that lead to (245), we now have

$$Corr(I_a, I_b) = \sum_{k,k'} \sum_{\alpha_a(k),\alpha_b(k)} \sum_{\alpha_a(k'),\alpha_b(k')} \left(C_k^{\alpha_a(k)} C_k^{\alpha_b(k)*}\right) \left(C_{k'}^{\alpha_a(k')*} C_{k'}^{\alpha_b(k')}\right) \tag{248}$$

where the amplitudes of a and of b are now characterized also by the parameters α_a and α_b. To show that in this case the correlation may exceed the Rayleigh law (245), suppose that there are n possible values for the parameter k, and m possible values for α. The average intensity (247) is a sum of $n \times m$

terms, so that $\langle I_a \rangle \langle I_b \rangle$ contains $n^2 \times m^2$ terms. On the other hand, from (248) we see, that the correlation includes $n^2 \times m^4$ terms which, if $m > 1$, is larger than $n^2 \times m^2$. The additional disordered degrees of freedom thus essentially change the correlation function, through the addition of many contributions that otherwise would not exist. The above-Rayleigh correlation is thus not so surprising. One "kind" of disorder, *e.g.* that corresponds to the position of scatterers, leads to the Rayleigh correlation (245), which is enhanced above the ordered system correlation (241). Similarly, another disordered degrees of freedom (*e.g.* Zeeman quantum numbers), which come *in addition* to the previous one, keep enhancing the correlation above the Rayleigh limit. We note finally that the "internal" degrees of freedom, denoted in this section by $\alpha_{a,b}$, are not necessarily quantum. They can be of any kind, quantum or classical.

In this chapter we have shown that when light is multiply scattered by atoms, atomic Zeeman degeneracy enhances the scattered intensity correlation above the Rayleigh limit. We have explicitly calculated this enhancement effect, and also explained it qualitatively on a general ground, by showing that the additional degrees of freedom result in many more contributions to the correlation than to the average intensity. In the case where the atomic ground state is not Zeeman degenerate, we have obtained the same results as already known for classical scatterers.

.

CHAPTER 6

Effects of an external magnetic field and of the motion of scatterers

In this chapter we discuss two effects that modify the correlation amplification discussed in the previous chapter. The first effect is the application of an external magnetic field, which removes some atomic transitions from resonance. As we shall see, however, the external field affects only the correlation cross section, while leaving the intensity *total* cross section unchanged, thus reducing the intensity correlation. The result is a sharp resonance-like curve of the correlation as a function of the field, which might be found useful for accurate level crossing spectroscopy.

The second correlation-limiting mechanism we shall study is associated with the motion of scatterers. Unlike the external magnetic field, this effect cannot be easily monitored, and it leads to a dephasing that reduces the amplified correlation.

The chapter is organized as follows. In Section 6.1 we modify the model presented in Chapter 5 so as to include the effect of the magnetic field, and calculate the dependence of the correlation function on this field. Section 6.2 presents the so-called *level-crossing spectroscopy*, which relies on the Lorentzian dependence of the scattering cross section on the external field to measure atomic parameters. This method is based on the Hanle and Franken effects, which thus serve as a reference to the present available resolution of level-crossing experiments. In Section 6.3, we consider the motion of the scatterers and its influence on the intensity correlation function.

6.1 Effect of a magnetic field on the correlation

As discussed earlier, the enhanced correlation cross section, relative to the intensity one, is at the basis of the amplified correlation. Therefore, an applied magnetic field H is expected to affect this enhancement, since it generally changes the single scattering cross section by removing the atomic level degeneracy (Zeeman splitting). In this section we show that the amplified correlation is sensitive to the application of a field, and calculate the corresponding functional dependence [1]. In fact, a strong enough field reduces $\mathcal{V}^{(c)}$ so that the enhancement condition $\mathcal{V}^{(c)} > \mathcal{V}^{(i)}$ does not apply anymore.

We begin by rewriting the generalized vertex (148) in the presence of an applied magnetic field

$$\mathcal{V}^{(c)} = \frac{1}{J^2} \sum_{m_i} \frac{\langle j_g m_2 | U(\hat{\varepsilon}_1, \hat{\varepsilon}_2) | j_g m_1 \rangle \langle j_g m_4 | U(\hat{\varepsilon}_3, \hat{\varepsilon}_4) | j_g m_3 \rangle^*}{(\omega - \omega_{m_1 m_e} + i\Gamma/2)(\omega - \omega_{m_3 m'_e} - i\Gamma/2)} \tag{249}$$

where we have defined the energy difference $\hbar\omega_{ij} = E_j - E_i$, and for simplicity unimportant pre-factors have been omitted. Also, as defined previously, $U(\hat{\varepsilon}, \hat{\varepsilon}') = \sum_M (\mathbf{d} \cdot \hat{\varepsilon}'^*) |M\rangle\langle M| (\mathbf{d} \cdot \hat{\varepsilon})$. The intensity vertex $\mathcal{V}^{(i)}$ is obtained by setting $m_1 = m_3$, $m_2 = m_4$, $\hat{\varepsilon}_1 = \hat{\varepsilon}_3$, and $\hat{\varepsilon}_2 = \hat{\varepsilon}_4$. Assuming a broad band light and averaging over the photon frequency ω, we obtain the Breit-Franken differential cross section [38]

$$\mathcal{V}^{(i)} = \frac{1}{J} \sum_{m_1 m_2} \sum_{m_e m'_e} \frac{B_{12}(m_e) B_{12}^*(m'_e)}{i\omega_{m'_e m_e} + \Gamma} \tag{250}$$

where $B_{12}(m_e) = \langle m_2 | \hat{\varepsilon}_2^* \cdot \mathbf{d} | m_e \rangle \langle m_e | \mathbf{d} \cdot \hat{\varepsilon}_1 | m_1 \rangle$. The broad band assumption is for convenience only. For a weak enough magnetic field, both broad band and monochromatic light give similar differential scattering cross sections [39]. This is valid when H is weak enough so that $\omega_{m'_e m_e} < \Gamma$.

The applied magnetic field H removes the level degeneracy and leads to a Zeeman splitting $\hbar\omega_{m'_e m_e} = g\mu_0 H(m_e - m'_e)$, so that two kinds of terms appear in (250). Terms for which $m_e = m'_e$, are independent of the magnetic field and they lead to the incoherent scattering cross section. The terms $m_e \neq m'_e$ depend on the magnetic field and they describe interferences between two distinct scattering amplitudes. Suppose that for $H = 0$, the excited level is degenerate. As the magnetic field increases, the interference contribution is gradually suppressed, because of the difference in the evolution of the two states $|m_e\rangle$ and $|m'_e\rangle$. Alternatively, the quantities $\omega_{m'_e m_e}$ get larger and reduce the contribution $m_e \neq m'_e$. This shows up as a Lorentzian resonance about the level-crossing point (Hanle and Franken effects, see Section 6.2), whose width ΔH_F is determined by the condition $\omega_{m'_e m_e} \simeq \Gamma$ (for $m_e \neq m'_e$), so that [38, 40]

$$\Delta H_F \simeq \frac{\hbar\Gamma}{g\mu_0} \tag{251}$$

up to a prefactor that depends on the slopes of the crossing levels [41].

Although the differential scattering cross section (250) depends on H, the total cross section σ obtained from it does not. To see this, we perform the

summation over the two independent outgoing polarizations in (250). The relevant terms has the form

$$\sum_{\hat{\varepsilon}_2 \perp \mathbf{k}} \langle m_2|\hat{\varepsilon}_2^* \cdot \mathbf{d}|m_e\rangle\langle m_e'|\hat{\varepsilon}_2 \cdot \mathbf{d}|m_2\rangle = \sum_{\mathbf{k}} (\varepsilon_{2\alpha}\varepsilon_{2\beta} + \varepsilon_{2\alpha}'\varepsilon_{2\beta}')\langle m_2|d_\alpha|m_e\rangle\langle m_e'|d_{-\beta}|m_2\rangle \ , \tag{252}$$

where $\mathbf{k}$ is the outgoing wave vector, and α, β are the polarization components that allow the transitions according to the electric dipole selection rules. The integration over $\mathbf{k}$ imposes $\alpha = -\beta$, which implies that the H-dependent interference terms $m_e \neq m_e'$ do not contribute to σ. Since the average transmitted intensity is proportional to $l/L = 1/n\sigma L$ [2] (see also (229)), $\overline{T}_{ab}$ is also independent of H within our approximations.

To observe the effect of the field H on the multiple scattering speckle pattern, we thus have to consider the correlation functions. To this purpose we use (236), which is the expression for the enhanced correlation ($\gamma_0^{(c)}$ is negative). Looking at (236), we see that the effect of the field H enters only in $\gamma_c \equiv |\gamma_0^{(c)}|$ that we now evaluate. From (199), $\gamma_0^{(c)}$ depends on $u_0^{(c)}$, the largest eigenvalue of $\mathcal{V}^{(c)}\mathcal{P}$. For small enough H, we can express this eigenvalue to lowest order in the dimensionless field

$$s = \frac{g\mu_0 H}{\hbar\Gamma} \tag{253}$$

as

$$u_0^{(c)}(s) \simeq u_0^{(c)}(0) - \beta s^2 \tag{254}$$

where β is a constant that depends on the specific scattering atom. This expression results from (249), inserting $\omega - \omega_{m_1 m_e} \simeq \omega - \omega_{m_3 m_e'} \simeq g\mu_0 H/\hbar$. Therefore, for small enough s we may write

$$\mathcal{V}^{(c)}(s) \simeq \mathcal{V}^{(c)}(0)\frac{1}{1+4s^2} \simeq \mathcal{V}^{(c)}(0)(1-4s^2) \tag{255}$$

so that the eigenvalues of $\mathcal{V}^{(c)}(s)$ behave as in (254). The corresponding damping rate becomes

$$\gamma_0^{(c)}(s) \simeq \gamma_0^{(c)}(0) + \frac{2\beta\, c\, a_{j_g j_e}}{3u_0^{(c)2}\, l}s^2 \tag{256}$$

which allows us to write the dependence of $X_0 \equiv X(0)$, defined before (235), on s as

$$X_0(s) = b\sqrt{|f_0 - f_2 s^2|} \tag{257}$$

with $f_0 = (2a_{j_g j_e}/u_0^{(c)}) - 3$ and $f_2 = 2a_{j_g j_e}\beta/u_0^{(c)2}$. To obtain the field dependence of the correlation we thus have to find the factor β (all other quantities in (257) are already known). β is found by calculating numerically $u_0^{(c)}(s)$ for many values of s and then, by fitting, evaluating β from (254). All is left now is to substitute (257) into (236), leading to the dependence of $C \equiv C_{abab}$ on the dimensionless field s, presented in Figure 15. It shows a resonance line whose FWHM ΔH_M is about $0.2\hbar\Gamma/g\mu_0$, a fifth of the FWHM ΔH_F corresponding to the Franken and Hanle effects. The curve in Figure 15 is obtained for $b = 5$, and its FWHM is a specific case of the more general result

$$\Delta H_M = \Delta H_F \frac{a}{b} \ , \tag{258}$$

where the factor a is of the order of unity. Relation (258) has been obtained numerically by considering various atomic transitions and values of b. Figure 16 shows the results, which are in a complete agreement with the linear dependence (258). From the exponential term in (236), and after substituting (257), the slope a is given roughly as $1/\sqrt{f_2}$.

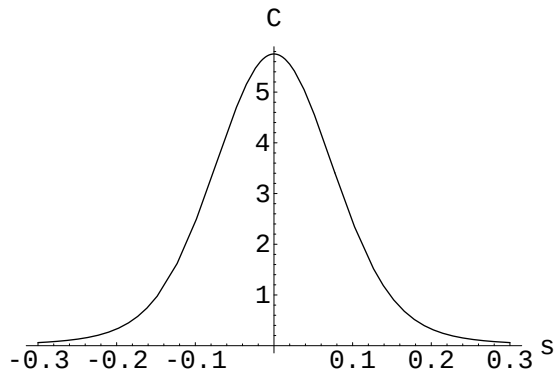

Figure 15: *The dependence of $C \equiv C_{abab}$ on the dimensionless field $s = g\mu_0 H/\hbar\Gamma$. In this figure $b = 5$, and the FWHM is accordingly about 0.2.*

The result (258) is unique in that it does not provide any "natural" bound on the accuracy achieved in level-crossing spectroscopy. Practically, technical considerations like Doppler shifts, absorption, and other dephasing and damping mechanisms that were ignored here, are supposed to limit the accuracy. However, according to the present analysis the accuracy is, in principle, not limited. Various authors discuss possibilities to improve the accuracy of level-crossing experiments (see next section) by a factor of 2 or 3, while from

(258) one can improve it by orders of magnitude by just increasing the optical depth. We now try to explain, in a somewhat intuitive way, this nontrivial result.

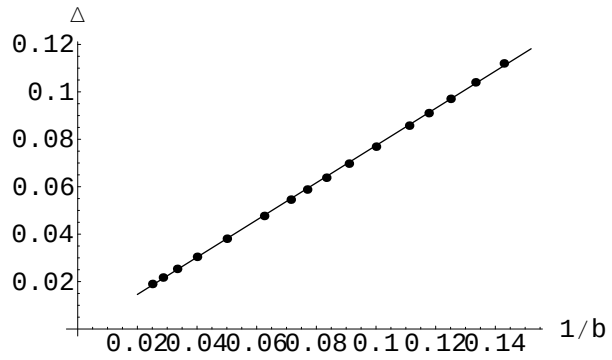

Figure 16: *A numerical calculation of the FWHM Δ for various values of b. The linear dependence of Δ on $1/b = l/L$ is clearly observed.*

The correlation decrease due to the magnetic field originates in the fact that most of the contributions to $\mathcal{V}^{(c)}$, that do not contribute to $\mathcal{V}^{(i)}$, are suppressed by the field. An example of such a process is shown in Figure 13 (Chapter 5). Most of these contributions get smaller as the Zeeman splitting grows. As explained above, the total cross section of a photon scattering upon an atom does not change with H (for small enough field). However, the previous derivation of this property of the total cross section does not hold anymore for the correlation. Trying to calculate a correlation cross section σ_c from $\mathcal{V}^{(c)}$, the outgoing polarization dependent part is now $\sum_{\hat{\varepsilon}_2,\hat{\varepsilon}_4\perp\mathbf{k}}\langle m_2|\hat{\varepsilon}_2^*\cdot\mathbf{d}|m_e\rangle\langle m_e'|\hat{\varepsilon}_4\cdot\mathbf{d}|m_4\rangle$, and we *cannot* conclude from summing polarizations and integrating over $\mathbf{k}$'s that the field-dependent terms do not contribute. From (199), the behavior of the correlation is mainly determined by $u_0^{(i)} - u_0^{(c)}$, while the intensity is dominated by the stable mode $\gamma_0^{(i)} \propto u_0^{(i)} - u_0^{(i)} = 0$. As already mentioned, $u_0^{(i)} = 2a_{j_g j_e}/3$ is proportional to the true total scattering cross section. By analogy, $u_0^{(c)}$ is proportional to the correlation cross section σ_c, determined by $\mathcal{V}^{(c)}$, in the same way σ is determined by $\mathcal{V}^{(i)}$. Therefore, the correlation, which depends strongly on σ_c, is much more sensitive to the external field than the intensity.

The free propagation of intensity inside a random medium, *i.e.* between two scattering events, decays as $e^{-R/l}$ where R is the distance of propagation

(see Chapter 2). In other words, the probability to propagate freely, without any scattering, for time periods longer than l/c is negligible. Since $\sigma_c > \sigma$, we have $l > l_c$ because $l = 1/n\sigma$ and $l_c = 1/n\sigma_c$. This means that, theoretically, the free propagation probability which corresponds to the correlation Diffuson $\mathcal{D}^{(c)}$, should decay as e^{-R/l_c}. However it *does not*. Each amplitude building up $\mathcal{D}^{(c)}$ still decays as $e^{-R/l}$, since it is the real cross section σ that dominates the propagation properties of the wave amplitudes. Only the *coupling* of two amplitudes, related to two different photons as explained above, is what forms σ_c. This brings about an effective gain, e^G, which can be found from

$$e^G e^{-R/l_c} = e^{-R/l} \tag{259}$$

leading to

$$G = R\frac{(l - l_c)}{ll_c} = \frac{R}{l}\frac{3}{2a_{j_g j_e}}(u_0^{(c)} - u_0^{(i)}) \tag{260}$$

where we have used the fact that $u_0^{(i)} = 2a_{j_g j_e}/3 \propto \sigma$ and $u_0^{(c)} \propto \sigma_c$, with the same proportionality factor, so that $l/l_c = u_0^{(c)}/u_0^{(i)}$. The total gain in a typical multiple scattering path, e^{G_T}, is obtained by replacing R in (260) by the length of a typical diffusive path cL^2/D. Thus

$$G_T = \frac{9}{2a_{j_g j_e}} b^2 (u_0^{(c)} - u_0^{(i)}) \ . \tag{261}$$

We now replace $u_0^{(c)}$ by $u_0^{(c)}(0) - \beta s^2$. The total gain along the whole path is

$$e^{G_T} = A e^{-\frac{9}{2a_{j_g j_e}} b^2 \beta s^2} \tag{262}$$

with $A = \exp[\frac{9}{2a_{j_g j_e}} b^2 (u_0^{(c)}(0) - u_0^{(i)})]$. From this we can find the width ΔH_M by imposing $\frac{9}{2a_{j_g j_e}} b^2 \beta (\Delta s)^2 = 1$, leading to

$$\Delta H_M \simeq \Delta H_F \frac{1}{b} \ , \tag{263}$$

(ΔH_F is defined in (251)) in agreement with (258).

Another intuitive argument for the dependence of ΔH_M on $1/b$ arises from (249). Assuming the typical value for the detuning, $\delta = s\Gamma \simeq \omega_{m_i m_j}$, we see that

$$\mathcal{V}^{(c)}(H) \simeq \mathcal{V}^{(c)}(0) \frac{\Gamma^2}{\delta^2 + \Gamma^2} \tag{264}$$

which shows the well known Lorentzian behavior of the resonance fluorescence scattered intensity as a function of δ. In this case the total cross section, in the presence of a magnetic field, also behaves like $1/(\delta^2+\Gamma^2)$. It is therefore reduced to half its maximum value $1/\Gamma^2$ for $\delta=\Gamma$. If, for example, the photon undergoes *two* successive scattering events, then for $\delta=\Gamma$ the two-scattering cross section is reduced to $1/4$ of its maximum value. This is because every single scattering cross section is reduced by a factor of $1/2$. The half width of the two-scattering cross section is therefore achieved for $\delta=\Delta_2$, where Δ_2 is the detuning for which the single scattering cross section is reduced by a factor of $1/\sqrt{2}$. According to the same reasoning, if the photon undergoes n scattering events before emerging, the half width of the n-scattering cross section will be achieved for $\delta=\Delta_n$ given by

$$\Delta_n=\Gamma\sqrt{2^{1/n}-1} \tag{265}$$

Δ_n is the detuning for which the single scattering cross section is reduced by a factor of $1/\sqrt[n]{2}$ (for example, $\Delta_1=\Gamma$). Since $2^{1/n}=e^{ln2/n}$, then for $n\gg 1$ it holds that

$$\Delta_n=\Gamma\sqrt{ln2/n}\ . \tag{266}$$

Finally, as already mentioned, for diffusive multiple scattering we have $n=(L/l)^2$ so that

$$\Delta_{n=(L/l)^2}\simeq\frac{l}{L}\Gamma \tag{267}$$

which also agrees with (258). This means that if the characteristic Zeeman splitting exceeds $(l/L)\hbar\Gamma$, most of the contributions to the correlation become negligible, and the correlation returns (more or less) to its nondegenerate value. The enhanced correlation is thus a phenomenon much more sensitive to a magnetic field, than other phenomena such as the Franken or Hanle effects. In the so-called level-crossing spectroscopy discussed below, one uses effects like Franken or Hanle to measure the energy width of atomic states. The full width at half maximum (FWHM) of these phenomena are directly related to the accuracy of measurements that can be achieved. It is clear therefore, that a phenomena as described here, that is orders of magnitude more sensitive to a magnetic field (*i.e.*, its FWHM is orders of magnitude smaller), might be very useful to improve the precision of these experiments.

6.2 Level-crossing spectroscopy

The changes in the differential scattering cross section of light, resonant with the $6^1s_0 \rightarrow 6^3p_1$ transition in Mercury, as a function of an applied magnetic field is called the *Hanle effect*, after W. Hanle, who has studied this problem in 1924 [42]. This is a variant of the level-crossing spectroscopy, which takes advantage of the dependence of the differential scattering cross section on an applied magnetic field, in order to obtain experimentally atomic parameters, such as the natural width Γ. In the experiment of Hanle, the two atomic levels are Zeeman degenerate in the absence of a magnetic field, so that the application of the field removes this degeneracy. Other experiments use an atomic structure which is non-degenerate in zero field, while at some specific values a level-crossing occurs which creates degeneracy. For example, the earliest level-crossing experiment was performed by Colegrove *et.al.* [43, 44]. In this experiment, the scattering of light corresponding to the transitions $2^3s_1 \rightarrow 2^3p_1$ and $2^3s_1 \rightarrow 2^3p_2$ of Helium was studied. In this case, the two excited states have different energies at zero field. However, for some value of the field a level-crossing occurs between the $m = 2$ sublevel of 2^3p_2 and the $m = 0$ sublevel of 2^3p_1 for a field strength of about $0.08T$. Measuring the differential scattering cross section about this and other crossing points, allowed Colegrove *et. al.* to determine experimentally the fine-structure separation between the 2^3p_1 and 2^3p_2 levels. In both cases, sweeping the magnitude of the field about the level-crossing (or zero field) point and measuring the resulted scattered intensity line, allows for the experimental determination of atomic parameters.

Consider the Breit-Franken cross section (250), and suppose that the ground state $|g\rangle$ is non-degenerate, while the excited state is two-fold degenerate and composed of the sublevels $|m\rangle$ and $|m'\rangle$, (250) then becomes,

$$\mathcal{V}^{(i)} = \frac{|B_{12}(m)|^2}{\Gamma} + \frac{|B_{12}(m')|^2}{\Gamma} + 2Re\frac{B_{12}(m)B_{12}^*(m')}{i\omega_{m'm} + \Gamma} \quad . \tag{268}$$

The first two terms on the *r.h.s* of (268) are the incoherent contributions of the scattering processes $|g\rangle \rightarrow |m\rangle \rightarrow |g\rangle$ and $|g\rangle \rightarrow |m'\rangle \rightarrow |g\rangle$, and are field independent. The third term amounts to the interference between these two kinds of scattering processes. It is seen that the interference term contributes as long as $\omega_{m'm} < \Gamma$. This corresponds to a width, in terms of the magnetic field, of $\Delta H = \hbar\Gamma/g\mu_0 \equiv \Delta H_F$ mentioned above, which determines the accuracy (or resolution) of the level-crossing experiment. The possibility,

presented in the previous section, of reducing significantly ΔH by a factor l/L, typically of the order of $1/10$, in the case of intensity correlation, thus may be experimentally useful.

6.3 Motion of the scatterers - time dependent correlation

In Section 3.4 of Chapter 3 we have described the temporal dependence of the classical intensity correlation, which results from the random motion of the scatterers. The quantity of interest is the temporal correlation function $C(\tau)$, which is the correlation between the transmitted intensity at two different times, t and $t+\tau$, averaged over both the disorder and the initial time t. The result, (96) in Chapter 3, depends on the quantity $L_\gamma(\tau) = \sqrt{2Dl\tau_b/c\tau}$, where τ_b is defined in (95) to be the characteristic time for the scatterers to move a distance comparable to the light wavelength λ. In Chapter 2 we have given an expression for the Diffuson function in the slab geometry. The result (50) depends on the characteristic length $L_\gamma(\mathbf{q}) = \sqrt{D/(\gamma + Dq^2)}$. The first expression for L_γ is a special case of the second one, obtained for $q = 0$ and

$$\gamma = \frac{c\tau}{2l\tau_b} \quad . \tag{269}$$

Using this identification and the results of Chapter 2, we can express the τ-dependent Diffuson also as

$$\mathcal{D}^{(c)}(\mathbf{r}, \mathbf{r}', \tau) = \int_0^\infty \mathcal{D}_0(\mathbf{R}_\perp, z, z', t) e^{-\gamma t} \tag{270}$$

where $\mathcal{D}_0$ is the Diffuson obtained for $\gamma = 0$, and the superscript (c) indicates that this Diffuson corresponds to the correlation. The intensity Diffuson is obtained, in this *classical* case, by setting $\gamma = 0$. A more rigorous calculation leads to exactly the same result [2].

We now wish to find the temporal correlation function in the case of degenerate atomic scatterers. A suggested setup for measuring this function is shown in Figure 17. As we saw in the previous chapter, when the scatterers are Zeeman degenerate atoms, an amplification term shows up via the exponential $e^{\gamma_c t}$ that multiplies the Diffuson. Combining the result (202) of Chapter 5 and (270), we find

$$\mathcal{D}^{(c)}(\mathbf{r}, \mathbf{r}', \tau) = Y_0^{(c)} \int_0^\infty dt \;\; \mathcal{D}_0(\mathbf{R}_\perp, z, z', t) \;\; e^{(\gamma_c - \gamma)t} \tag{271}$$

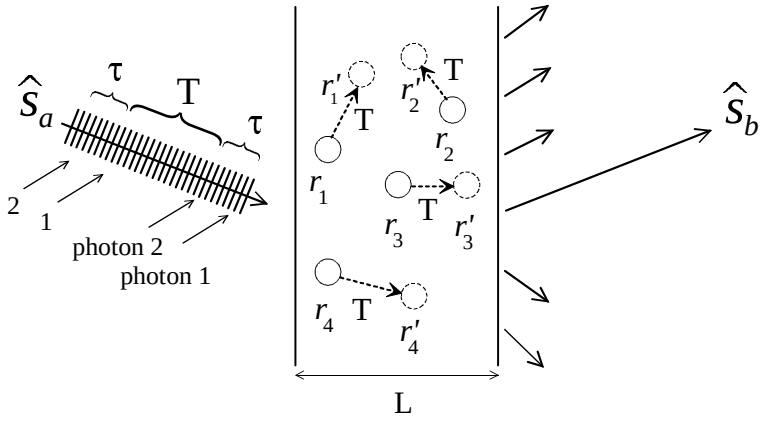

Figure 17: *A suggested experimental setup for measuring $C(\tau)$. A laser beam, incoming along $\mathbf{s}_a$, falls on the atomic gas and is measured along $\mathbf{s}_b$. A first measurement of the outgoing intensity is taken at $t = 0$, corresponding to a bunch of photons represented as "photon 1". A time τ later, a second measurement is taken corresponding to "photon 2". The time τ is short enough so that the atoms stay at rest between $t = 0$ and $t = \tau$. Therefore, photons 1 and 2 see the same spatial configuration of scatterers. The two photons, however, experience different internal atomic states due to all other photons that have been scattered between the arrivals of photon 1 and photon 2. This measuring process is repeated after a time T, during which the scatterers move, what realizes the spatial disorder average.*

where we have ignored all diffusion modes except for the amplified mode, and where $\gamma_c \equiv |\gamma_0^{(c)}|$. Also, here $\gamma_c > 0$ corresponding to correlation amplification, and $\gamma > 0$ by the definition (269). There is a competition, therefore, between γ_c and γ, and an immediate conclusion is that the amplification exists as long as $\gamma_c > \gamma$, namely for $\tau < \tau_{amp}$ where

$$\tau_{amp} = \frac{2l\tau_b}{c}\gamma_c \ . \tag{272}$$

The dimensionless quantity defined as

$$\chi \equiv \frac{l}{c}\gamma_c \tag{273}$$

characterizes the "amount" of amplification in the medium, since it is the ratio between the characteristic time for amplification and the elastic mean

free time between two successive scattering events l/c. As such, $\chi \sim 1$, for example, means that the amplification occurs on a time scale of only one or two scattering events, and thus corresponds to strong amplification that becomes significant after only few scatterings. On the other hand, if $\chi \ll 1$, many scattering events take place before the amplification starts to be important. The limit $\chi \ll 1$ therefore corresponds to weak amplification. The relation $\tau_{amp} = 2\chi\tau_b$, obtained from (272) and (273), leads to the identification of the regime $\tau_{amp} \sim \tau_b$ with strong amplification, and of $\tau_{amp} \ll \tau_b$ with weak amplification. For strong amplification, the correlation is enhanced as long as the temporal separation τ is less than the dephasing time τ_b, which is the classical limitation (Section 3.4). For a weak amplification, the correlation ceases to be enhanced already for a very small temporal separation, namely, for a very small dephasing between amplitudes that belong to different pulses.

The integral in (271) may be evaluated as in Section 5.5. The result is similar to (236) of Chapter 5, except for the additional dependence on τ via the decay rate γ

$$\sqrt{Corr(\tau)} = \frac{3bY_0^{(c)}}{4\pi}\left(\frac{\sin^2(\frac{X(\tau)}{b})}{X(\tau)\sin X(\tau)} - 2\sin^2(\frac{\pi}{b})\frac{e^{-\pi^2+X^2(\tau)}}{\pi^2 - X^2(\tau)}\right) \qquad (274)$$

with $X(\tau) = L\sqrt{(\gamma_c - \gamma)/D}$, which is the quantity $X(\mathbf{q})$ defined before (235) of Chapter 5, with $\mathbf{q} = 0$ and including the additional decay time γ. $X(\tau)$ is real as long as $\gamma_c > \gamma$. For $\gamma_c = 0$ we restore the classical results of Chapter 3, in the same way it was done for the angular correlation function after (236). As before, the last term on the *r.h.s* of (274) corresponds to the amplification. From this term we may conclude a modified condition for correlation amplification, that is

$$X^2(\tau) > \pi^2 \qquad \text{(amplification)} \qquad (275)$$

which leads to

$$\tau < 2\tau_b(\chi - \pi^2\eta) = \tau_{amp} - 2\tau_b\pi^2\eta \qquad \text{(amplification)} \qquad (276)$$

with $\eta \equiv 1/3b^2$. In the diffusive limit, however, $\eta \ll 1$ and we restore the previous condition, $\tau < \tau_{amp}$.

From (274), we can also estimate the characteristic time scale for the amplified correlation to decrease as a function of τ, by defining $\exp[-(3L^2/2l^2\tau_b)\tau_\Delta] = 1/e$. This characteristic time τ_Δ is therefore

$$\tau_\Delta = 2\tau_b\eta \ . \qquad (277)$$

This is quite an intuitive result, because η is the inverse of the number of scattering events in a typical diffusion trajectory, namely, the Thouless time τ_D divided by l/c. Moreover, τ_b is the characteristic time for one scatterer to move a distance λ from its origin. As a result, if two pulses, separated in time by τ_b, are scattered off this scatterer, a dephasing comparable to π is brought about between scattering amplitudes corresponding to different pulses. Accordingly, if a trajectory includes $1/\eta$ scattering events, it is sufficient that every scatterer move only $\eta\lambda$ from its origin to cause a total dephasing of about π. This is because each scatterering event contributes to the total dephasing along the scattering trajectory.

Finally, we would like to comment on quantum mechanical motion of the scatterers, which may be subjected to a certain potential, as in electromagnetic trapping for example, that holds them in some small region of space. In this case it is convenient to consider each atom as a quantum mechanical harmonic oscillator, denoting by $|\{n\}\rangle$ its quantum state corresponding to the external degrees of freedom. Restricting ourselves to the case of two atoms, and ignoring internal atomic degrees of freedom, the scattered intensity is given, by analogy to (138) in Chapter 5, as [33]

$$\mathcal{T} = F|\langle\{n_f\}|e^{-i\mathbf{q}\cdot\mathbf{R}_1}+e^{-i\mathbf{q}\cdot\mathbf{R}_2}|\{n_i\}\rangle|^2 = 2F[1+\cos(\mathbf{q}\cdot\mathbf{d})e^{-\langle(\mathbf{q}\cdot\mathbf{u})^2\rangle_q/2}] \ . \quad (278)$$

Here $|n_i\rangle$ ($|n_f\rangle$) are the initial (final) states of the atoms motion, $\hat{\mathbf{u}}$ is a quantum mechanical operator which corresponds to the atoms relative position's departure from the equilibrium $\mathbf{d}$, and $\langle\cdots\rangle_q$ is a thermal average over the quantum numbers $|n_i\rangle$. The classical disorder discussed above, if it exists, concerns only the classical relative position $\mathbf{d}$. In other words, the above averaging $\langle\cdots\rangle$ is performed only over $\mathbf{d}$. Two limiting cases appear in (278). The first is the quantum limit, in which the characteristic departure from $\mathbf{d}$ is significant, namely $\rho \equiv \sqrt{\langle\hat{\mathbf{u}}^2\rangle_q} \gg \lambda$. In this case, for $|\mathbf{q}| \sim 2\pi/\lambda$,

$$e^{-\langle(\mathbf{q}\cdot\mathbf{u})^2\rangle_q/2} \simeq 0 \quad (279)$$

and $\mathcal{T} = 2F$ does not depend on $\mathbf{d}$. Therefore, the correlation function is 0. This result is quite obvious, since a significant quantum motion means also a large uncertainty in atoms position. If this uncertainty exceeds λ, no interference can occur since the various amplitudes are no longer coherent among themselves. The quantum motion, therefore, "kills" the cross terms which is at the basis of the enhanced correlation. On the other hand, there

is the classical limit where the quantum motion is negligible, namely $\rho \ll \lambda$. In this case,

$$e^{-\langle(\mathbf{q}\cdot\mathbf{u})^2\rangle_q/2} \simeq 1 \tag{280}$$

and we restore the classical disorder results discussed above.

In this chapter we have considered two mechanisms that reduce the correlation function, namely, an applied magnetic field and the motion of scatterers, and obtained the functional dependence of the correlation on both of them. In the first case, we have found that the correlation decays as a function of the field, with a FWHM that depends on $1/b$, which might be useful experimentally. In the second case, the correlation decays roughly as $1/b^2$ as a function of time. We have also obtained the times for which an amplification of the time-dependent correlation holds.

.

APPENDIX A

The propagator W

In (189) of Chapter 5 we have defined the function $W(\mathbf{Q})$ which corresponds to the polarization *independent* part of propagation of the intensity between two successive scattering events. As such, its form may be derived from the scalar theory discussed in Chapter 2, in which the Drude-Boltzmann approximated propagator, P_{DB}, was said to represent also the free propagation between scattering events. The two quantities must therefore be proportional, $W \propto P_{DB}$. In the real space-time representation, $P_{DB}(\mathbf{r}, \mathbf{r}', t)$ has dimensions of 1/volume. Assuming translation invariance, the spatial dependence of P_{DB} is only on $\mathbf{R} = \mathbf{r}' - \mathbf{r}$. The Fourier representation $P_{DB}(\mathbf{Q})$ (which is also time integrated) with $\mathbf{Q}$ being the Fourier variable of $\mathbf{R}$, has thus dimensions of time. Since $W(\mathbf{Q})$ is a dimensionless quantity, it is conventionally defined as

$$W(\mathbf{Q}) = \frac{3}{2}\frac{c}{l_{cl}} P_{DB}(\mathbf{Q}) \tag{A.1}$$

where l_{cl} is the mean free path corresponding to classical scatterers.

The diffusion regime amounts, among others, to the condition $\omega(l/c) \ll 1$. This condition results from the approximation, according to which the typical time for a diffusion process, t, is much larger than the typical time between two successive scattering events, namely, $t \gg l/c$. Within this approximation, the Fourier space representation of P_{DB} is given as [2]

$$P_{DB}(\mathbf{Q}) = \frac{l}{c}\left(1 - \frac{DQ^2 l}{c}\right) \tag{A.2}$$

where $D = cl/3$ is the 3-dimensional diffusion coefficient. The function $W(\mathbf{Q})$ is thus given by the dimensionless expression

$$W(\mathbf{Q}) = \frac{3}{2}\frac{l}{l_{cl}}\left(1 - \frac{DQ^2 l}{c}\right) \quad . \tag{A.3}$$

In (126) of Chapter 4 the total cross section was given, which depends on the degeneracy of the atomic scatterer. Since the case $j_g = 0$, $j_e = 1$ corresponds

to classical scatterer, we see that $\langle\sigma\rangle/\langle\sigma\rangle_{cl} = a_{j_g j_e}$, leading to $l/l_{cl} = 1/a_{j_g j_e}$. Finally, thus

$$W(\mathbf{Q}) = \frac{3}{2a_{j_g j_e}} \left(1 - \frac{DQ^2 l}{c}\right) \quad . \tag{A.4}$$

APPENDIX B

The spectral decomposition theorem

Taken from [35].

Version 1

Let A be an $n \times n$ matrix with n distinct eigenvalues $\lambda_1, ..., \lambda_n$. Then A can always be represented in the form

$$A = \lambda_1 T_1 + \cdots + \lambda_n T_n \tag{B.1}$$

where the $n \times n$ matrices $T_1, ..., T_n$ have the following properties:

a) $T_i^2 = T_i$.

b) $T_i T_j = 0$ for $i \neq j$.

c) $T_1 + \cdots + T_n = I$, with I being the $n \times n$ unit matrix.

Version 2

Let B be an $n \times n$ hermitian matrix with k (not necessarily equal to n) distinct eigenvalues $\lambda_1, ..., \lambda_k$. Then B can always be represented in the form

$$B = \lambda_1 T_1 + \cdots + \lambda_k T_k \tag{B.2}$$

where the $n \times n$ matrices $T_1, ..., T_k$ have the following properties:

a) $T_i^2 = T_i$.

b) $T_i T_j = 0$ for $i \neq j$.

c) $T_1 + \cdots + T_k = I$, with I being the $n \times n$ unit matrix.

.

APPENDIX C

The $6j$ symbols

Consider the sum of three angular momenta

$$\mathbf{J} = \mathbf{j} + \mathbf{j}' + \mathbf{j}'' \tag{C.1}$$

The summation process can be done, for example, by first coupling $\mathbf{g}' = \mathbf{j} + \mathbf{j}'$, and then $\mathbf{J} = \mathbf{g}' + \mathbf{j}''$. It can also be performed as follows: first $\mathbf{g}'' = \mathbf{j} + \mathbf{j}''$, and then $\mathbf{J} = \mathbf{g}'' + \mathbf{j}'$. These two coupling schemes correspond to two different basis sets for the state space. The $6j$ symbols are related to the coefficients that connect these two bases, and play a similar role to the Clebsch-Gordan coefficients. The definition of the $6j$ symbols is [32]

$$\langle j'g'', JM | g'j'', J'M' \rangle = \delta_{JJ'}\delta_{MM'}\sqrt{(2g'+1)(2g''+1)}(-)^{j+j'+j''+J} \left\{ \begin{array}{ccc} j' & j & g' \\ j'' & J & g'' \end{array} \right\} \tag{C.2}$$

where the *l.h.s* is the product of two state vectors corresponding to the two coupling schemes.

Some properties:

1) In order for the $6j$ symbol not to be zero, the triads $(jj'g')$, $(j'Jg'')$, $(j''jg'')$, and $(j''Jg')$ should satisfy the triangular inequality and have an integral sum.

2) A $6j$ symbol is invariant in a cyclic permutation of its columns, and in an exchange of two elements of the first line with the corresponding elements in the second line.

3) Relation to the $3j$ symbols

$$\begin{aligned} \sum_{gm}(-)^{g+m}(2g+1) \left\{ \begin{array}{ccc} j_1 & J_1 & g \\ J_2 & j_2 & f \end{array} \right\} \left(\begin{array}{ccc} j_1 & J_1 & g \\ m_1 & M_1 & -m \end{array} \right) \left(\begin{array}{ccc} j_2 & J_2 & g \\ m_2 & M_2 & m \end{array} \right) \\ = (-)^{j_2+J_1+f+g} \sum_{M} \left(\begin{array}{ccc} j_1 & j_2 & f \\ m_1 & m_2 & -M' \end{array} \right) \left(\begin{array}{ccc} J_1 & J_2 & f \\ M_1 & M_2 & M \end{array} \right) \end{aligned} \tag{C.3}$$

4) Orthogonality:

$$\sum_{x}(2x+1) \left\{ \begin{array}{ccc} a & b & x \\ c & d & f \end{array} \right\} \left\{ \begin{array}{ccc} c & d & x \\ a & b & g \end{array} \right\} = \delta_{fg}\frac{1}{2f+1} \tag{C.4}$$

.

APPENDIX D

Publications

This appendix includes three articles we have written [1]. The first one, concerning the amplified correlation (Chapter 5), is already published in the Physical Review Letters. The second article has been accepted for publication in the Journal of Modern Optics. It summarizes the results of both Chapters 5 and 6 (except for Section 6.3). The third one, submitted to the Europhysics Letters, focuses on the study presented in Section 6.1.

.

Bibliography

[1] O. Assaf and E. Akkermans, Phys. Rev. Lett. **98** 083601 (2007), E. Akkermans and O. Assaf, to be published in J. Mod. Opt. (2007), E. Akkermans and O. Assaf, submitted to Europhys. Lett. (2007), O. Assaf and E. Akkermans, Technion preprint (2007), E . Akkermans and O. Assaf, arXiv:cond-mat/0610454 v1 (2006).

[2] E. Akkermans and G. Montambaux, *Mesoscopic physics of electrons and photons*, Cambridge University Press (2007).

[3] J. P. Barrat, J. Phys. Rad. **20** 633 (1959).

[4] A. Omont, J. Phys. Rad. **26** 576 (1965).

[5] R. Berkovitz *et. al.*, Phys. Rep. **238** 135 (1994).

[6] E. Akkermans *et. al.*, J. Phys. France **49** 77 (1988).

[7] E. Akkermans *et. al.*, J. Physique Lett. **46** L-1045 (1985).

[8] P. E. Wolf *et. al.*, Phys. Rev. Lett. **55** 2696 (1985).

[9] M. P. van Albada *et. al.*, Phys. Rev. Lett. **55** 2692 (1985).

[10] B. Shapiro, Phys. Rev. Lett. **57** 2168 (1986).

[11] F. Scheffold *et. al.*, Phys. Rev. ? **56** 10942 (1997).

[12] J. F. de Boer *et. al.*, Phys. Rev. B **45** 658 (1992).

[13] R. A. Webb *et. al.*, Phys. Rev. Lett. **54** 2696 (1985), P. A. Lee *et. al.*, Phys. Rev. Lett. **55** 1622 (1985).

[14] D. J. Pine *et. al.*, Phys. Rev. Lett. **60** 1134 (1988).

[15] C.A. Muller *et. al.*, Phys. Rev. A **64** 053804-1 (2001).

[16] C.A. Muller *et. al.*, J. Phys. A: Math. Gen. **35** 10163 (2002).

[17] G. Labeyrie *et. al.*, Phys. Rev. Lett. **83** 5266 (1999).

[18] G. Labeyrie *et. al.*, J. Opt. B: Quantum Semiclass. Opt. **2** 203902-1 (2000).

[19] T. Jonckheere *et. al.*, Phys. Rev. Lett. **85** 4269 (2000).

[20] Y. Bidel *et. al.*, Phys. Rev. Lett. **88** 203902-1 (2002).

[21] S. Chandrasekhar, *Radiative transfer*, Dover, N.Y. (1960).

[22] I. Freund *et. al.*, Phys. Rev. Lett. **61** 2328 (1988).

[23] G. Maret *et. al.*, Z. Phys. B **65** 409 (1987).

[24] R. Loudon, *The quantum theory of light*, Oxford University Press (1983).

[25] C. Cohen-Tannoudji, B. Diu, F. Laloe *Quantum mechanics*, John Wiley (1977).

[26] J. D. Jackson, *Classical electrodynamics* (John Wiley), 1998.

[27] C. Cohen-Tannoudji, J. Dupont-Roc, G. Grynberg, *Atom-photon interactions*, Wiley (1992).

[28] M. Weissbluth, *Photon-atom interactions*, Academic Press (1988).

[29] W. Heitler, *The quantum theory of radiation*, Oxford (1954).

[30] A. R. Edmonds, *Angular momentum in quantum mechanics*, Princeton university press (1957).

[31] G. Baym, *Lectures on quantum mechanics*, W. A. Benjamin (1973).

[32] A. Messiah, *Quantum mechanics*, North-Holland (1962).

[33] W. M. Itano *et. al.*, Phys. Rev. A **57** 4176 (1998).

[34] M. E. Rose, *Elementary theory of angular momentum*, John Wiley (1957).

[35] J. de Pillis, *Linear Algebra*, Holt, Rinhehart and Winston, Inc. (1969).

[36] W. Happer *et. al.*, Phys. Rev. **160** 23 (1967).

[37] W. Happer *et. al.*, Phys. Rev. **163** 12 (1967).

[38] P.A. Franken, Phys. Rev. **121**, 508 (1961).

[39] W. Rasmussen *et. al.*, Opt. Comm. **12** 315 (1974).

[40] C. Cohen-Tannoudji, *Atoms in electromagnetic fields* (World Scientific), 1994.

[41] E. Arimondo *et. al.*, Rev. Mod. Phys. **49**, 31 (1977).

[42] W. Hanle, Z. Phys. **30**, 93 (1924).

[43] B. H. Bransden and C. J. Joachain, *Physics of atoms and molecules*, Prentice Hall (2003).

[44] F. D. Colegrove *et. al.*, Phys. Rev. Lett., **3** 420 (1959).

101 (2004).